2020

MODELING THE EFFECTS OF HYDROLOGIC SERVICE PAYMENTS ON THE HYDROLOGY OF TROPICAL MONTANE WATERSHEDS IN CENTRAL VERACRUZ, MEXICO.

Sergio Miguel López Ramírez
Michigan Technological University, slopezra@mtu.edu

MODELING THE EFFECTS OF HYDROLOGIC SERVICE PAYMENTS ON THE HYDROLOGY OF TROPICAL MONTANE WATERSHEDS IN CENTRAL VERACRUZ, MEXICO.

By

Sergio Miguel López Ramírez

A DISSERTATION

Submitted in partial fulfillment of the requirements for the degree of

DOCTOR OF PHILOSOPHY

In Civil Engineering

MICHIGAN TECHNOLOGICAL UNIVERSITY

2020

This dissertation has been approved in partial fulfillment of the requirements for the Degree of DOCTOR OF PHILOSOPHY in Civil Engineering.

Department of Civil and Environmental Engineering

Dissertation Co-Advisor:	*Dr. Alex Mayer*
Dissertation Co-Advisor:	*Dr. Veronica L. Webster*
Committee Member:	*Dr. Fengjing Liu*
Committee Member:	*Dr. Leonardo Saenz*
Department Chair:	*Dr. Audra Morse*

Table of Contents

List of figures

List of tables

Preface

Chapter 2 is a republication of a journal article published in *Hydrological Processes* (López Ramírez et al., 2020a).

Chapter 3 is a republication of a journal article under review in the *Journal of Hydrology* (López Ramírez et al., 2020b).

Chapter 4 is under preparation to be submitted to *Journal of Environmental Management.*

Acknowledgements

This material is based upon work supported by the National Science Foundation Award Number: 1313804. This National Science Foundation grant has been awarded to the University of New Hampshire with a subcontract agreement with Michigan Technological University. Funding was also provided by Michigan Technological University through the Doctoral Finishing Fellowship Award.

We thank the landowners of the micro-catchments for permitting us to work on their land. We would also like to thank León Rodrigo Gómez Aguilar, Carlos Lezama, and Víctor Vásquez for their great help in the field. Finally, we would like to acknowledge the valuable comments of Tadesse Alemayehu during the calibration of the SWAT-T model.

Abstract

An analysis of the effects of the Land Use Land Cover (LULC) change and its impacts on the hydrological cycle of tropical montane catchments influenced by cloud forest (TMCF) is developed in Central Veracruz, Mexico. This work started with the analysis of data from monitored-micro-catchments with contrasting LULC. Later the suitability of an improved version of the Soil and Water Assessment Tool model for the Tropics (SWAT-T) was evaluated. Finally, potential future land use scenarios, including conservation targeting alternatives were evaluated using a calibrated Seasonal Water Yield model as part of the Integrated Valuation of Ecosystem Services and Tradeoffs framework (InVEST-SWY).

High-resolution rainfall and streamflow timeseries suggested no statistical difference in the regulation capacity of high flows in 20 years of natural regeneration, compared to the mature forest. In terms of baseflow sustenance, the mature forest and intermediate age forest better promote this hydrologic service than the other land uses. Shade coffee exhibited a high capacity to modulate peak flows comparable to that of mature forest, and an intermediate capacity to sustain baseflow. Finally, forty years of intense pasture management caused a fivefold greater peak flow response and a lower baseflow compared to mature forest.

SWAT-T accurately simulated the observed low fraction of surface runoff. However, it incorrectly predicted the dominance of lateral flow, instead of the deep groundwater flow observed from isotope-based studies. Moreover, SWAT-T underestimated the influence of rainfall interception losses in forests. The temperature-based potential evapotranspiration methods produced the best model fit (KGE = 0.75, NSE = 0.54, PBIAS = 4.6%), but overestimated the PET in land covers with lower rainfall interception. Finally, the model largely overestimates the low flow in managed land covers, while underestimating it in forests.

The InVEST-SWY model predicted that forest conservation policy will produce a slight decrease in the annual water yield at catchment scale due to larger evapotranspiration rates observed in forests. However, the model was unable to mimic the effects of forest conservation on dry-season baseflow. InVEST-SWY exhibited a poor performance at interannual scale and needs improvements to incorporate the water storage capacity of the soils.

1 Introduction

Forests provide valuable contributions to people but continue to be threatened by land use change. Payments for watershed services or payments for hydrological services (PHS) programs are increasingly popular water management alternatives to improve the provisioning of ecosystem services such as water supplies (Brouwer et al., 2011). However, Inadequate targeting and the lack of measurement and modeling of the changes in hydrological services constitute two key obstacles that may considerably hamper PHS success (Wunder et al., 2020).

The central Veracruz zone is one of the pioneer areas adopting PHS programs in Latin America; this program started in 2003 as part of the National PHS program adopted by Mexico (Muñoz-Piña et al., 2008). Our work is centered on the Gavilanes and Pixquiac catchments. The Gavilanes catchment (area = 41 km^2) is the main source of water for the city of Coatepec, Veracruz, Mexico (García et al., 2004). The Pixquiac catchment (area = 106 km^2) provides 38% of the water supply for the Veracruz state capital of Xalapa (Paré and Gerez, 2012). The two catchments comprise part of the Antigua River basin (area = 1,565 km^2). Today areas receiving PHS payments cover 27% of the surface of the two studied catchments. These payments are aimed at increasing dry season baseflow.

A variety of tools have been developed or enhanced for assessing the hydrological services and more guidance is needed regarding the applicability of such tools in tropical environments (Vigerstol and Aukema, 2011). Two of the most prominent tools for the evaluation of seasonal water supply are: a) the SWAT model, which represents traditional and complex hydrologic tools, and, b) the InVEST-SWY model, that represents newer and parsimonious ecosystem services tools. Both models required similar spatial inputs: topography, land use, soils. However, SWAT requires daily climate data, while InVEST-SWY uses monthly timesteps. Thus, an advantage of the latter is that you can obtain a quicker assessment of the water budget, but you lose accuracy in the calibration of hydrological processes. Nonetheless, in the literature both models have been rated as capable to realistically represent seasonal water supply and consistently predict spatial distribution of baseflow (i.e., Hamel et al.,2020, and Willemen et al., 2019). More work is needed in the evaluation of the strengths and limitations of these models in monitored catchments.

In these areas, several field studies have shed light regarding the hydrologic functioning of contrasting land covers: including measurements of rainfall interception (i.e., Holwerda et al., 2010, Holwerda et al., 2013, González-Martínez, and Holwerda, 2018), monitoring of headwater micro-catchments (Muñoz-Villers et al., 2013), mean transit times estimates using stable isotopes (Muñoz-Villers et al., 2016), among others. However, most studies were reported at the upper band (>2100 m a.s.l.) or lower bands of the cloud forest belt (< 1300 m a.s.l.). Moreover, local hydrological modeling efforts and program evaluations have relied on secondary datasets (i.e., Mokondo et al., 2018, Asbjornsen et al., 2017). Two main knowledge gaps were identified. First, a need to better understand the land use effects of forest and managed land covers at the mid-

elevation band (1200-2100 m a.s.l.). Second, scale-up and integrate lessons learned across multiple spatial and temporal scales. We primarily contributed to better understand headwater catchment functioning through monitoring. Further, we combined innovating modeling methodologies to scale up experimentally derived results using two popular tools to evaluate environmental services: SWAT and InVEST-SWY models. Below is a detailed description of the steps we took.

1.1 Chapter 2

Chapter 2 presents the results of a study conducted in five neighboring headwater micro-catchments located in the TMCF region of Veracruz, Mexico. The research questions addressed by the hydrologic measurements and analysis were: (a) how does age of forest recovery affect streamflow?; (b) what are the effects of TMCF conversion to shaded coffee on streamflow?; and, (c) what are the effects of TMCF conversion to intense pasture management on streamflow? The hydroclimatic data were acquired over a four-year period by recording high-resolution rainfall and streamflow measurements (10 min) (2015-2019). To analyze the data and compare between micro-catchments and associated dominant land uses, we used a series of hydrologic indices related to streamflow variability at daily and storm-event scales. At the storm-event scale we used statistical analysis, including the non-parametric Dunn's test and the Analysis of Covariance (ANCOVA), to assess whether responses between micro-catchments were statistically different.

1.2 Chapter 3

Chapter 3 evaluates the suitability of the SWAT-T model to simulate discharge in a catchment dominated by tropical montane cloud forest (TMCF) located in Central Veracruz, Mexico. We hypothesize that by contrasting calibrated SWAT-T models against local hydrologic and vegetation observations (e.g. streamflow and leaf area index) and ecohydrological parameters, such as canopy storage capacities of different vegetation covers, we can identify model weaknesses and strengths for analyzing the hydrological consequences of land use change in these environments. Specifically, (a) we evaluate the performance of three PET methods in the SWAT-T model and (b) assess the accuracy of the model to simulate streamflow over the full range of the flow duration curve in four micro-catchments with contrasting land covers (mature and intermediate age TMCF, shade coffee, and pasture). To the best of our knowledge, this is the first study to apply a framework based on metrics from across the flow duration curve in the calibration of SWAT-T, together with the evaluation of the model at micro-catchments with contrasting land covers in areas influenced by tropical montane cloud forest and managed land covers.

1.3 Chapter 4

Chapter 4 presents the modeling results of future ecosystem services outcomes in PHS programs in watersheds in Veracruz, Mexico. This work evaluates targeting strategies by combining (a) a calibrated hydrology model (integrating results from local monitoring across different scales in forested and managed land covers) with (b) a land change model (LCM) that simulates future land cover patterns in response to PHS program coverage and targeting strategies. To the best of our knowledge this is the first study to model rainfall interception in SWY using locally derived parameters for two elevation bands of TMCF forests. Moreover, this study reviews the InVEST-SWY strengths and weaknesses to represent interannual quickflow and baseflow dynamics.

1.4 References

Asbjornsen, H., Manson, R.H., Scullion, J.J., Holwerda, F., Muñoz-Villers, L.E., Alvarado-Barrientos, M.S., Geissert, D., Dawson, T.E., McDonnell, J.J., Bruijnzeel, L.A., 2017. Interactions between payments for hydrologic services, landowner decisions, and ecohydrological consequences: synergies and disconnection in the cloud forest zone of central Veracruz, Mexico. Ecology and Society 22(2): 25. https://doi.org/10.5751/ES-09144-220225

Brouwer, R., Tesfaye, A., Pauw, P. (2011). Meta-analysis of institutional-economic factors explaining the environmental performance of payments for watershed services. *Environmental Conservation, 38,* 380-392.

García, C.I., Martínez, A.A., Ramírez, A., Cruz, A.N., Rivas A.J., Domínguez, L., 2004. La relación agua-bosque: delimitación de zonas prioritarias para pago de servicios ambientales hidrológicos en la cuenca del río Gavilanes, Coatepec, Veracruz. Last consulted on November 4, 2020 at: http://www2.inecc.gob.mx/publicaciones2/libros/528/relacion.pdf

González-Martínez, T.M., Holwerda, F., 2018. Rainfall and fog interception at the lower and upper altitudinal limits of cloud forest in Veracruz, Mexico. Hydrological processes 32, Issue 25, Pages 3717-3728. https://doi.org/10.1002/hyp.13299

Hamel, P., Valencia, J., Schmitt, R., Shrestha, M., Piman T., Sharp, R. P., Francesconi, W., Guswa A. J., 2020. Modeling seasonal water yield for landscape management: Applications in Peru and Myanmar. Journal of Environmental Management 270. https://doi.org/10.1016/j.jenvman.2020.110792

Holwerda, F., Bruijnzeel, L.A., Muñoz-Villers, L.E., Equihua, M., Asbjornsen, H., 2010. Rainfall and cloud water interception in mature and secondary lower montane cloud forests of Central Veracruz, Mexico. Journal of Hydrology, 384, 84–96. https://doi.org/10.1016/j.jhydrol.2010.01.012

Holwerda, F., Bruijnzeel, L.A., Barradas, V.L., Cervantes, J., 2013. The water and energy exchange of a shaded coffee plantation in the lower montane cloud forest zone of central Veracruz, Mexico. Agricultural and Forest Meteorology 173,1– 13. http://dx.doi.org/10.1016/j.agrformet.2012.12.015

Mokondoko, P., Manson, R.H., Ricketts, T.H., Geissert, D., 2018. Spatial analysis of ecosystem service relationships to improve targeting of payments for hydrological services. PLoS ONE 13 (2): e0192560. https://doi.org/10.1371/journal.pone.0192560

Muñoz-Piña, C., Guevara, A., Torres, J.M., Braña, J., 2008. Paying for the hydrological services of Mexico's forests: analysis, negotiations and results. Ecological Economics 65, 725–736. https://doi.org/10.1016/j.ecolecon.2007.07.031

Muñoz-Villers, L.E., McDonnell, J. J., 2013. Land use change effects on runoff generation in a humid tropical montane cloud forest region. Hydrology and Earth System Sciences 17, 3543–3560. https://doi.org/10.5194/hess-17-3543-2013

Muñoz-Villers, L.E., Geissert, D.R., Holwerda, F., McDonnell, J.J., 2016. Factors influencing stream baseflow transit times in tropical montane watersheds. Hydrology and Earth System Sciences 20, 1621-1635. doi:10.5194/hess-20-1621-2016

Paré, L., & Gerez, P. (2012). *Al filo del agua: Cogestión de la subcuenca del río Pixquiac, Veracruz* (1st ed.). Delegación Tlalpan, México, D.F., INE-Semarnat, ISBN 978-607-7908-89-0.

Vigerstol, K.L., Aukema, J.E., 2011. A comparison of tools for modeling freshwater ecosystem services. Journal of Environmental Management 92, issue 10, 2403-2409. https://doi.org/10.1016/j.jenvman.2011.06.040

Willemen, L., Crossman, N. D., Newsom, D., Hughell, D., Hunink, J. E., Milder, J.C., 2019. Aggregate effects on ecosystem services from certification of tea farming in the Upper Tana River basin, Kenya. Ecosystem services 38, 100962. https://doi.org/10.1016/j.ecoser.2019.100962

Wunder, S., Börner, J., Ezzine-de-Blas, D., Feder, S., Pagiola, S., 2020. Payments for Environmental Services: Past Performance and Pending Potentials. Annual review of resource economics 12, issue 1, 209-234. https://doi.org/10.1146/annurev-resource-100518-094206

2 Land use change effects on catchment streamflow response in a humid tropical montane cloud forest region, central Veracruz, Mexico

2.1 Abstract

Tropical montane cloud forests (TMCF) are recognized for their capacity to maintain high dry-season baseflow and a host of other ecosystem services. Substantial areas of TMCF have been converted to pasture and crops such as coffee, while in other areas TCMF are recovering. However, little is known about the effects of this complex dynamic on catchment hydrology. We investigated the effect of land use on rainfall-runoff response in five neighboring headwater micro-catchments in central Veracruz, Mexico, dominated by either mature TMCF (MF), young (20 yr-old) and intermediate (40 yr-old) naturally regenerating TMCF (YF and IF, respectively), shaded coffee (SC), and an intensively grazed pasture (IP). We used a 4-year record of high-resolution rainfall and streamflow (10 min) data, collected from 2015 to 2019. These data were analyzed via comparison of hydrologic metrics that summarize streamflow responses at various time scales and magnitudes. Results showed no statistical difference in the regulation capacity of high flows in the micro-catchment with 20 years of natural regeneration, compared to the MF. In terms of baseflow sustenance, our results support the hypothesis that MF and IF better promote this hydrologic service than the other land uses. SC exhibited a high capacity to modulate peak flows comparable to that of MF, and an intermediate capacity to sustain baseflow, suggesting that the integrated functioning of this micro-catchment was largely preserved. Finally, forty years of intense pasture management was found to have degraded the soil hydraulic properties of IP; mainly, reducing its infiltration capacity, causing a fivefold greater peak flow response and a lower baseflow compared to MF.

2.2 Introduction

Understanding the impact of land use change on hydrology remains a major global research issue and it is fundamental to the effective management of water resources (Evaristo & McDonnell, 2019; Foley et al., 2005). Land use change is not linear, nor does it follow a unique direction. Across the world, large areas are losing forest, but forest regeneration is occurring elsewhere. (Bjørn, 2001; Paré & Gerez, 2012). In the tropics, particularly in developing countries, deforestation is still a prominent environmental problem (Wolfersberger et al., 2015). In these areas, conversion from forests to pastures for cattle raising or to cash crop agriculture are common land-use change activities, along with urbanization (ICO, 2010; Navarrete, 2016; Richardson & Peres, 2016). However, urbanization has also caused mass migration to urban centers and abandonment of rural livelihoods (Paré and Gerez, 2012), leaving lands in a regeneration process. Little is known about the effects that this complex land use change dynamic has on the hydrologic cycle. In particular, the effect of regeneration of forest and agroforestry systems, such as

shaded coffee cultivation, remain poorly understood (Evaristo & McDonnell, 2019; Muñoz-Villers et al., in review).

A significant gap persists in our understanding of the impacts of conversion of the tropical montane cloud forest (TMCF) on seasonal hydrologic variability, particularly for low and high flow regimes (Brown et al., 2005; Bruijnzeel, 2004). Apart from being among the world's most valuable terrestrial ecosystems in terms of species richness and levels of endemism (Bruijnzeel et al., 2011; Martínez et al., 2009), TMCFs are recognized for their marked capacity to capture, store, and purify fresh water that benefit millions of people downstream across the tropics (Sáenz & Mulligan, 2013). Despite their importance, by the year 2000, between 45% and 55% of TMCFs worldwide were converted to other land uses (Bruijnzeel et al., 2011; Scatena et al., 2010). Approximately 15% of TMCF sites listed by WCMC-UNEP as having confirmed cloud forest presence (Aldrich et al., 1997) occur in andosols (FAO-UNESCO, 2007). Volcanic soils are recognized not only for having a high-water storage capacity (Nanzyo, 2002), but also for being fragile and particularly difficult to restore (Meza-Pérez & Geissert-Kientz, 2006). It's unclear how land use activities such as cultivation of crops or cattle grazing affect the hydrologic functions of these environments and the implications for downstream communities (Bruijnzeel et al., 2011; Sáenz et al., 2014; Toledo-Aceves et al., 2011). Thus, under an anticipated future world with increasing water stress (IPCC, 2018), TMCFs, and particularly those located in volcanic regions, represent a high conservation priority.

Another major gap in our knowledge of TMCFs is the degree to which restoration of hydrologic functions occurs from forest regeneration after disturbance (Bruijnzeel, 2004; Bruijnzeel et al., 2011). A slow return to pre-disturbance hydrology may be expected in TMCFs, since these environments have slower vegetative growth rates due to reduced radiation from clouds (Bruijnzeel et al., 2011; Fahey et al., 2015). In central Veracruz, Mexico, Muñoz-Villers and McDonnell (2013) reported that 20 years of natural regeneration may be enough to largely restore the original hydrologic conditions of local TMCF. However, uncertainty remains on whether the time required to restore hydrologic functions depend on land use history (Muñoz-Villers & McDonnell, 2013). Further information on the hydrologic functioning of both naturally regenerating forests and shade coffee is relevant for informing Payments for Ecosystem Services (PES) Programs, since PES programs often promote these landcovers, with the assumption that they provide hydrologic benefits compared to those of mature forests (Marin-Castro et al., 2016; Saenz et al., 2014). Hydrological Services (HS) are part of the PES schemes that encompass benefits such as water supply and the mitigation of flood damage. HS are commonly defined by hydrologic attributes such as quantity and timing of flow (Brauman et al., 2007). Water supply services are often linked with baseflow metrics, while peak flow is regularly associated with flood mitigation.

Another critical area of tropical land use change research is understanding of the hydrologic effects of TMCF conversion to perennial crops, such as shade coffee plantations. Coffee is an important cash crop, providing income to about 26 million

people in approximately 50 coffee producing countries, mainly located on humid tropical mountains (ICO, 2010). In addition, shade coffee has been valued not only for conserving a large part of the biological diversity of the TMCF (De Beenhouwer et al., 2013), but also for the wide variety of environmental services they provide, including pollination, soil stability, pest regulation (De Beenhouwer et al., 2013), high carbon sequestration compared to annual crops (Lewis et al., 2019), and a higher soil hydraulic conductivity compared to intensively grazed pasture (Muñoz-Villers & McDonnell, 2013; Tobón et al., 2010). However, when shade coffee plantations have been compared with natural and restored native forests, they have exhibited reduced carbon sequestration (Lewis, et al., 2019), lower soil hydraulic conductivity values, and lower stream water quality (Marín-Castro et al., 2016; Martinez et al., 2009; Pérez-Pérez & Muñoz-Villers, 2016).

Finally, there is substantial evidence that forest conversion to pasture is associated with an increase in annual streamflow totals because of the lower evapotranspiration of the replacement vegetation (Bruijnzeel, 2004; Muñoz-Villers & McDonnell, 2013; Ogden, 2013). In contrast, this conversion has been shown to result in strong declines in dry season flows, as pastures show much lower rainfall infiltration, mainly due to soil compaction, which leads to insufficient replenishment of groundwater reserves during rainy seasons (Bruijnzeel, 2004; Muñoz-Villers et al., 2015). Moreover, reduced rainfall infiltration can result in higher and more rapid peak flows, which may exacerbate flash flooding (Bonell & Bruijnzeel, 2005).

A common approach used to understand land use effects on runoff generation is to compare the hydrology of neighboring micro-catchments with different land covers but similar size, topography, soils, geology and climate (Muñoz-Villers et al., 2012; Muñoz & McDonnell, 2013; Ogden, 2013). We followed this approach to create our experimental design to assess the hydrologic impacts of TMCF conversion and natural regeneration, in combination with rainfall and runoff indices, and associated statistical tests. This study uses daily and event streamflow measurements to investigate differences in hydrologic functioning between headwater micro-catchments dominated by mature TMCFs, regenerating forests, pastures, and shade coffee plantations in a region dominated by volcanically-derived soils. Two particularly novel aspects of our work are that (1) it assesses whether replacing land covers (such as shade coffee plantations) can offer comparable hydrologic services to those of mature TMCFs and (2) it considers the timeframes needed for naturally regenerating TMCFs to approximate the hydrologic regulatory capacity of mature TMCFs.

This paper presents the results of a study conducted in five neighboring headwater micro-catchments located in the TMCF region of Veracruz, Mexico. The research questions addressed by the hydrologic measurements and analysis were: (a) how does age of forest recovery affect streamflow?; (b) what are the effects of TMCF conversion to shaded coffee on streamflow?; and, (c) what are the effects of TMCF conversion to intense pasture management on streamflow? The hydroclimatic data were acquired over a four-year period by recording high-resolution rainfall and streamflow measurements (10 min) (2015-2019). To analyze the data and compare between micro-catchments and associated

dominant land uses, we used a series of hydrologic indices related to streamflow variability at daily and storm-event scales. At the storm-event scale we used statistical analysis, including the non-parametric Dunn's test and the Analysis of Covariance (ANCOVA), to assess whether responses between micro-catchments were statistically different.

2.3 Methodology

2.3.1 Study site

The research was carried out in five headwater micro-catchments (0.137 – 0.446 km^2) located between 1241 m a.s.l. and 1713 m a.s.l. in the TMCF zone in central Veracruz, Mexico (Figure 2-1). A detailed description of the characteristics of each micro-catchment is provided in Table 2-1. The micro-catchments are drained by first or second-order perennial streams and are located within the catchments of the Pixquiac and Gavilanes rivers (106 and 42 km^2, respectively), which are, in turn, sub-catchments of the Antigua River basin (1565 km^2). The micro-catchments where chosen based on the dominance of five Land Use Land Cover (LULC) categories of interest within each micro-catchment: mature forest (MF; 100% of total cover; Table 2-1), intermediate age secondary forest (IF; 77%), young secondary forest (YF; 68%), shade coffee plantations (SC; 94%), and high-intensity pasture (IP; 63%). Together these land uses comprise 89% of LULC in the Pixquiac and Gavilanes sub-watersheds (Von Thaden-Ugalde, unpublished data). The most important land use change in the last 40 years in the Pixquiac and Gavilanes catchments is TMCF regeneration. For example, in the Pixquiac catchment, forest cover increased from 6561 ha in 1975 to 7685 ha by 2004 (Paré & Gerez, 2012). Recent land use maps have confirmed that the forest cover has remained constant during the last decade and accounts for around 79 % of the study area (CONANP et al., 2015).

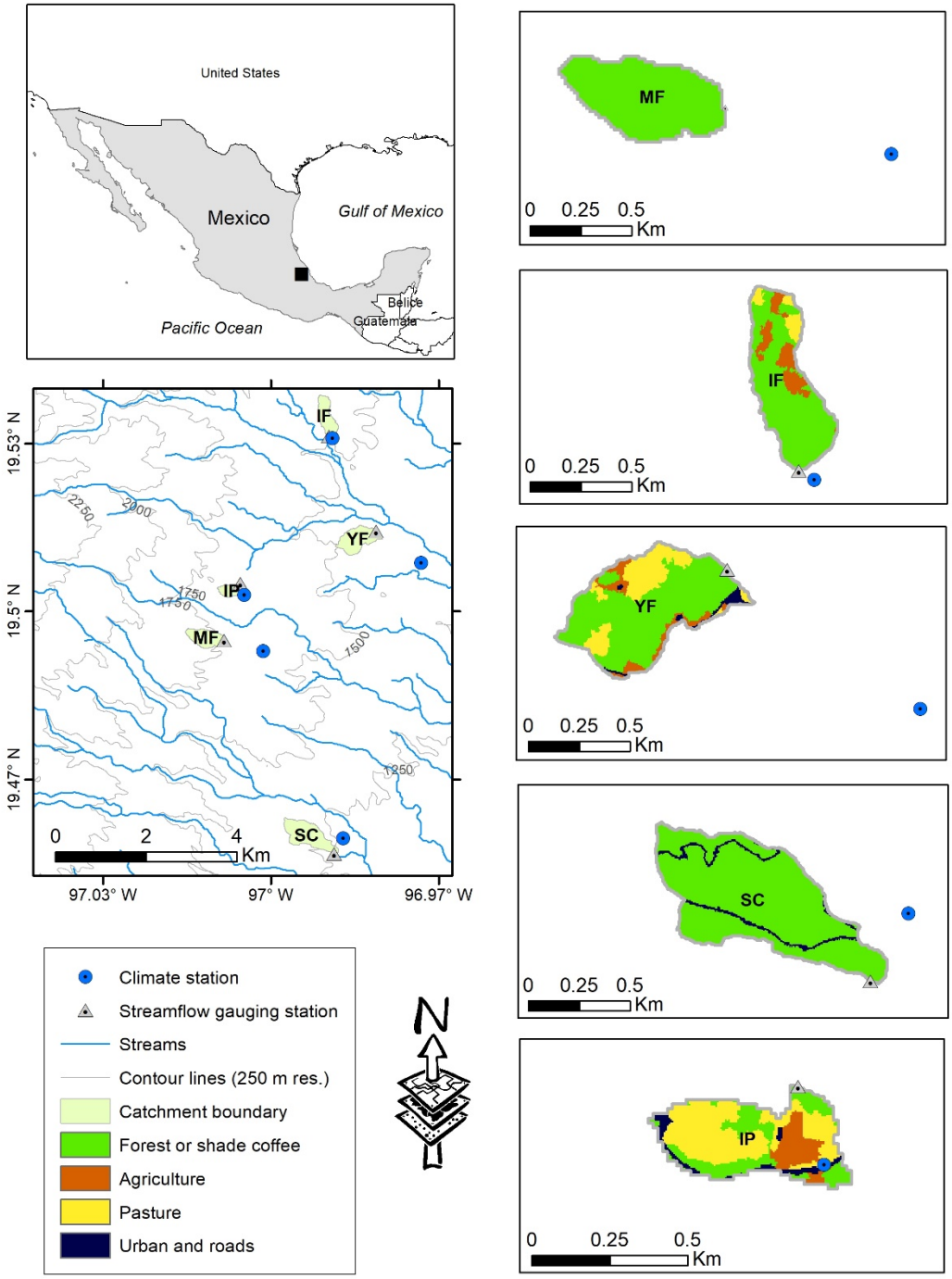

Figure 2-1: Location of the study area in central Veracruz, Mexico, and maps of the study micro-catchments showing land use-land cover distributions and locations of instrumentation. Sources: (INEGI; 2013). Mature forest (MF), intermediate forest (IF), young forest (YF), shade coffee (SC), and intensive pasture (IP).

The MF micro-catchment is dominated by old-growth TMCF (> 50 years old) with low disturbance; less than 10% of the area is covered by a 15-year-old secondary forest. The IF site is mainly covered by 40-year-old TMCFs (> 77 % of the area). The remaining proportion of the IF micro-catchment is pasture land and annual crops (mainly maize) located in the upper parts. The YF micro-catchment is covered (> 68% of the area) by 20-year-old TMCF, with the remaining area of pasture and maize (Von-Thaden U., unpublished data). The overstory of these TMCFs is dominated by *Quercus spp, Oreomunnea mexicana, Turpinia insignis, Liquidambar styraxiflua, Carpinus tropicalis, Clethra macrophylla* (Williams-Linera & Vizcaíno-Bravo, 2016, García-Franco et al., 2008), with greater heterogeneity in the IF and YF micro-catchments. The mean tree height in the three micro-catchments is similar and ranges between 20-25 m, with a few larger trees reaching more than 30 m in height. The three micro-catchments have similar mean leaf area index (LAI), see Table 2-1. LAI was measured with a LAI-2200C Plant Canopy Analyzer (LI-COR, 2019) over a 500 m transect in each of the micro-catchments. These measurements were taken during the rainy season (July 8 to August 20, 2019) in the early-morning hours (6:45 to 8:00 am), before the sunset or under cloudy conditions to avoid scattering effects.

The SC micro-catchment has been covered by shaded coffee for more than 80 years (Marín-Castro et al., 2016), with 94 % of the land area dominated by this land cover. This production system retains some trees to provide shade to the coffee. However, coffee cultivation in the area includes management practices such as removal of the herbaceous groundcover, pruning, fertilization, and agrochemical applications. The original vegetation in the IP micro-catchment was TMCF, which was cleared more than 40 years ago (Paré & Gerez, 2012; and local inhabitants, personal communication). Since then, the pasture has been heavily grazed by sheep, goats and cows (> 63% of the land area), with grass height generally less than 5 cm, compaction from livestock is present. In addition, approximately 10% of IP is covered by cropland (maize and, more recently, potatoes) and associated shrub-dominated fallows.

The soils in the micro-catchments are classified as Umbric Andosols derived from volcanic ash, with clay and silty clay as dominant textures (Campos-Cascaredo, 2010; Paré & Gerez, 2012). Topsoils in all micro-catchments are characterized by low bulk densities (< 0.7 g cm^{-3}) due to the abundance of noncrystalline materials and organic matter. In general, soils in TMCFs exhibit lower bulk densities in comparison to pasture and coffee, revealing less soil compaction (Looker N., unpublished data; Table 2-1). In addition, soil profiles are generally deep (A + B horizons > 1 m and C + Cr horizons > 10 m on ridges and backslopes) and moderately well developed (Karlsen, 2010) in all micro-catchments, favoring good water storage. Moreover, the soils in the region are generally underlined by andesitic saprolite, with high permeability ranging from 0.05 to 0.08 mm h^{-1} (Gabrielli & McDonnell, 2011; Karlsen, 2010; Muñoz-Villers & McDonnell, 2012). Although we did not measure bedrock hydraulic properties here, we observed the presence of saturated saprolite on various road cuts in our study sites. Field-saturated hydraulic conductivities (K_{fs}) were measured in 2017 at the soil surface (5-15 cm) in points distributed spatially across the five micro-catchments using the constant head

Guelph permeameter method (Elrick et al., 1989). The results are presented in Table 2-1 (Looker, unpublished data).

The general climate is classified as humid temperate with abundant rains during the summer (Koppen classification modified by García, 2004). The mean daily temperature ranges between 16 to 18 °C, the mean of the maximum daily temperature ranges between 22 and 24 °C, and the mean of the minimum daily temperature is between 12 and 13 °C. The mean daily relative humidity is between 86 and 90% and the mean annual precipitation values range from 1500 to 3000 mm (Shinbrot et al., in review.; SMN, 2015; Williams-Linera & Vizcaíno-Bravo, 2016). Approximately 80% of the rainfall falls as convective storms during the wet season (May–October), when the region is under the influence of the easterly trade wind flow. During the dry season (November–April), rainfall is generally associated with cold fronts and characterized by light rains and drizzle (Holwerda et al., 2010). Annual values of cloud water interception account for less than 2% of the total rainfall in the region (Holwerda et al., 2010).

Table 2-1: Topographic, land cover and soil physical characteristics of the five study micro-catchments. Where available, the standard deviation (SD) is provided. Mean K_{fs} is the geometric mean because this variable is log normally distributed, whereas for the other variables the mean is an arithmetic mean. Mature forest (MF), intermediate forest (IF), young forest (YF), shade coffee (SC), and intensive pasture (IP).

	MF	**IF**	**YF**	**SC**	**IP**
Area (km^2) [b]	0.242	0.224	0.343	0.446	0.137
Surface 3D, (km^2) [b]	0.262	0.233	0.349	0.461	0.143
Mean elevation (m a.s.l.)[c]	1756	1604	1453	1284	1655
Mean slope (°) [b]	20 ± 8	14 ± 7	8 ± 5	12 ± 7	12 ± 10
Percent forest or coffee cover [c]	100%	77%	68%	94%	29%
Percent of pasture and crops cover [c]	0%	23%	29%	0%	63%
Percent of urban and roads [c]	0%	0%	3%	6%	8%
Soil saturated hydraulic conductivity (K_{fs}) at 20-cm depth (mm h^{-1})[a]	125 ± 2.1	127 ± 2.1	95 ± 2.4	48 ± 3.4	26 ± 2

	MF	IF	YF	SC	IP
Bulk density at 0-5 cm (g cm^{-3}) [a]	0.19 ± 0.08	0.31 ± 0.09	0.29 ± 0.15	0.62 ± 0.13	0.37 ± 0.1
Surface soil texture mean percentage of Clay [a]	49	42	44	48	41
Surface soil texture mean percentage of Silt [a]	40	50	38	41	52
Surface soil texture mean percentage of Sand [a]	11	8	18	10	7
Aspect [b]	E-NE	SW-SE	NE-E	S-SE	NE-E
Leaf area index (LAI) (m^2 m^{-2}) [d]	5.93 ± 0.9	5.96 ± 1.22	5.91 ± 1.31	4.3 ± 1.71	-

[a] Berry et al., in prep.

[b] Estimated from INEGI (2013)

[c] Land use map distributed by CONANP et al. 2015

[d] See text for description of the LAI measurement methods.

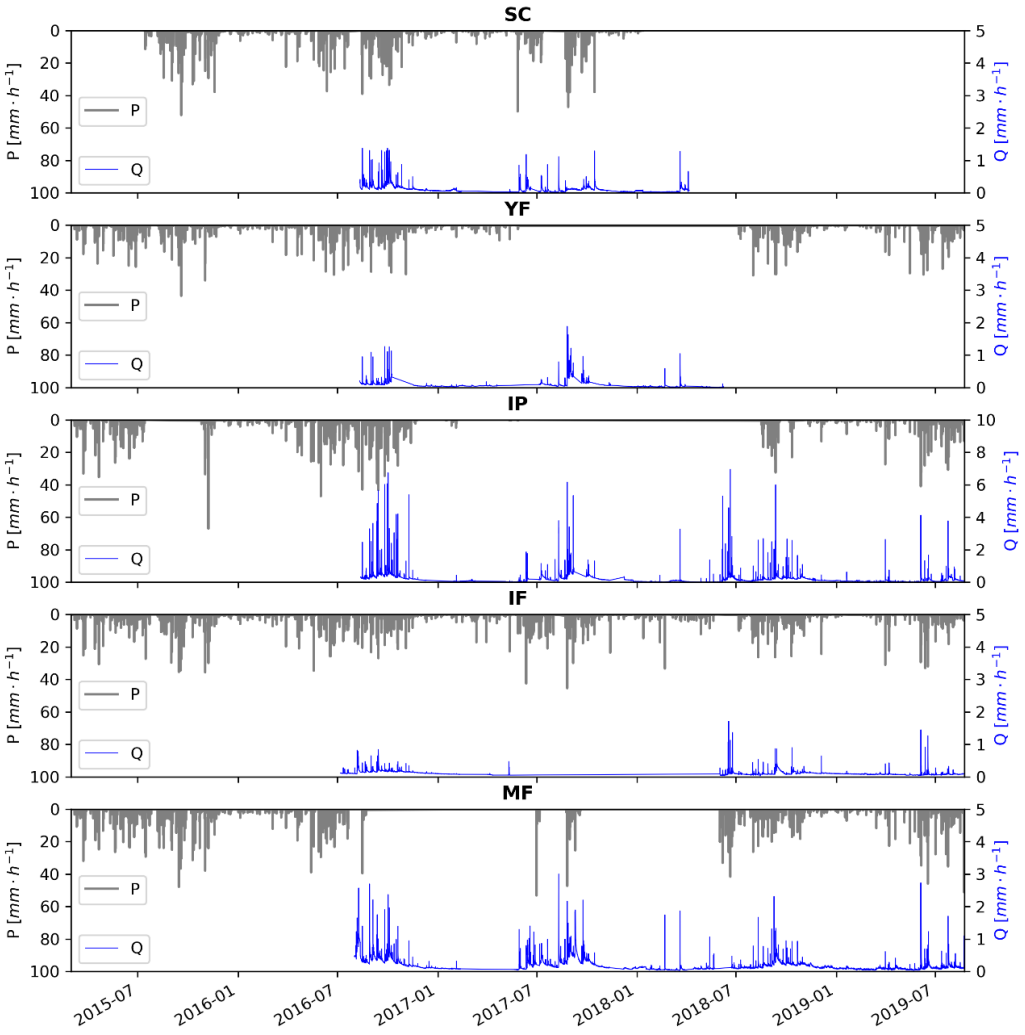

Figure 2-2: Hourly depths of rainfall, P (top y axis; grey bars) and streamflow, Q (bottom y axis; blue lines), as measured at the five study micro-catchments from Feb 26, 2015 to Aug 23, 2019. Mature forest (MF), intermediate forest (IF), young forest (YF), shade coffee (SC), and intensive pasture (IP).

2.3.2 Hydrometeorological measurements

Rainfall was measured with climate stations located in clearings (> 30 m from forest edge) in each of the five study micro-catchments (Figure 2-1). The stations were equipped with tipping bucket rain gauges equipped with dataloggers (Campbell Scientific and Davis), with resolutions between 0.1 mm and 0.2 mm and recording readings every 10 to 15 minutes (Figure 2-2). Streamflow was measured using V-notch weirs at the micro-catchment outlets (90° angle for the YF, IF, MF, IP and 120° for the SC micro-catchment). The 120° angle was used in SC because this micro-catchment has a larger area and the design peak discharge was larger. Water levels were registered every 1.5 min

using Solinst water level sensors paired with barometric pressure recorders. Water levels were converted to streamflow (L s^{-1}) using experimental stage-discharge relationships for the weirs based on rating curves derived from volumetric and salt dilution measurements of discharge (ASTM D5242-92, 2013; Moore, 2005).

Rainfall measurements in the five micro-catchments started in February 2015, whereas discharge data collection began in July 2016. The monitoring of discharge continued only to July 2018 in the SC and YF. For MF, IF and IP, rainfall and streamflow measurements continued until August 2019 (Figure 2-2). Damage to the equipment by animals and problems with access to the sites led to periodic gaps in the streamflow and rainfall data; on average, these gaps account for around 25% of the period of record, for streamflow and rainfall.

Since a range of hydrological conditions (e.g. slope) were observed in each micro-catchment, standardized metrics and statistics across the land covers were applied (Nainar et al., 2018; Ochoa-Tocachi et al., 2016). The streamflow data was normalized by the contributing micro-catchment true areas, rather than planar areas (Figure 2-2), as suggested by Zhang et al., (2011) and Kienzle (2010). Surface areas were estimated using a triangulated irregular network (TIN) model, created by transforming a 15-m DEM (INEGI, 2013) into a continuous 3-dimensional surface, according to the method proposed by Jenness (2004) and Zhang et al., (2011). This procedure was conducted using 3D Analyst Tools in ArcMap version 10.5.1.

2.3.3 Data process and analysis

Streamflow and rainfall data were resampled to daily timesteps as mean daily streamflow and sum of daily rainfall and a set of metrics were calculated for each micro-catchment to compare their hydrologic regimes. Table 2-2 presents definitions for each metric. To estimate runoff ratios, only days containing paired values of rainfall and runoff were selected. The following parameters were computed: average daily rainfall (MP), average daily runoff (MQ), and runoff ratio (RR) (Muñoz-Villers & McDonnell, 2013; Sawicz et al., 2011). All the available data of rainfall was used to estimate the annual ratio of days with zero precipitation (DAYP0), and daily rainfall variability (PVAR). Likewise, the complete dataset of discharge was used to compute the daily flow variability (QVAR), flow duration curve (FDC), slope of the flow duration curve (SFDC), mean annual high flow ($MAHF$), and mean annual low flow ($MALF$) (Kelleher et al., 2015; Nainar et al., 2018; Ochoa-Tocachi et al., 2016; Ogden et al., 2013; Price et al., 2011; Tetzlaff & Soulsby, 2008). Additionally, the baseflow recession constant (k) was obtained from the master recession curve (MRC) using the matching strip method (Toebes & Strang, 1964) during the period where the minimum rainfall inputs were identified in the dry season (Chapman, 1999). Note that a larger k value indicates slow drainage and greater storage capacity (Murphy & Stallard, 2012).

Table 2-2: Definition of the hydrological indices analyzed in the study.

Index	**Reference formula**	**Units**	**Definition**
N		day	Number of days where complete data of rainfall and runoff is available
MP	$\bar{P}_n$	mm day^{-1}	Average daily rainfall during the period where both rainfall and streamflow are available (n)
MQ	$\bar{Q}_n$	mm day^{-1}	Average daily runoff over the period where both rainfall and streamflow are available (n)
RR	$\bar{Q}_n / \bar{P}_n$	-	Ratio between average daily runoff and average daily rainfall (Ochoa-Tocachi et al., 2016).
PVAR	σ_P / P_{mean}	mm mm^{-1}	Coefficient of variation in daily precipitation over the entire monitoring period, standard deviation divided by mean (Ochoa-Tocachi et al., 2016)
DAYP0	$D_{p<RGres} / D_{total}$	-	Fraction of days with zero precipitation with respect to the total number of days over the monitoring period (Ochoa-Tocachi et al., 2016).
QVAR	$\sigma_Q \ / \ Q_{mean}$	mm mm^{-1}	Coefficient of variation in daily flows over the monitoring period, standard deviation divided by mean (Ochoa-Tocachi et al., 2016).
FDC		-	Flow duration curve is the distribution of probabilities of streamflow being greater than or equal to a specified magnitude plotted on a semi-log scale. (Muñoz & McDonnell, 2013).

Index	Reference formula	Units	Definition
SFDC	$S_{FDC} = \frac{ln(Q_{33}) - ln(Q_{66})}{0.66 - 0.33}$	-	Slope of the flow duration curve. Calculated using the method of Zhang et al. (2008) modified by Sawicz et al. (2011).
MAHF	Q_5	mm day^{-1}	Mean annual high flow calculated as the mean of the 5st percentile of the FDC (Muñoz & McDonnell, 2013)
MALF	Q_{95}	mm day^{-1}	Mean annual low flow calculated as the mean of the 95st percentile of the FDC (Muñoz & McDonnell, 2013)
k	$Q_d = Q_0 \cdot exp(-t/\tau)$ $Q_d = Q_0 \cdot k^t$	-	MRC is described using linear reservoir theory (Chapman, 1999), where Q_0 and Q_d are the flows (mm day^{-1}) at time 0 and t (days), respectively, τ is the turnover time of the groundwater storage (days) and k is the recession constant (Ogden, 2013; Muñoz & McDonnell, 2013)

To assess stream response to precipitation and runoff response in the studied micro-catchments, 266 storm events were examined during the period from July 1st, 2016 to August 10th, 2018. For this analysis, ten-minute rainfall and streamflow data were used to graphically separate streamflow into quickflow (direct flow in response to a rainfall event) and baseflow (the delayed flow from storage), following the approach of Hewlett and Hibbert (1967). The hydrograph separation was performed using the slope constant method (see Mosley, 1979). Storms were defined as periods with more than 0.2 mm of rainfall, separated by a dry period of at least 3 h (Muñoz-Villers & McDonnell, 2013). For each storm event, the following parameters were calculated: total rainfall (P_{ev} [mm]), total runoff (Q_t [mm]), quickflow (Q_{qf} [mm]), baseflow (Q_{bf} [mm]), peak flow (Q_{peak} [mm h^{-1}]) and the 24 h antecedent precipitation (AP [mm]). Furthermore, we calculated the lag time (T_L [h]), defined as the time between peak rainfall and peak flow, and the time to peak (T_p [h]), defined as the time between the onset of storm and peak flow (Mosley, 1979).

2.3.4 Statistical methods

Statistical tests were applied to detect differences in the hydrologic responses across the micro-catchments. Since the distribution of storm events did not follow the normality assumption (Shapiro-Wilk test), we chose the non-parametric Kruskal-Wallis H test followed by the post-hoc Dunn's test ($\alpha = 0.05$) (Nainar et al., 2018). The latter test was used to make multiple pairwise comparisons based on approximations to the actual rank statistics. The Dunn's (1961) Bonferroni adjustment was used for multiple comparisons, and the results are displayed in box-and-whisker plots supplemented by alphabet groupings (Yamada, 2013). These statistics were carried out with the R software v.3.5.3.

The storm parameters (Q_t, Q_{qf}, Q_{bf}, Q_{peak}) were positively correlated with the total event rainfall (P_{ev}). Consequently, to control for the effects of this covariation, two approaches were applied. First, the parameters were normalized by rainfall event (Q_t/P_{ev}, Q_{qf}/P_{ev}, Q_{bf}/P_{ev}) and subsequently compared with the non-parametric methods listed above. Second, a multiple regression analysis was conducted on each hydrologic variable against P_{ev} across the five micro-catchments, followed by an analysis of covariance (ANCOVA) of the resulting linear models in R software v.3.5.3. (Baumer et al., 2017; Nainar et al., 2018; Staelens et al., 2008; Verma et al., 2018).

In the ANCOVA, we modeled the land cover-specific relationship between P_{ev} and each of the storm parameters using a multiple linear regression model (Equation 1) with a distinct slope and intercept for each land cover:

$$Y = \alpha_0 + \beta_0 P_{ev} + \alpha_1 x_1 + \beta_1 x_1 P_{ev} + \alpha_2 x_2 + \beta_2 x_2 P_{ev} + \alpha_3 x_3 + \beta_3 x_3 P_{ev} + \alpha_4 x_4 + \beta_4 x_4 P_{ev} + \varepsilon \quad (1)$$

Where the regression coefficients $\alpha_0, \alpha_1, \alpha_2, \alpha_3, and\ \alpha_4$ represent the intercepts and the coefficients $\beta_0, \beta_1, \beta_2, \beta_3, and\ \beta_4$ are the slopes. The reference land cover is MF, and x_1 through x_4 are indicator variables for IF, YF, SC, and IP.

ANCOVA was used to determine the following model (Schneider et al., 2015):

$$Y_{i,j} = \mu + \alpha_i + \beta_i\left(X_{i,j} - \overline{X_\iota}\right) + \varepsilon_{i,j} \quad (2)$$

where $Y_{i,j}$ is the response of streamflow (Q_t, Q_{qf}, Q_{bf}, Q_{peak}) in micro-catchment *i* to storm *j* with total rainfall $X_{i,j,}$ $\overline{X_\iota}$ represents the means of total rainfall in the micro-catchments, and $\varepsilon_{i,j}$ represents the residuals. We can rearrange Equation 2 to express the ANCOVA on the original response variable (*Y*) as a regular ANOVA on values of *Y* that have been adjusted, according to their linear dependence on *X*:

$$Y_{i,j} - \beta_i(X_{i,j} - \overline{X_\iota}) = \mu + \alpha_i + \varepsilon_{i,j} \quad (3)$$

This approach allows for comparing the slope, intercept, and residual variances for two regression equations based on a two-tail F-test. If statistically significant differences in

slopes, intercepts, or residual variances are found, then the regressions describing streamflow response (Q_t, Q_{qf}, Q_{bf}, Q_{peak}) for each land cover can be regarded as statistically different.

2.4 Results

2.4.1 Rainfall and runoff hydrologic metrics

During the study period, as described in section 2.3, mean annual precipitation (*P*) was higher in MF (2607 mm), followed by IP (2340 mm), SC (2135 mm), IF (1840 mm), and YF (1649 mm). The micro-catchments located in the north and with lower elevations have lower rainfall, while rainfall is highest to the southwest at higher elevations (≈ 1700 m a.s.l.). Rainfall was not necessarily correlated with elevation, as observed in SC and YF, which had relatively high rainfalls at lower elevations. However, the micro-catchments located at lower elevations (YF and SC) exhibited higher daily precipitation variation (PVAR) and percent of days without rainfall (DAYP0) (see Table 2-3).

Figure 2-3b shows the rainfall duration curve for daily rainfall across the study micro-catchments. The highest runoff ratio (Table 2-3 and Figure 2-3c) occurred in the IP (0.69), followed by MF (0.67), IF (0.58), YF (0.53), and SC (0.46). In general, the micro-catchments with higher annual precipitation presented a higher RR. However, this index is also controlled by other factors, including land use; in our case, IP had the highest RR and SC had the smallest RR, despite similar rainfall. The FDC for runoff (Figure 2-3a), the slope of the FDC (SFDC), and the coefficient of variation in daily flows (QVAR) exhibited complex responses across the micro-catchments (Table 2-3). YF showed the highest QVAR, followed by IP, SC, MF and IF. This metric agrees with most of the results for SFDC, where IP had the second highest streamflow variability and MF and IF presented the lowest SFDC.

The mean annual high flow (MAHF) metric appears to be influenced by slope and soil infiltration capacity. IP showed the highest high flow followed by MF, SC, YF and IF (Table 2-3). The reduced infiltration capacity of IP appears to be the main explanatory variable for MAHF; however, the high MAHF observed in MF can be also linked to its steep slope (20°). Interestingly, in IF, a high infiltration capacity (127 mm h^{-1}) appears to be a stronger controlling factor than slope (14°), explaining why this micro-catchment has the lowest MAHF. MF presented the highest MALF, followed by IF, SC, IP, and YF (Table 2-3). In the five micro-catchments *k* was relatively high, from 0.978 to 0.993, indicating slow drainage and high storage. It should be stressed, that *k* is bounded ($k \leq 1$) and *k* often is above 0.80 even in mesoscale catchments (Thomas et al., 2013).

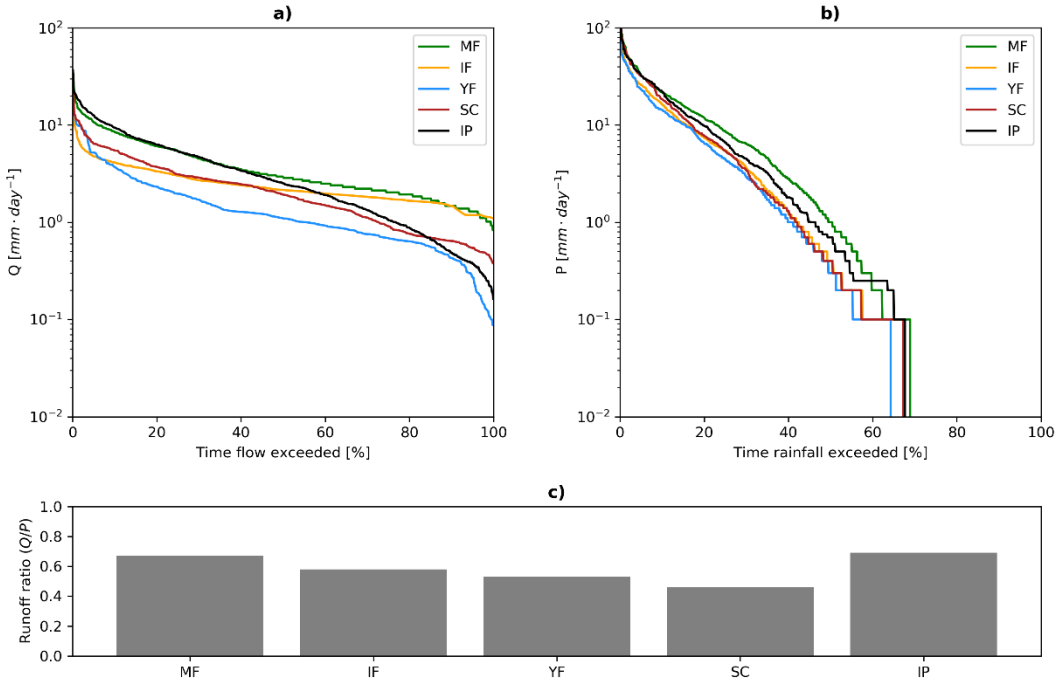

Figure 2-3: Plots showing the a) flow-duration curve; b) rain-duration curve; c) runoff ratio (RR) for study micro-catchments in central Veracruz, Mexico. Mature forest (MF), intermediate forest (IF), young forest (YF), shade coffee (SC), and intensive pasture (IP).

Table 2-3: Computed meteorological and runoff-related coefficients of the different catchments, where available, the standard deviation (SD) is provided. Mature forest (MF), intermediate forest (IF), young forest (YF), shade coffee (SC), and intensive pasture (IP).

Index	MF	IF	YF	SC	IP
N	469	642	209	360	467
MP	6.47	4.64	3.29	6.67	6.00
MQ	4.35	2.67	1.74	3.05	4.14
RR	0.67	0.58	0.53	0.46	0.69
PVAR	1.86	2.07	2.10	2.18	1.99

Index	MF	IF	YF	SC	IP
DAYP0	0.31	0.32	0.36	0.33	0.32
QVAR	0.83	0.51	1.13	0.91	1.05
SFDC	1.79	1.01	1.82	2.22	3.04
MAHF (± SD)	10.7 ± 0.25	4.7 ± 0.05	5.2 ± 0.01	6.5 ± 0.12	12.5 ± 0.35
MALF (± SD)	1.29 ± 0	1.18 ± 0	0.26 ± 0.01	0.54 ± 0	0.37 ± 0
k	0.989	0.993	0.978	0.986	0.980

2.4.2 Catchment event response

During the study period, a total of 266 discrete rainfall events were analyzed, including 51 events in MF, 79 in IF, 31 in YF, 60 in SC, and 45 events in IP (Table 2-4). The Dunn's test (Figure 2-4a) shows that the Q_t/P_{ev} metrics were significantly different between micro-catchments. In Table 2-4, it can be observed that the mean Q_t/P_{ev} is higher in IP followed by MF, SC, YF and IF. For IP and MF, values of Q_t/P_{ev} were not statistically different, nor were the responses from IF, YF and SC (alphabet groups in Figure 2-4a). Using the more robust ANCOVA test, the $Q_t - P_{ev}$ regressions were significantly different among all land uses (Table 2-4). Thus, the linear models presented in Figure 2-4e had different slopes and intercepts compared to MF, which was used as a control against the other human-modified landscapes (Equation 1). YF and IF presented moderate slopes which translates to less response towards storm magnitude, while MF and IP had steeper slopes.

The Q_{qf}/P_{ev} ratios were significantly different among land uses (Figure 2-4b). IP presented the highest mean Q_{qf}/P_{ev} followed by SC, YF, MF, and IF (Table 2-4). The Q_{qf} - P_{ev} regressions have significantly different slopes and intercepts (Table 2-5, Figure 2-4f). This analysis distinguished two main groups: IP, SC and MF, which have similar and flashier responses; versus IF and YF, which were statistically different and less flashy than MF. The Q_{bf}/P_{ev} metric is also different across micro-catchments (Table 2-4). Figure 2-4c distinguishes two main groups, IP and MF, with a higher Q_{bf}/P_{ev}, while IF, YF and SC had lower response. This finding is associated with the higher elevation and higher rainfall in MF and IP. The slope of the Q_{bf} - P_{ev} regression lines (Figure 2-4g and Table 2-5) is steeper in MF compared to the rest of the sites.

The mean 24-hour antecedent precipitation (AP) ranged between 4.55 to 11.75 mm (Table 2-4) and exhibited a weak correlation ($r < 0.15$) with the storm parameters (Q_t,

Q_{peak}, Q_{qf}, Q_{bf}). We considered the Q_{qf}/Q_t and Q_{bf}/Q_t (Table 2-4), because these are normalized by total streamflow. Average baseflow (Q_{qf}/Q_t) at the storm event scale was higher in the MF (81%), closely followed by IF (77%). In the SC, YF, and IP micro-catchments, the baseflow component was lower (70%, 67%, and 66%, respectively). These indices relate well with the recession constant *k* (Table 2-3), where IF and MF had higher values, while IP and YF exhibited lower results.

Peak flow (Q_{peak}) also differs significantly between micro-catchments, where IP is significantly different from the other micro-catchments (Figure 2-4d). IP also differs significantly in its peak flow interaction with rainfall. Table 2-5 and Figure 2-4h show that this micro-catchment had a five-fold larger peak flow to rainfall ratio, compared to MF. The rest of the micro-catchments had smaller values of intercepts and slopes compared to MF. These linear regression models exhibited the highest adjusted R^2 (0.78, Table 2-5). Time to peak (T_p) and lag time (T_L) presented a similar pattern of responses (Table 2-4) where IF had the largest T_p and T_L, followed by YF, IP, MF, and SC.

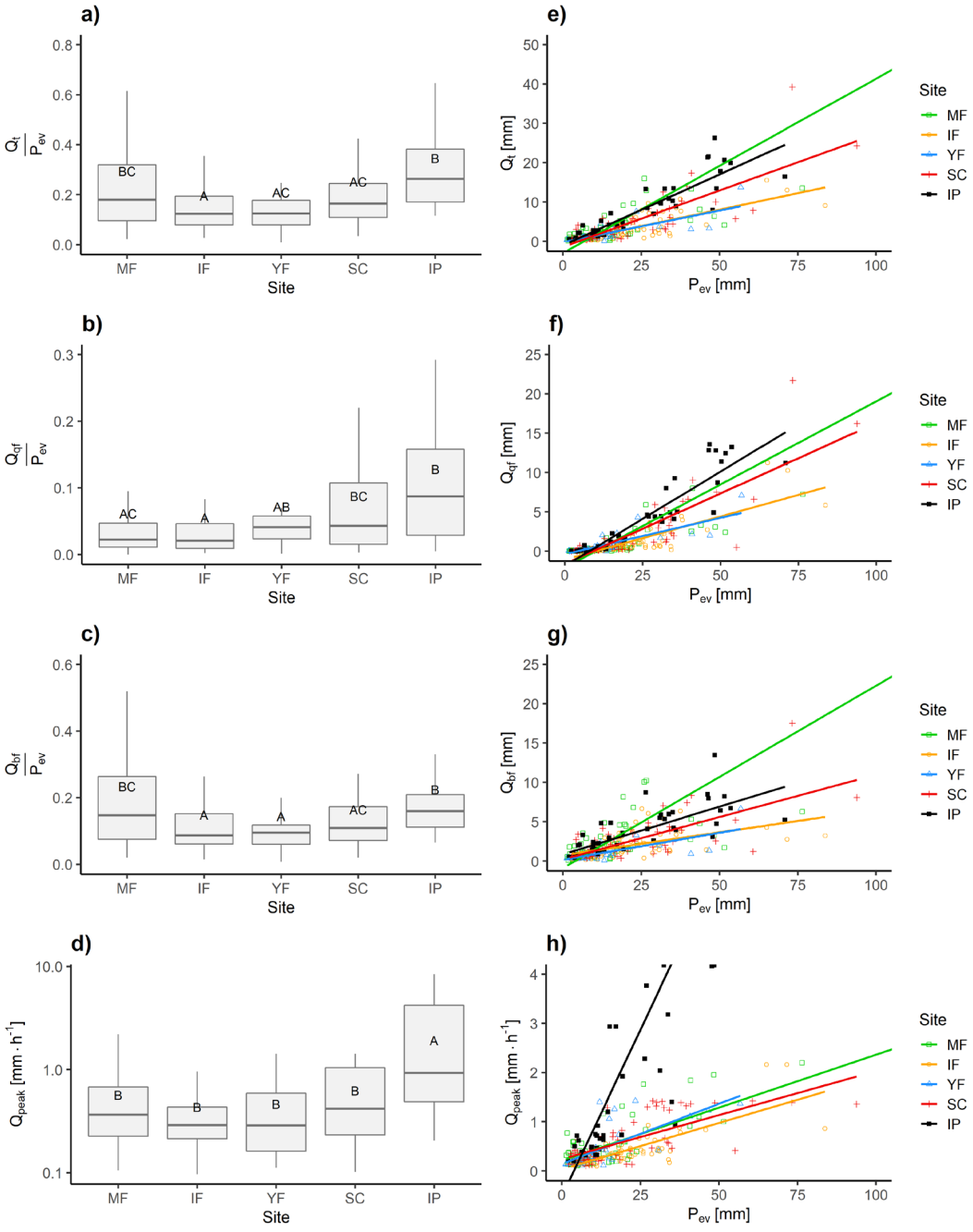

Figure 2-4: Differences in hydrological variables (left, Dunn's test; right, multiple regression) between the micro-catchments. Dunn´s test results are displayed in left box and whisker plots supplemented by alphabet groupings. Mature forest (MF), intermediate forest (IF), young forest (YF), shade coffee (SC), and intensive pasture (IP).

Table 2-4: Summary of rainfall and storm runoff characteristics (mean ± standard deviation) for the five study micro-catchments. Mature forest (MF), intermediate forest (IF), young forest (YF), shade coffee (SC), and intensive pasture (IP).

	MF	**IF**	**YF**	**SC**	**IP**
n	51	79	31	60	45
AP	10.6 ± 14.12	7.8 ± 11.68	4.55 ± 6.85	8.05 ± 10.92	11.75 ± 16.97
Q_t/P_{ev}	0.25 ± 0.19	0.14 ± 0.08	0.15 ± 0.1	0.21 ± 0.15	0.29 ± 0.13
Q_{qf}/P_{ev}	0.05 ± 0.06	0.03 ± 0.04	0.05 ± 0.04	0.07 ± 0.06	0.11 ± 0.09
Q_{bf}/P_{ev}	0.2 ± 0.17	0.11 ± 0.06	0.1 ± 0.07	0.14 ± 0.12	0.18 ± 0.1
Q_{peak} [mm h^{-1}]	0.59 ± 0.56	0.4 ± 0.36	0.49 ± 0.45	0.62 ± 0.46	2.66 ± 2.79
Q_{qf}/Q_t	0.19 ± 0.16	0.23 ± 0.17	0.33 ± 0.18	0.3 ± 0.21	0.34 ± 0.22
Q_{bf}/Q_t	0.81 ± 0.16	0.77 ± 0.17	0.67 ± 0.18	0.7 ± 0.21	0.66 ± 0.22
T_p [h]	2.98 ± 3.13	4.35 ± 3.83	3.62 ± 1.87	2.85 ± 2.49	3.56 ± 1.95
T_L [h]	1.17 ± 1.29	2.24 ± 3.16	2.2 ± 1.51	0.93 ± 1.09	1.98 ± 0.94

Table 2-5: Coefficients of intercept (I) and slope (S), F-value, p-value and adjusted r-squared (R_a^2) for ANCOVA regressions of hydrologic metrics against land use. **Bold** indicates statistical significance ($\alpha = 0.05$). Mature forest (MF), intermediate forest (IF), young forest (YF), shade coffee (SC), and intensive pasture (IP).

Y	MF		IF		YF		SC		IP		F-value	p-value	R_a^2
	α_0	β_0	α_1	β_1	α_2	β_2	α_3	β_3	α_4	β_4			
	I	S	I	S	I	S	I	S	I	S			
Q_t	-2.92	0.44	**-0.29**	**0.17**	**-0.18**	**0.16**	-1.37	**0.29**	-0.98	0.36	67.5	<0.05	0.69
Q_{qf}	-2.06	0.21	**-1.06**	**0.11**	**-0.36**	**0.09**	-1.60	0.18	-1.86	0.24	89.3	<0.05	0.75
Q_{bf}	-0.87	0.23	**0.77**	**0.06**	0.18	**0.07**	0.23	**0.11**	**0.89**	**0.12**	39.6	<0.05	0.57
Q_{peak}	0.21	0.02	0.03	0.02	0.15	0.02	0.24	0.02	**-0.52**	**0.14**	106.7	<0.05	0.78

2.5 Discussion

2.5.1 How does age of forest recovery affect streamflow?

The vegetation properties were similar for the three forested micro-catchments in terms of LAI (Table 2-1), tree height, and dominant species; yet, important differences were observed in the streamflow at daily and event scales. At the daily scale, the MF and IF presented similar responses characterized by lower variability in their daily flows, higher water storage capacity (high recession constants), and higher *MALF*, compared to that of the YF (Table 2-3). Figure 2-3a shows that, during the dry season (flow exceeded more 75% of the time), the IF had a streamflow closer to that of MF. These results correlate well with the soil infiltration capacity, where, MF and IF show a similar and higher K_{fs}, compared to the YF. Thus, our results suggest that daily scale hydrologic regime of the IF more closely resembles that of MF than that of a YF. However, the YF micro-catchment also had the lowest annual rainfall inputs and the highest rainfall variability (PVAR and DAYP0), in addition to a greater land cover heterogeneity (Figure 2-1), which may have obscured the response of this land cover. While MF and IF have dominant land covers in their respective micro-catchments (100% and 77% respectively), the YF covers only 68% of the area and the rest of the micro-catchment is covered by more developed land. It has been shown in other studies that 20% or less forest removal may cause substantial effects on peak flow and water yield (Bosch & Hewlett, 1982, Schueler et al., 2009; Evaristo & McDonnell, 2019). However, the mean annual low flow (Table 2-3) for YF is similar to the results reported by Muñoz-Villers and McDonnell (2013) for a 20 yr-old regenerating forest in a neighboring micro-catchment (0.21 mm day^{-1}), while the mean annual high flow estimates (Table 2-3) were significantly smaller compared to the same study (32 mm day^{-1}).

YF and IF showed a lower Q_t/P_{ev} (Table 2-4) which is associated with lower AP over the analyzed events; although, this result can also be influenced by the high K_{fs} of IF. In terms of baseflow normalized by total runoff Q_{bf}/Q_t, all three forested micro-catchments have a high baseflow percentage (Table 2-4): MF (81%), IF (78%), and YF (67%). This metric is positively correlated with the percent of forest cover. Similar results of high baseflow dominance during storms were previously reported in this region for an old-growth TMCF by stable isotope-based experiments (Table 2-3 from Muñoz-Villers & McDonnell, 2012), where groundwater dominated up to 90% of the storm runoff during the wet season. In terms of quick flow and total runoff responses to rainfall, YF and IF were less responsive to storm magnitude compared to MF (Figure 2-4e and Figure 2-4g). The steeper slope of the MF (Figure 2-4g) may support the hypotheses of higher baseflow contribution to the hydrograph during storm events. Similar effects were previously reported for an old-growth TMCF, a 20-yr old TMCF, and a pasture micro-catchment (Muñoz-Villers & McDonnell, 2013). The peak flow response to rainfall was very similar for the three forested micro-catchments (Table 2-5, Figure 2-4d). These results indicate that the three forests present a similar capacity to attenuate peak flows. Our work supports the hypothesis that the secondary forests contribute to restore the hydrologic

responses to pre-disturbance conditions. Nonetheless, uncertainty remains to confirm this hypothesis, since the micro-catchments were not entirely, nor equally, dominated by the studied forests, as indicated earlier.

We were not able to completely answer the question of whether forest age impacts hydrology, in terms of baseflow maintenance and peak flow, because differences in slope, elevation and percent of forest cover among the three micro-catchments may have influenced our results. For instance, the MF micro-catchment has a steeper mean slope than that of IF and YF, being 6° and 12° greater, respectively. Steep slopes have been associated with higher quickflow, and lower lag time and time to peak responses (Mu et al., 2015; Nainar, 2018), as observed in our study (Figure 2-4e-f and Table 2-4). On the other hand, steeper slopes have also been linked with higher water storage capacity (Karlsen, 2010; Gabrielli & McDonnell, 2011; Sayama et al., 2011; Uchida et al., 2008). Thus, the steeper slope of MF may explain its higher contribution from baseflow and its high runoff ratio (0.67). Additionally, the higher mean elevation of MF (1756 m a.s.l.), compared to that of IF (1604 m a.s.l.) and YF (1453 m a.s.l.) correlates with its higher RR. An additional source of uncertainty is the use of the constant slope hydrograph separation method; nonetheless, this type of method is commonly used for catchment comparisons; a major drawback is the lack of standard hydrograph separation techniques (Blume et al., 2007). The use of normalized metrics (by area, slope, precipitation and streamflow) is expected to minimize the effects of these confounding parameters.

Our findings strongly support that 20 and 40 years of natural forest regeneration are sufficient to restore large part of the hydrology on micro-catchments previously occupied by intensive pastureland and annual crops (local inhabitants' communication). These results suggest that, despite the commonly accepted notion that these forests have high ET rates, both young and mature forests can provide important hydrological services, such as dry-season baseflow sustenance and modulation of peak flow, due to the higher infiltration rates and water storage capacities.

2.5.2 What are the effects of TMCF conversion to shaded coffee on streamflow?

At the daily scale, SC had a lower mean streamflow and lower runoff ratio, despite having similar rainfall inputs compared to MF. In the dry season, SC also showed a slightly lower mean annual low flow (MALF), and a lower recession constant (k) (Table 2-3). A significantly lower RR and MALF was expected in SC, because this micro-catchment is located at a lower elevation (472 m difference), which promotes a higher evapotranspiration (ET) (Ramirez et al., 2017), while ET in the MF is likely to be energy-limited. ET rates are lower at higher elevations, mainly due to lower atmospheric demand driven by lower temperatures and higher relative humidity, which reduces water losses from ET and increases runoff amounts (Saenz et al., 2014; Ramirez et al., 2017). Additionally, the soil evaporation (E_s) in a shaded coffee farm may account for around 13% of the total ET (Holwerda & Meesters, 2019), while the dense canopy (see LAI, Table 2-1) in MF can minimize E_s (Levia et al., 2011). Although SC has lower LAI

(Table 2-1), resulting in lower interception (approximately 10% to 15% ET) compared to MF (Holwerda et al., 2010; Holwerda et al., 2013; Ponette-González et al., 2010), its increased soil evaporation due to more open, unvegetated area can offset the higher interception, resulting in higher ET and lower streamflow. SC had a significantly lower RR than MF, as expected, but it also exhibited a relatively higher MALF and *k*, when compared to the other studied land covers (Table 2-3) and with previous studies (Muñoz-Villers & McDonnell, 2013), regardless of the expected higher ET described earlier. This suggests that SC may preserve a large part of its original capacity to sustain baseflow during the dry season, associated with its higher soil infiltration capacity when compared to IP (Table 2-1).

At the event scale, the Dunn's test indicated that the hydrologic response of SC in terms of total runoff, quickflow, baseflow and peak flow were not statistically different (alphabet grouping Figure 2-4a-d) compared to the MF. The metric normalized by streamflow (Q_{bf}/Q_t) also suggested that SC has larger dominance of baseflow compared to YF and IP (Table 2-4). Finally, the ANCOVA analysis showed that the quick flow and peak flow responses were not significantly different between SC and MF (Table 2-5). These findings indicate that the SC micro-catchment has a similar capacity to modulate peak flow compared to that of MF. However, the average time to peak and lag time responses of the SC were the lowest (Table 2-4), suggesting a faster response, even though this micro-catchment has the largest area of the studied sites (Table 2-1), and larger areas are normally associated with longer T_p and T_L (Wurbs & Wesley, 2002.). We attribute this result to the fact that SC has an intermediate soil infiltration capacity (48 mm h^{-1}) and the highest soil bulk density (Table 2-1). This is likely associated with management practices such as the continuous removal of herbaceous groundcover (Martínez et al., 2009). Our results agree with previous research conducted in the study region which suggested that shade coffee soils had higher bulk density and lower soil porosity than forest soils, in addition to intermediate saturated hydraulic conductivities (Geissert & Ibáñez, 2008; Marin-Castro et al., 2016). Our study supports the hypothesis that shade coffee preserves a large part of the pre-disturbance capacity to sustain baseflow and modulate peak flow, despite the differences in elevation and slopes that may have affected our results.

2.5.3 What are the effects of TMCF conversion to intensive pasture management on streamflow?

The mean daily streamflow and runoff ratio was slightly higher in IP in comparison to the MF. Additionally, IP showed lower water storage capacities to sustain low flows during the dry season (see *k* in Table 2-3). The IP also presented a higher variability on its streamflow regime and the steepest SFDC of all the studied micro-catchments. This result was further verified by the higher MAHF in IP (Table 2-3). Both results are consistent with IP's lower infiltration capacity (K_{fs} = 26 mm h^{-1}), which is less than a quarter of the benchmark value in MF (K_{fs} = 125 mm h^{-1}). These findings also agree with previous research indicating decreased infiltration capacity after forest removal and grazing, triggering an increase in surface runoff (Bruijnzeel, 1988; Ogden, 2013). Additionally,

the reduced soil infiltration may have diminished the micro-catchment's capacity to recharge and store water, causing a lower MALF. Finally, the IP and MF presented a higher RR compared to the rest of the sites; the RR in MF is also higher in comparison to the existing literature (Evaristo & McDonnell, 2019; Hibbert, 1969; Muñoz-Villers et al., 2015). MF and IP are both located at higher elevations receiving greater annual inputs of rainfall (Table 2-1). ET rates are lower at higher elevations, as described in previous paragraphs. Additionally, forested landscapes have higher interception (Holwerda et al., 2010) that may increase ET; this can explain the higher RR observed IP compared to MF. On the other hand, forests have also been linked with higher runoff coefficients attributable to the higher percent of stemflow around the tree base (Levia & Germer, 2015).

At the event scale, the total rainfall - runoff regression line for MF had a slightly steeper slope than the IP regression (Figure 2-4e); although, these differences were not statistically significant (Figure 2-4a). The IP exhibited a statistically steeper slope for the rainfall - quick flow relationship (Figure 2-4b), while in MF baseflow was more dominant over the analyzed storms Q_{bf}/Q_t (81% in MF, versus 66% in IP). In forested areas, stemflow is higher and may promote locally concentrated input of water causing a rapid recharge of groundwater by preferential flow mechanisms through macropores and roots (Levia et al., 2011). When assessing the rainfall - peak flow relationships (Figure 2-4h), the IP had a statistically different and flashier response (Table 2-4 and Table 2-5). These results agree with previous studies (Bruijnzeel, 1988; Muñoz-Villers & McDonnell, 2013; Ogden, 2013), which found that peak flow may increase in pasture due to reduced soil infiltration capacity (K_{fs}) and its higher soil bulk density (Table 2-1).

The volcanic soils in the region are known to have high water storage capacities (Campos et al., 2001; Dubroeucq et al., 2002). Previous research in the study area reported that 50 years of cropping caused a moderate reduction of soil structural stability followed by a reduction of water retention at field capacity and permanent wilting point, with potentially negative implications on soil hydrologic response (Meza-Pérez & Geissert-Kientz, 2006). The micro-catchment that has undergone 40 years of intense pasture management indicate inferior soil hydraulic properties, reduced baseflow sustenance, and increase in peak flow by up to five times compared to the MF.

2.6 Conclusions

Daily streamflow regimes of an intermediate age forest closely resembled a mature forest; however, storm runoff event responses across the three forested micro-catchments were not statistically different. Our results support the hypothesis that older forests are associated with better soil conditions, particularly higher soil infiltration capacity and thus greater recharge of subsurface water storages.

Despite the potential changes in the water and energy balance due to forest conversion to shade coffee alternatives, the capacity to sustain baseflow in a shaded coffee dominated micro-catchment was largely preserved, relative to the forested micro-catchments. The

shaded coffee cultivation also preserved the soil capacity to modulate peak flows during storms.

The pasture-dominated micro-catchment showed a lower baseflow compared to the mature forest, and a fivefold greater peak flow response, despite similar rainfall rates. In the pasture-dominated site, 40 years of intense pasture management has deteriorated the hydraulic properties of the underlying volcanic soils, mainly in terms of reduced infiltration capacity.

The major implications of our findings for managers of payments for watershed services and other programs promoting conservation of hydrologic services are: 1) shade coffee may provide similar hydrologic services to forests in these types of programs, but more work on coffee farms with different management practices is needed to support this hypothesis; 2) higher conservation priority should be given to mature and older regenerating TMCF, particularly those located at higher elevations; and 3) conversion to pasture should be avoided, and best management practices such as rotational ranching should be promoted in the existing pasture land to minimize the deterioration of soil hydraulic properties. More research is needed to better understand the energy and mass dynamics on regenerating TMCF across a wider range of elevations and forest ages.

2.7 References

Aldrich, M., Billington, C., Edwards, M., & Laidlaw, R. (1997). A Global Directory of Tropical Montane Cloud Forests. UNEP-World Conservation Monitoring Centre: Cambridge, UK. https://www.unep-wcmc.org/resources-and-data/tropical-montane-cloud-forest-sites

Archer, J. R., & Smith, P. D. (1972). The relation between bulk density, available water capacity, and air capacity of soils. *Journal of Soil Science*, *December 1972, Vol.23*(4), pp. 475-480. https://doi.org/10.1111/j.1365-2389.1972.tb01678.x

ASTM D5242-92 (2013). Standard Test Method for Open-Channel Flow Measurement of Water with Thin-Plate Weirs, ASTM International, West Conshohocken, PA, 2013, www.astm.org

Baumer, B. S., Kaplan, D. T., & Horton, N. J. (2017). *Modern Data Science with R*. Ebook, CRC Press Taylor & Francis Group. https://mdsr-book.github.io/

Bjørn, L. (2001). *The Skeptical Environmentalist: Measuring the Real State of the World*. Cambridge University Press, UK, ISBN 0 521 01068 3 (pb.)

Blume, T., Zehe, E., & Bronstert, A. (2007). Rainfall—runoff response, event-based runoff coefficients and hydrograph separation. *Hydrological Sciences Journal, 52:5*, pp. 843-862. DOI: https://doi.org/10.1623/hysj.52.5.843

Bosch, J. M., & Hewlett, J. D. (1982). A review of catchment experiments to determine the effect of vegetation changes on water yield and evapotranspiration. *Journal of Hydrology*, *55*(1982) pp. 3-23.

Bonell, M., & Bruijnzeel, L. A. (2005). *Forests, Water and People in the Humid Tropics: Past, Present, and Future Hydrological Research for Integrated Land and Water Management*. Cambridge University Press, UK, ISBN 0 521 82953 4

Brauman, K. A., Daily, G. C., Duarte, T. K., Mooney, H. A. (2007). The nature and value of ecosystem services: an overview highlighting hydrologic services. *The Annual Review of Environment and Resources, 32* (2007), pp. 67-98. Doi:10.1146/annurev.energy.32.031306.102758

Brown, A. E., Zhang, L., McMahon, T. A., Western, A. W., & Vertessy, R. A. (2005). The review of paired catchments studies for determining changes in water yield resulting from alterations in vegetation. *Journal of Hydrology*, 310 (2005), 28–61. doi:10.1016/j.jhydrol.2004.12.010

Bruijnzeel, L. A. (2004). Hydrological functions of tropical forests: not seeing the soil for the trees?. *Agriculture, Ecosystems and Environment 104* (2004), pp. 185–228. doi:10.1016/j.agee.2004.01.015

Bruijnzeel, L. A., Burkard, R., Carvajal, A., Frumau, A., Köhler, L., Mulligan, M.,…, & Tobón, C. (2006). Hydrological impacts of converting tropical montane cloud forest to pasture, with initial reference to northern Costa Rica. Final Technical Project, January 31, 2006. https://www.researchgate.net/publication/233758018

Bruijnzeel, L. A., Mulligan, M., & Scatena, F. S. (2011). Hydrometeorology of tropical montane cloud forests: emerging patterns. *Hydrological Processes. 25* (3), pp. 465–498. DOI: 10.1002/hyp.7974

Campos, C. A., Oleschko, K., Cruz, H. L., Etchevers, D. B. J., & Hidalgo, M. C. (2001). Estimation of Allophane and its Relationship with Other Chemical Parameters in Mountain Andisols of the Volcano Cofre de Perote, *Terra, Vol. 19*, No. 2, 2001. https://chapingo.mx/terra/contenido/19/2/art105-116.pdf

Campos, C. A. (2010). Response of soil inorganic nitrogen to land use and topographic position in the Cofre de Perote Volcano (Mexico). *Environmental Management (2010),* pp. *46*: 213. https://doi.org/10.1007/s00267-010-9517-z

Chapman, T. (1999). A comparison of algorithms for stream flow recession and baseflow separation. *Hydrological Processes, 13*, pp. 701–714, 1999.

CONANP, CONAFOR, INECC y FMCN- Proyecto C6 cuencas costeras (2015). “Mapa de uso de suelo y vegetación 2014 en la cuenca del río la Antigua” a partir de los

productos elaborados por Brockmann Consult con apoyo de GeoVille y financiados por el programa EOWorld de la Agencia Espacial Europea-Banco Mundial.

De Beenhouwer, M., Aerts, R., & Honnay, O. (2013). A global meta-analysis of the biodiversity and ecosystem service benefits of coffee and cacao agroforestry. *Agriculture, Ecosystems and Environment. 175*, pp. 1–7. http://dx.doi.org/10.1016/j.agee.2013.05.003.

Dubroeucq, D., Geissert, D., Barois, I., & Ledru, M. P. (2002). Biological and mineralogical features of Andisols in the Mexican volcanic highlands. *Catena, 49*(3), pp. 183–202. https://doi.org/10.1016/S0341-8162(02)00043-7

Dunn, O. J. (1961). Multiple comparisons among means. *Journal of the American Statistical Association*. *56* (203), pp. 52-64.

http://www.jstor.org/stable/2282330

Evaristo, J. & McDonnell, J. J. (2019). Global analysis of streamflow response to forest management. *Nature, vol 570*, 455. https://doi.org/10.1038/s41586-019-1306-0

Elrick, D. E., Reynolds, W. D., & Tan, K. A. (1989). Hydraulic Conductivity Measurements in the Unsaturated Zone Using Improved Well Analyses. *Groundwater Monitoring & Remediation, 9*(3), pp. 184–193. https://doi.org/10.1111/j.1745-6592.1989.tb01162.x

Fahey, T. J., Sherman, R. E., & Tanner, E. V. J. (2015). Tropical montane cloud forest: environmental drivers of vegetation structure and ecosystem function. *Journal of Tropical Ecology*, pp.1 -13, Available on CJO 2015 doi:10.1017/S0266467415000176

FAO-UNESCO (2007). Digitized Soil Map of the World, at 1:5.000.000 scale. FAO-UN - Land and Water Division. http://www.fao.org/geonetwork/srv/en/main.home?uuid=446ed430-8383-11db-b9b2-000d939bc5d8

Foley, J. A., DeFries, R., Asner, G. P., Barford, C., Bonan, G., Carpenter, S. R.,…, & Snyder, P. K. (2005). Global Consequences of Land Use, *Science, 22*, pp. 570–574, 2005. DOI:10.1126/science.1111772

Gabrielli, C. P., & McDonnell, J. J. (2011). An inexpensive and portable drill rig for bedrock groundwater studies in headwater catchments. *Hydrological Processes. 26*, pp. 622 – 632 (2011). DOI:10.1002/hyp.8212

García-Franco, J. G., Castillo-Campos, G., Mehltreter, K., Martínez, M. L., & Vázquez, G. (2008). Composición florística de un bosque mesófilo del centro de Veracruz, México, *Boletín de la Sociedad Botánica de México, 83*, pp. 37–52, 2008.

Garcia, E. (2004). *Modificaciones al sistema de clasificación climática de Köppen (5th ed.)*. México, D. F., Instituto de Geografía UNAM, Núm.6, 90 pp., ISBN 970-32-1010-4. http://www.igeograf.unam.mx/sigg/utilidades/docs/pdfs/publicaciones/geo_siglo21/serie_lib/modific_al_sis.pdf

Geissert, D., & Ibáñez, A. (2008). *Agroecosistemas cafetaleros de Veracruz: biodiversidad, manejo y conservación.* México D.F., Instituto de Ecología A.C. (INECOL) e Instituto Nacional de Ecología (INE-SEMARNAT), pp. 213–221. ISBN 970-709-112-6.

Hewlett, J.D., & Hibbert, A.R. (1967). Factors Affecting the Response of Small Watersheds to Precipitation in Humid Areas. *International Symposium on Forest Hydrology, Pergamon, Pennsylvania State University*, New York, pp. 275-290.

Hibbert, A. R. (1969). Water Yield Changes after Converting a Forested Catchment to Grass. *Water Resources Research, Vol. 5*, Issue3, June 1969, pp. 634-640. https://doi.org/10.1029/WR005i003p00634

Holwerda, F., Bruijnzeel, L. A., Muñoz-Villers, L. E., Equihua, M., & Asbjornsen, H. (2010). Rainfall and cloud water interception in mature and secondary lower montane cloud forests of central Veracruz, Mexico. *Journal of Hydrology, 384*, pp. 84–96, 2010. doi:10.1016/j.jhydrol.2010.01.012

Holwerda, F., Bruijnzeel, L. A., Barradas, V. L., Cervantes J. (2013). The water and energy exchange of a shaded coffee plantation in the lower montane cloud forest zone of central Veracruz, Mexico. *Agricultural and Forest Meteorology, 173*, pp. 1– 13, 2013. http://dx.doi.org/10.1016/j.agrformet.2012.12.015

Holwerda, F., & Meesters, A. G. C. A. (2019). Soil evaporation in a shaded coffee plantation derived from eddy covariance measurements. *Journal of Geophysical Research: Biogeosciences, 124*, pp. 1472–1490. https://doi.org/10.1029/2018JG004911

ICO (2010). Employment Generated by the Coffee Sector. London: International Coffee Organization. *www.ico.org/documents/icc-105-5e-employment.pdf*

INEGI (2013). Continuo de Elevaciones Mexicano (CEM). Instituto Nacional de Estadística, Geografía e Informática, México. http://www.beta.inegi.org.mx/app/geo2/elevacionesmex/index.jsp

IPCC (2018). Summary for Policymakers. In: Global warming of 1.5°C. An IPCC Special Report on the impacts of global warming of 1.5°C above pre-industrial levels and related global greenhouse gas emission pathways, in the context of strengthening the global response to the threat of climate change, sustainable development, and efforts to eradicate poverty [V. Masson-Delmotte, P. Zhai, H. O. Pörtner, D. Roberts, J. Skea, P. R. Shukla, A. Pirani, W. Moufouma-Okia, C. Péan, R. Pidcock, S. Connors, J. B. R.

Matthews, Y. Chen, X. Zhou, M. I. Gomis, E. Lonnoy, T. Maycock, M. Tignor, T. Waterfield (eds.)]. World Meteorological Organization, Geneva, Switzerland, 32 pp.

Jenness, J. S. (2004). Calculating landscape surface area from digital elevation models. *Wildlife Society Bulletin 2004, 32*(3): pp. 829–839. https://pdfs.semanticscholar.org/50b3/81cae049f3d04068cbfb47adad74d5a44fa5.pdf

Karlsen, R. (2010). Stormflow processes in a mature tropical montane cloud forest catchment, Coatepec, Veracruz, Mexico. MSc. thesis, VU Univ., Amsterdam, Netherlands, 110 pp.

Kienzle, S. W. (2010). Effects of area under-estimations of sloped mountain terrain on simulated hydrological behavior: a case study using the ACRU model. *Hydrological Processes*, Wiley Online Library. DOI: 10.1002/hyp.7886

Lewis, S. L., Wheeler, C. E., Mitchard, E. T. A., & Koch A. (2019). Restoring natural forests is the best way to remove atmospheric carbon. *Nature 568*, pp. 25-28 (2019). doi: 10.1038/d41586-019-01026-8

Levia, D.F, Carlyle-Moses, D., & Tanaka, T. (2011). Forest hydrology and Biogeochemistry, Synthesis of Past and Future Directions. Springer Dordrecht Heidelberg London New York, USA, e-ISBN 978-94-007-1363-5.

Levia, D. F., & Germer S. (2015). A review of stemflow generation dynamics and stemflow-environment interactions in forests and shrublands. *Reviews of Geophysics 53*, pp. 673–714. doi:10.1002/2015RG000479.

LI-COR 2019. LAI-2200C Plant Canopy Analyzer Instruction Manual. Copyright©2013–2019, LI-COR, Inc., Publication Number:984-14112. https://licor.app.boxenterprise.net/s/fqjn5mlu8c1a7zir5qel

Marín-Castro, B. E., Geissert, D., Negrete-Yankelevich, S., & Gómez-Tagle, C. A. (2016). Spatial distribution of hydraulic conductivity in soils of secondary tropical montane cloud forests and shade coffee agroecosystems. *Elsevier Geoderma 283* (2016) pp. 57–67. http://dx.doi.org/10.1016/j.geoderma.2016.08.002

Martínez, M. L., Pérez-Maqueo, O., Vázquez, G. A, Castillo-Campos, G., García-Franco, J., Mehltreter,…, & Landgrave, R. (2009). Effects of land use change on biodiversity and ecosystem services in tropical montane cloud forests of Mexico. *Forest Ecology and Management 258* (2009), pp. 1856–1863. doi:10.1016/j.foreco.2009.02.023

Meza-Pérez, E., & Geissert, D. (2006). Estabilidad de estructura en andisoles de uso forestal y cultivados. *Terra Latinoamericana, vol. 24*, núm. 2, pp. 163-170. http://www.redalyc.org/articulo.oa?id=57311108002

Moore, D. (2005). Slug injection using salt in solution. *Streamline watershed Management Bulletin Vol. 8*, No. 2, printed in Canada, ISSN 1705-5989.

Mosley, M. P. (1979). Streamflow Generation in a Forested Watershed, New Zealand, *Water Resources Research, Vol. 15*, No. 4, pp. 795-806, August 1979.

Mu, W., Yu, F., Li, C., Xie, Y., Tian, J., Liu, J., & Zhao, N. (2015). Effects of rainfall intensity and slope gradient on runoff and soil moisture content on different growing stages of spring maize. *Water 7*, pp. 2990–3008. https://doi.org/10.3390/w7062990

Muñoz-Villers, L. E., Holwerda, F., Gómez-Cárdenas, M., Equihua, M., Asbjornsen, H., Bruijnzeel, L. A.,…, & Tobón, C. (2011). Water balances of old-growth and regenerating montane cloud forests in central Veracruz, Mexico. *Journal of Hydrology* 462–463 (2012), pp. 53–66. doi:10.1016/j.jhydrol.2011.01.062

Muñoz-Villers, L. E., & McDonnell, J. J. (2012). Runoff generation in a steep, tropical montane cloud forest catchment on permeable volcanic substrate. *Water Resources Research, 48*, W09528, doi:10.1029/2011WR011316.

Muñoz-Villers, L. E. & McDonnell, J. J. (2013). Land use change effects on runoff generation in a humid tropical montane cloud forest region. *Hydrology and Earth System Sciences, 17*, pp. 3543–3560, 2013. doi:10.5194/hess-17-3543-2013

Muñoz-Villers, L. E., Holwerda, F., Alvarado-Barrientos, M. S., Geissert, D., Marín-Castro, B., Gómez-Tagle, A.,…, & Bruijnzeel, L. A. (2015). Hydrological effects of cloud forest conversion in central Veracruz, Mexico. *Bosque, vol. 36*, num. 3, 2015, pp. 395-407. DOI: 10.4067/S0717-92002015000300007

Muñoz-Villers, L. E., Geissert, D. R., Holwerda, F., & McDonnell J. J. (2016). Factors influencing stream baseflow transit times in tropical montane watersheds. *Hydrology and Earth System Sciences, 20*, pp. 1621–1635, 2016. doi:10.5194/hess-20-1621-2016

Muñoz-Villers, L. E., Geris, J., Alvarado-Barrientos, S., Holwerda, F., & Dawson, T. E. (2019). Coffee and shade trees show complementary use of soil water in a traditional agroforestry ecosystem, *Hydrology and Earth System Sciences. Discuss*., https://doi.org/10.5194/hess-2019-329, in review.

Murphy, S. F., & Stallard, R. F. (2012). Water quality and landscape processes of four watersheds in eastern Puerto Rico. *U.S. Geological Survey Professional Paper* 1789, 292 pp.

Nainar, A., Tanaka, N., Bidin, K., Annammala, K. V., Ewers, R. M., Reynolds, G., & Walsh, R.P.D. (2018). Hydrological Dynamics of Tropical Streams on a Gradient of Land-use Disturbance and Recovery: A Multi-Catchment Experiment, *Journal of Hydrology (2018)*. doi: https://doi.org/10.1016/j.jhydrol.2018.09.022

Nanzyo, M. (2002). Unique properties of volcanic ash soils. Consulted online: https://pdfs.semanticscholar.org/8efa/44e080456ab71dbb6ea168802f88f364feae.pdf

Navarrete, D. (2016). Conversion from Forests to Pastures in the Colombian Amazon Leads to Contrasting Soil Carbon Dynamics Depending on Land Management Practices. *Global Change Biology 22*.10 (2016), pp. 3503–3517. doi: 10.1111/gcb.13266

Ochoa-Tocachi, B. F., Buytaert, W., De Bièvre, B., Célleri, R., Crespo, P., Villacís, M.,…, & Arias, S. (2016). Impacts of land use on the hydrological response of tropical Andean catchments. *Hydrological Processes. 30*, pp. 4074–4089. https://doi.org/10.1002/hyp.10980

Ogden, F. L., Crouch, T. D., Stallard, R. F., & Hall J. S. (2013). Effect of land cover and use on dry season river runoff, runoff efficiency, and peak storm runoff in the seasonal tropics of Central Panama. *Water Resources Research, 49*, pp. 8443–8462. doi:10.1002/2013WR013956

Paré, L., & Gerez, P. (2012). *Al filo del agua: Cogestión de la subcuenca del río Pixquiac, Veracruz* (1st ed.). Delegación Tlalpan, México, D.F., INE-Semarnat, ISBN 978-607-7908-89-0.

Pérez-Pérez, H., & Muñoz-Villers L. E. (2016). Impacto del cambio en el uso del suelo en la conductividad hidráulica del suelo y sus implicaciones hidrológicas (Centro de Veracruz México). IV Congreso Nacional de Manejo de Cuencas Hidrográficas.

Ponette-González, A. G., Weathers, K. C., & Curran, L. M. (2010). Water inputs across a tropical montane landscape in Veracruz, Mexico: synergistic effects of land cover, rain and fog seasonality, and interannual precipitation variability. *Global Change Biology, 16*: pp. 946-963. doi:10.1111/j.1365-2486.2009.01985.x

Price, K., Jackson, C. R., Parker, A. J., Reitan, T., Dowd, J., & Cyterski M. (2011). Effects of watershed land use and geomorphology on stream low flows during severe drought conditions in the southern Blue Ridge Mountains, Georgia and North Carolina, United States. *Water Resources Research, 47*, W02516. doi:10.1029/2010WR009340

Ramírez, B. H., Teuling, A. J, Ganzeveld, L., Hegger, Z., Leemans, R. (2017). Tropical Montane Cloud Forests: Hydrometeorological variability in three neighboring catchments with different forest cover. *Journal of Hydrology 552*, pp. 151–167. http://dx.doi.org/10.1016/j.jhydrol.2017.06.023

Richardson, V. A., & Peres, C. A. (2016). Temporal decay in timber species composition and value in Amazonian logging concessions. *PLoSOne 11*, e0159035. https://doi.org/10.1371/journal.pone.0159035

Sáenz, L. & Mulligan, M. (2013). The role of Cloud Affected Forests (CAFs) on water inputs to dams. *Ecosystem Services 5* (2013) e69–e77. http://dx.doi.org/10.1016/j.ecoser.2013.02.005

Sáenz, L., Mulligan, M., Arjona, F., & Gutierrez, T. (2014). The role of cloud forest restoration on energy security. *Ecosystem Services 9* (2014), pp. 180–190. http://dx.doi.org/10.1016/j.ecoser.2014.06.012

Sayama, T., McDonnell, J. J., Dhakal, A., & Sullivan, K. (2011). How much water can a watershed store?. *Hydrological Processes, 25,* pp. 3899–3908, (2011). DOI: 10.1002/hyp.8288

Sawicz, K., Wagener, T., Sivapalan, M., Troch, P. A., & Carrillo, G. (2011). Catchment classification: empirical analysis of hydrologic similarity based on catchment function in the eastern USA. *Hydrology and Earth System Sciences, 15*, pp. 2895–2911, doi:10.5194/hess-15-2895-2011

Scatena, F. N, Bruijnzeel, L. A, Bubb, P., Das, S. (2010). Setting the stage. *In Tropical Montane Cloud Forests: Science for Conservation and Management*, Cambridge University Press: Cambridge, UK, pp. 3–13. DOI: 10.1017/CBO9780511778384.003

Schneider, B. A., Avivi-Reich, M. & Mozuraitis, M. (2015) A cautionary note on the use of the Analysis of Covariance (ANCOVA) in classification designs with and without within-subject factors. *Frontiers in Psychology 6*:474. doi: 10.3389/fpsyg.2015.00474

Schueler, T. R., Fraley-McNeal, L., & Cappiella, K. (2009). Is Impervious Cover Still Important? Review of Recent Research. *Journal of Hydrologic Engineering, Vol. 14*, No. 4, April 1, 2009. DOI. 10.1 061/(ASCE) 1 084-0699(2009) 14:4(309)

SMN (2015). Información Estadística Climatológica. Servicio Meteorológico Nacional, México. https://smn.conagua.gob.mx/es/climatologia/informacion-climatologica/informacion-estadistica-climatologica

Staelens, J., De Schrijver, A., Verheyen, K., & Verhoest, N. E. C. (2008). Rainfall partitioning into throughfall, stemflow, and interception within a single beech (Fagus sylvatica L.) canopy: influence of foliation, rain event characteristics, and meteorology. *Hydrological Processes 22*, pp. 33–45. https://doi.org/10.1002/hyp.6610

Tetzlaff, D., & Soulsby, C. (2008). Sources of baseflow in larger catchments – Using tracers to develop a holistic understanding of runoff generation. *Journal of Hydrology (2008) 359*, pp. 287– 302. doi:10.1016/j.jhydrol.2008.07.008

Thomas, B. F., Vogel, R. M., Kroll, C. N., & Famiglietti, J. S. (2013). Estimation of the base flow recession constant under human interference. *Water Resources Research.,49*, pp. 7366–7379. doi:10.1002/wrcr.20532.

Tobón, C., Bruijnzeel, L. A., Frumau, K. F. A., & Calvo-Alvarado, J. C. (2010). Changes in soil physical properties after conversion of tropical montane cloud forest to pasture in northern. Tropical Montane Cloud Forests. *Science for Conservation and Management*, pp. 502–515. https://doi.org/10.1017/CBO9780511778384.054

Toebes, C., & Strang, D. D. (1964). On recession curves 1 – recession equations, *Journal of Hydrology* (New Zealand) 3, pp. 2–14. https://www.jstor.org/stable/43944075

Toledo-Aceves, T., Meave, J. A., González-Espinosa, M., & Ramírez-Marcial, N. (2011). Tropical montane cloud forests: current threats and opportunities for their conservation and sustainable management in Mexico. *Journal of environmental management, 92* (3), pp. 974-981. doi:10.1016/j.jenvman.2010.11.007

Zhang, Y., Zhang, L., Yang, C., Bao, W., & Yuan, X. (2011). Surface area processing in GIS for different mountain regions. *Forestry Studies in China, 2011, 13*(4): pp. 311–314. DOI 10.1007/s11632-013-0403-7

Verma, S., Bartosova, A., Markus, M., Cooke, R., Um, M. J., & Park, D. (2018). Quantifying the Role of Large Floods in Riverine Nutrient Loadings Using Linear Regression and Analysis of Covariance. *Sustainability 2018,* 10, 2876. *doi:10.3390/su10082876*

Williams-Linera, G. & Vizcaíno-Bravo, Q. (2016). Cloud forests on rock outcrop and volcanic soil differ in indicator tree species in Veracruz, Mexico. *Revista Mexicana de Biodiversidad, 87* (2016), pp. 1265–1274. http://dx.doi.org/10.1016/j.rmb.2016.09.003

Wolfersberger, J., Delacote, P., & Garcia, S. (2015). An empirical analysis of forest transition and land-use change in developing countries. *Ecological Economics, 119*, pp. 241–251. https://doi.org/10.1016/J.ECOLECON.2015.08.018

Wurbs, R. A., & Wesley, P. J. (2002). *Water Resources Engineering*. Upper Saddle River, NJ 07458, Prentice Hall, USA, ISBN 0-13-081293-5.

Yamada, H., 2013. How to append alphabet of multiple comparison [WWW Document]. URL

https://sites.google.com/site/hymd3a/statistics/numbering (accessed 1.28.2020).

3 Performance of the SWAT model in predicting streamflow responses of contrasting land covers in tropical montane areas of Central Veracruz, Mexico

3.1 Abstract

Tropical montane cloud forests (TMCF) are often threatened by land use change despite their capacity to maintain high dry-season baseflow. A number of conservation policies have been implemented to protect these ecosystems. However, since most of the modeling tools used to assess these policies were developed for temperate zones with distinct hydrological regimes, more work is needed to evaluate model strengths and limitations in tropical contexts. This study assesses an improved version of the Soil and Water Assessment Tool model for the Tropics (SWAT-T). In this study, we evaluate the performance of SWAT-T in a mesoscale catchment (34 km^2), and in four micro-catchments with dominant land covers: intermediate age (IF) and mature forests (MF), shade coffee (SC), and pasture (IP). Potential evapotranspiration (PET) was calculated using three methods provided by SWAT-T: Penman-Monteith (PM), Hargreaves (HA), and Priestly-Taylor (PT). Plant growth and canopy water storage capacity were manually adjusted with field data. A sensitivity analysis of parameters and calibration of daily streamflow were conducted at the catchment scale. Furthermore, the calibrated models were evaluated at four micro-catchments using streamflow data. SWAT-T was capable of predicting the observed low fraction of surface runoff. However, SWAT-T incorrectly predicted the dominance of lateral flow, instead of the deep groundwater flow observed from isotope-based studies. Moreover, SWAT-T underestimated the influence of rainfall interception losses since evaporation is limited by daily PET in forests. For PET, HA produced the best model fit, while PT and PM underestimate evaporation from the wet forest canopy. In contrast, temperature-based PET methods overestimate PET in land covers with lower interception. Finally, the model largely overestimates the mean annual low flow in IP, while underestimating it in MF and IF. Taken together, these results indicate that SWAT-T requires improvements in the modeling of rainfall interception and groundwater dynamics to improve its application in areas dominated by TMCF.

3.2 Introduction

Integrating scientific knowledge about the effects of land use change on water quantity and quality is key for scaling up and improving catchment policy design (Naeem et al., 2015, Wright et al., 2018). Hydrological models have been used to assess the efficiency of management schemes for conserving hydrological services (Quintero et al., 2009, Bremer et al., 2020). Nonetheless, hydrological models are rarely evaluated with the necessary rigor, and in most cases, modelers evaluate management scenarios based on models calibrated using statistical criteria only from measured stream gauge data at the outlets, while potentially misrepresenting interior processes (Arnold et al., 2015, Hrachowitz et al., 2014). This issue remains a major challenge in hydrology, especially in

tropical montane areas characterized by poor availability of data and ecohydrological knowledge, less suitable modeling tools, and high spatial variability in climate, vegetation, and soils (Hamel et al., 2017, Wright et al., 2018). Better understanding and modeling of the response of the "hydrological signal" to land use change is key to the effective implementation, monitoring, and success of conservation policy (Guswa et al., 2014).

The Soil and Water Assessment Tool (SWAT) is a hydrological model originally developed to simulate complex hydrological processes on agricultural catchments (Arnold et al., 1998). In part, due to its open access policy and detailed documentation, but also because of important efforts to improve its calibration, the use of the model has extended beyond agricultural applications. SWAT has been used to assess and design conservation policies and management strategies around the world (Francesconi et al., 2016, Shrestha et al., 2018), including in forest-dominated catchments in the mountainous tropics (i.e., Quintero et al., 2009, Francesconi et al., 2016, Tuppad et al., 2010, Plesca et al., 2012). Today, SWAT exhibits an element of robustness in the simulation of streamflow responses for a wide range of topographic, soils, and land use conditions (Van Liew et al., 2007). Furthermore, compared with other modeling tools, SWAT excels in the process-level detail of its results and its capacity to incorporate available local data (Vigerstol and Aukema, 2011).

Various authors have reported successful SWAT model applications in mountainous tropical settings (Quintero et al., 2009, Shrestha et al., 2018), including tropical montane cloud forest in Mexico (Salas-Martínez et al., 2014, Sánchez-Galindo et al., 2017). However, to the best of our knowledge, none of these studies have evaluated the performance of the model at micro-catchments with contrasting land covers, and more work is needed to better understand the strengths and limitations of SWAT in these environments. Moreover, some authors have noted that SWAT shows a tendency to underperform in either very low or very high discharge events, particularly in forested areas (Qiu et al., 2012). However, most model evaluations have relied only on statistics measured at the outlet (Arnold et al., 2015). A recent introduction of signature metrics for different parts of the flow duration curve has shown that it is possible to achieve a balanced hydrograph with the SWAT model. Nonetheless, calibrating SWAT simultaneously for very high and very low flows is still challenging (Shrestha et al., 2018, Pfannerstill et al., 2014).

Evapotranspiration (ET) is one of the most important elements in the water cycle, but it is also among the most difficult processes to accurately estimate at the catchment scale (Aouissi et al., 2016). While the Potential Evapotranspiration (PET) is a commonly used index in estimating ET, the many methodologies available to calculate PET produce a wide range of values (Archibald and Walter, 2013). Additionally, forest PET values at the landscape level are often indirectly estimated using models that were developed for short crops and under specific climatic conditions (Lu et al., 2005). SWAT uses empirical PET methods to estimate the actual ET, including the temperature-based Hargreaves (HA), (Hargreaves and Samani, 1985), radiation-based Priestley-Taylor (PT) (Priestley and

Taylor, 1972), and the combined energy-mass transfer Penman-Monteith (PM) (Monteith, 1965) methods. The PM method is generally considered the best method when detailed weather data (daily solar radiation, air temperature, relative humidity, and wind speed) are available (Allen et al., 1998). However, a clear definition of the "best" method for hydrological computation is still not evident and the literature suggests that different methods perform better under certain climatic conditions, especially in data-scarce regions (i.e., Alemayehu et al., 2015, Samadi, 2017).

Recently, authors have suggested improvements to SWAT to better represent vegetation growth in tropical areas (SWAT-T), recognizing that SWAT assumes that vegetation enters a dormant period at the end of each growing season (i.e., in winter), while many tropical plant species exhibit drought-controlled dormancy or continuous growth throughout the year (Strauch and Volk, 2013, Alemayehu et al., 2017). This modified version improves the applicability of the model in tropical areas, especially in the calculations of ET. Nonetheless, SWAT-T has not been formally evaluated in areas characterized by tropical montane cloud forest.

In this study, we evaluated the suitability of the SWAT-T model to simulate discharge in a catchment dominated by tropical montane cloud forest (TMCF) located in Central Veracruz, Mexico. We hypothesize that by contrasting calibrated SWAT-T models against local hydrologic and vegetation observations (e.g. streamflow and leaf area index) and ecohydrological parameters, such as canopy storage capacities of different vegetation covers, we can identify model weaknesses and strengths for analyzing the hydrological consequences of land use change in these environments. Specifically, (a) we evaluate the performance of three PET methods in the SWAT-T model and (b) assess the accuracy of the model to simulate streamflow over range of the flow duration curve in four micro-catchments with contrasting land covers (mature and intermediate age TMCF, shade coffee, and pasture). To the best of our knowledge, this is the first study to apply a framework based on metrics from across the flow duration curve in the calibration of SWAT-T, together with the evaluation of the model at micro-catchments with contrasting land covers in areas influenced by tropical montane cloud forest and other land covers.

3.3 Material and methods

3.3.1 Study site

The research was carried out in four micro-catchments (0.137–0.446 km^2) and in the Gavilanes catchment (34 km^2) originally dominated by tropical montane cloud forest (TMCF) and located between 1226 m a.s.l. and 2962 m a.s.l. in central Veracruz, Mexico (Figure 3-1). A detailed description of the characteristics of the micro-catchments is provided in Table 3-1, and more details can be found in López-Ramírez et al. (2020). The micro-catchments are located within the subcatchments of the Pixquiac and Gavilanes rivers (areas = 106 and 42 km^2, respectively), which comprise part of the Antigua River basin (area = 1,565 km^2). The micro-catchments were chosen based on the contrasting

dominance of four land use/land cover (LULC) types within each micro-catchment, (see the LULC map in Figure 3-1) including mature forest (MF), intermediate age forest (IF), shade coffee plantations (SC), and high-intensity pasture (IP). Table 3-1 indicates the fractions of the four LULC types for each of the micro-catchments. Together, these four LULC types comprise around 70% of LULC in this study area (Von Thaden et al., 2019).

Table 3-1: Description and daily hydrologic indices observed at four micro-catchments. Table includes land use, slope and soil class corresponding to the HRUs use for model evaluation at micro-catchment scale.

	MF	**IF**	**SC**	**IP**
Area (km^2)[a]	0.242	0.224	0.446	0.137
Mean elevation (m a.s.l.)[a]	1756	1604	1284	1655
Mean slope (%)[a]	36%	25%	21%	21%
Percent forest or coffee cover[a]	100%	77%	94%	29%
Percent of pasture and crops cover[a]	0%	23%	0%	63%
Percent of urban and roads[a]	0%	0%	6%	8%
Leaf area index (LAI) (m^2 m^{-2})[a]	5.93 ± 0.9	5.96 ± 1.22	4.3 ± 1.71	-
Soil saturated hydraulic conductivity (Kfs) at 20-cm depth (mm hr^{-1})[a]	125 ± 2.1	127 ± 2.1	48 ± 3.4	26 ± 2
N (day) [a]	469	642	360	467
Average daily rainfall (mm day^{-1})[a]	6.47	4.64	6.67	6
Average daily runoff (mm day^{-1})[a]	4.35	2.67	3.05	4.14
Ratio between runoff and rainfall (-)[a]	0.67	0.58	0.46	0.69
Mean annual high flow (± SD) (mm day^{-1})[a]	10.7 ± 0.25	4.7 ± 0.05	6.5 ± 0.12	12.5 ± 0.35
Mean annual low flow (± SD) (mm day^{-1})[a]	1.29 ± 0	1.18 ± 0	0.54 ± 0	0.37 ± 0
Recession constant *k* (-) [a]	0.989	0.993	0.986	0.98
HRU Land use [b]	FRSE	FRSE2	COFF	PAST
HRU Soil[b]	105	105	205	305
HRU Slope (%)[c]	35 - 99	0-35	0 - 35	0 - 35

[a] López-Ramírez et al. (2020)
[b] Estimated from SWAT-T setup (See text for explanation)
[c] Estimated from SWAT-T setup (See section 2.4 in text for explanation)
Note: Where available, the standard deviation (SD) is provided

Abbreviations: a.s.l., above sea level; IF, intermediate forest; IP, intensive pasture; MF, Mature forest; SC, shade coffee.

The Gavilanes catchment is the main source of water for the city of Coatepec, Veracruz, Mexico (García et al., 2004), while the Pixquiac catchment provides 38% of the water supply for the Veracruz state capital of Xalapa (Paré and Gerez, 2012). The general climate is temperate humid (Garcia, 2004) with about 80% of the annual rainfall occurring during the wet season (May-October). Mean annual rainfall ranges from 1120 mm to 3185 mm to 855 mm as elevation increases from 1200 m a.s.l. to 2100 m a.s.l. to 3000 m a.s.l., respectively. Mean daily temperatures decrease from 19° to 5°C from 1200 to 3000 m a.s.l. (Holwerda et al., 2013; Muñoz-Villers et al., 2012, Muñoz-Villers et al., 2016). Annual values of cloud water interception account for less than 2% of the total rainfall in the region (Holwerda et al., 2010).

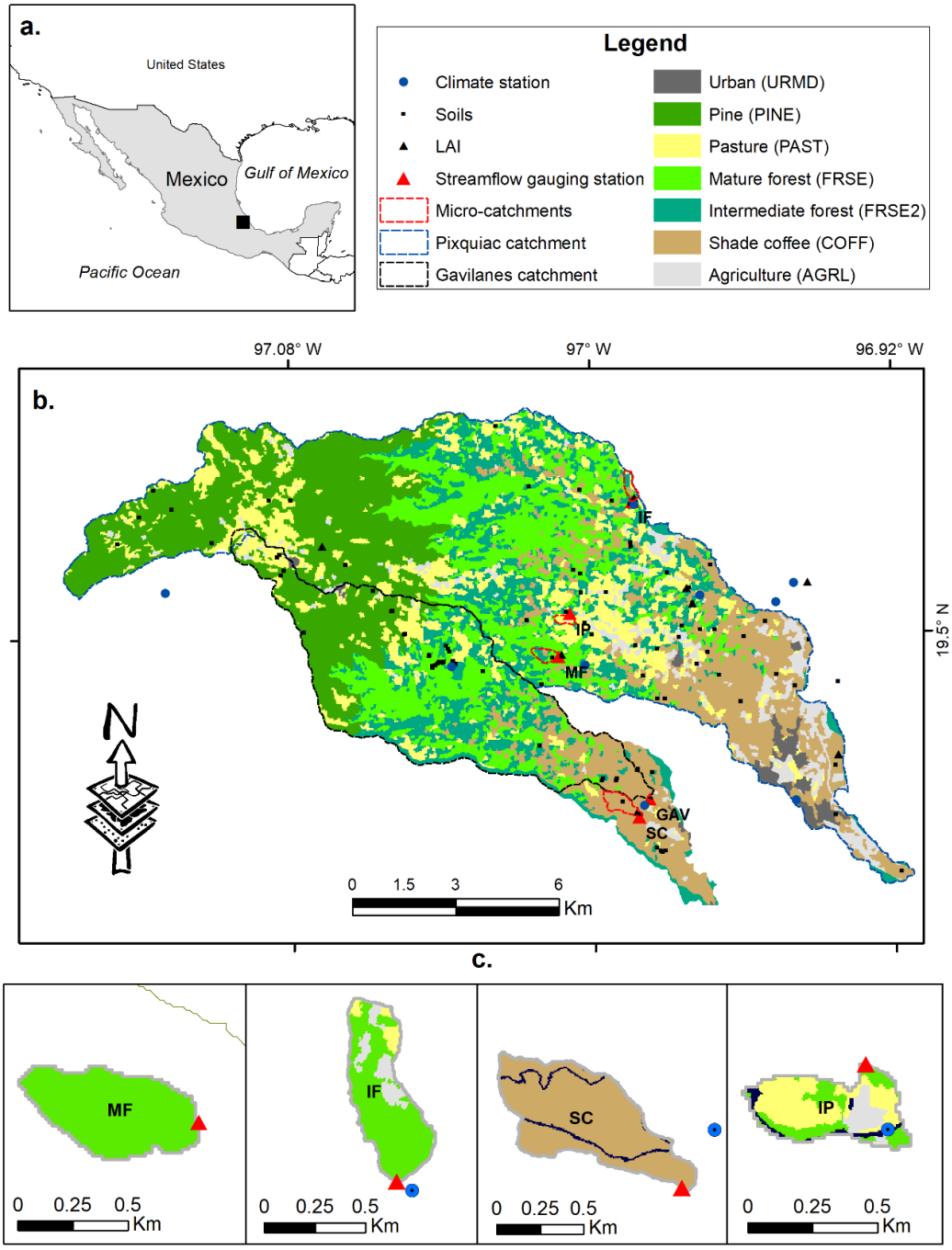

Figure 3-1: General location (a), the study area, including the Gavilanes and Pixquiac catchments (b), and four micro-catchments with different land use: mature TMCF (MF), intermediate TMCF (IF), shade coffee (SC), and pasture (IP) (c). The map includes sites where the leaf area index (LAI) and soil physical properties were observed. Note the codes presented in Legend correspond to the SWAT plant database (Neitsch et al., 2011).

The MF micro-catchment is completely dominated by old-growth TMCF (>50 years old) with low disturbance. IF is mainly covered by 40-year-old TMCF (>77% of the area) and scattered pastureland and annual crops (mainly maize) located in the upper parts of the catchment. The mean tree height in these micro-catchments is similar and ranges between 20 and 25 m (Vizcaíno-Bravo et al., 2020). These micro-catchments also have a similar mean leaf area index (LAI), see Table 3-1. The SC micro-catchment has been completely covered by shade coffee agroforestry for more than 80 years (Marín-Castro et al., 2016), with 94% of the land area dominated by this land cover. This production system retains some tree cover to provide shade to the coffee, but it exhibits a lower LAI (4.3 m^2 m^{-2}). The IP micro-catchment was largely cleared more than 40 years ago (López-Ramírez et al., 2020). Since then, pastures have been heavily grazed by sheep, goats, and cows (63% of the land area), 29% are young forests and 8% is covered by urban and roads.

The soils in these areas are mainly classified as Umbric Andosols derived from volcanic ash, with clay and silty clay as dominant textures (Campos, 2010; Paré and Gerez, 2012). Mineral soil horizons are characterized by low bulk densities (<0.7 g cm^{-3}) across land cover types due to the abundance of non-crystalline materials and organic matter; thick organic horizons (5-15 cm) often overly the mineral soil in TMCFs, but typically not in pastures and coffee plantations. Soil profiles are generally deep (A + B horizons >1 m and C + Cr horizons >10 m on ridges and backslopes) and moderately well developed (Karlsen, 2010), favoring good water storage. The soils in the region are generally underlined by andesitic saprolite, with high permeabilities ranging from 0.05 to 0.08 mm hr^{-1} (Karlsen, 2010; Muñoz-Villers and McDonnell, 2012). Although we did not measure bedrock hydraulic properties here, we observed the presence of saturated saprolite on various road cuts in our study sites. Field-saturated hydraulic conductivities are generally higher in TMCF areas in comparison to pasture and coffee (López-Ramírez et al., 2020).

3.3.2 The Soil and Water Assessment Tool (SWAT)

SWAT is a process-based, spatially distributed, continuous hydrological model (Arnold et al., 1998). This model allows the simultaneous simulation of hydrology, plant growth, sediment transport, and nutrient balances (Heidari et al., 2019). In SWAT, a basin is partitioned into sub-basins, which in turn, are subdivided into hydrological response units (HRUs) that represent a unique combination of land use, soil type, and slope class (Abiodun et al., 2018). SWAT includes five storage types to calculate the water balance: snow, the canopy, the soil profile, and the shallow and deep aquifers (Neitsch et al., 2011). When precipitation falls on any given day, canopy storage must be filled before any water is allowed to reach the soil surface. This process is controlled by the maximum amount of water that can be trapped in the canopy (CANMX) and the LAI. SWAT removes as much water as possible from canopy storage (up to the daily PET); this evaporation of intercepted rainfall is especially significant in forests (Neitsch et al., 2011). The model does not incorporate processes such as fog interception, which can be an important hydrological input in TMCF. This omission is unlikely to affect model

performance in our study area, as detailed micrometerological measurements have indicated that this process contributes relatively little to local water balance (Holwerda et al., 2010).

SWAT simulates ET as the sum of the evaporation from the canopy and from the soil, as well as plant transpiration. A comprehensive outline of ET calculations in SWAT is presented by Abiodun et al. (2018). SWAT has two important limitations that produce a significant underestimation of ET during the autumn and winter seasons in the tropics (Alemayehu et al., 2017). First, it assumes that trees and perennials enter a period of dormancy, at which point the LAI is set to a minimum value close to zero (Neitsch et al., 2011). This assumption does not realistically represent the seasonal dynamics (phenology) of foliage in the tropics in general or in the study area in particular (Williams-Linera, 1999, Alemayehu et al., 2017). Second, when leaf senescence exceeds leaf growth, SWAT models LAI with a linear decline usually dropping to zero (Neitsch et al., 2011), which rarely happens in humid tropical forests.

This study uses SWAT-T, which is a model version where the plant growth subroutine was adapted to basins located between 20° N and 20° S (Alemayehu et al., 2017). SWAT-T incorporates the logistic decline curve to model leaf senescence as suggested by Strauch and Volk (2013). Additionally, in this model the beginning of the new growth cycle for trees and perennials is triggered by a Soil Moisture Index, which occurs within a period defined by the user as the months at the end of the dry season (SOS1) and the beginning of the rainy season (SOS2). This formulation provides more flexibility for adjusting the growth cycle depending on the climatic and phenological characteristics of the study area and thus ensures more realistic ET simulations.

The curve number method (CN2) (Soil Conservation Service, 1972) is included in the SWAT and SWAT-T models to regulate the occurrence of surface runoff. The available soil water capacity (SOL_AWC) in different soil horizons controls the soil water storage at different soil depths. The hydraulic conductivity of the soil and the slope length for lateral subsurface flow (SOL_K and SLSOIL, respectively) determine the lateral flow travel time and regulate the lateral flow rate in the soil profile. Two parameters largely control the groundwater response: the groundwater delay (GWDELAY) represents the drainage time of the overlying geologic formations (days), while the baseflow recession constant (ALPHA_BF) represents the groundwater flow response to changes in recharge. The maximum canopy storage (CANMX) controls the maximum amount of water that can be intercepted and stored in a fully developed canopy. Finally, the soil evaporation factor (ESCO) is used to configure the contribution of soil water from different soil depths to evaporation. For a more detailed description of the model parameters, please refer to Neitsch et al. (2011).

3.3.3 Data for the SWAT model evaluation

Leaf area index

We combined ground-based leaf area index (LAI) measurements with MODIS satellite products. Maximum LAI was measured with the LAI-2200C Plant Canopy Analyzer (LI-COR, 2019) over a 500-m transect in ten plots with dominant land covers at different elevations: two mature TMCF (> 50 yr-old), two intermediate age TMCF (20 – 40 yr-old), two shade coffee plantations, three treeless agricultural land covers (maize, sugar cane, and pasture), and one pine forest (Figure 3-1). These measurements were taken during the rainy season (July 8 to August 20, 2019) in the early morning hours (6:45 a.m. to 8:00 a.m.), before sunset, or under cloudy conditions to avoid scattering effects. The MODIS satellite (Terra and Aqua) provide estimates of LAI on a 500-m grid every eight days at a world scale (Myneni et al., 2015). We extracted and analyzed 231 MODIS LAI composites from June 2014 to August 2019 to estimate the average daily LAI values for 10 pixels with homogeneous land covers representative of our LAI sampling sites. Clouds were masked, and mean LAI values were predicted for each day of the year by fitting local polynomial regressions (Ripley, 1998) in the *stats* Package (R Core Team, 2019) to the eight-day MODIS LAI estimates pooled across years (2014-2019).

Finally, we rescale the smoothed daily LAI using the observed LAI for each of our sites. In pine forests, we used the default SWAT max LAI value (5.0) since we did not have an accurate needle-to-shoot area ratio to adjust the observed LAI. In general, we observed that the MODIS algorithm (Myneni et al., 2015) produced acceptable results in the broadleaf forest (i.e., TMCF) and in the pine forest, while it significantly overestimated LAI in the shade coffee and in the pasture (Figure 3-3). These smoothed and rescaled MODIS LAI models were used to calibrate the SWAT-T vegetation growth module for simulating LAI (Figure 3-3).

Table 3 presents the SWAT-T model parameters that were adjusted during the manual calibration process. Initially, the minimum LAI (ALAI_MIN) and maximum potential LAI (BLAI) for each land cover class were based on the ground-based MODIS LAI model, which corresponds well with independent measurements in the study area (González-Martínez and Holwerda, 2018). The shape coefficients for the LAI curve (FRGRW1, FRGRW2, LAIMX1, LAIMX2) and the remaining parameters were adjusted by a trial-and-error process, based on values reported in the literature (i.e., Strauch and Volk 2013, Alemayehu et al., 2017), such that the SWAT-T-simulated LAI mimics the rescaled MODIS LAI.

Streamflow at the Gavilanes catchment

We used a two-year daily streamflow series from the Gavilanes catchment streamflow gauge (5/2/2015 - 4/30/2017). Water levels were measured every 10 min using water level sensors paired with barometric pressure recorders. Recorded levels were converted to streamflow (L s^{-1}) using experimental stage-discharge relationships based on rating

curves derived from salt dilution measurements of discharge (Moore, 2005). The streamflow data were resampled (mean) to daily timesteps (Figure 3-4).

Streamflow at four micro-catchments

Within each micro-catchment (Figure 3-1c), streamflow and rainfall were measured from 2015 to 2019. For streamflow, V-notch weirs were installed at each micro-catchment outlet, and the water level was logged every 1.5 minutes using a Solinst water level sensor (model 3001) paired with a barometric pressure recorder (model 3001). We calculated the streamflow (L s^{-1}) using field-derived rating curves generated via volumetric and salt dilutions measurements of discharge (Moore, 2005). Please see López-Ramírez et al. (2020) for more details.

3.3.4 Methodology

The methodological approach presented in Figure 3-2 consisted of setting up SWAT-T models to use each of the three PET methods, followed by a manual calibration of plant growth and canopy interception capacity. Next, an automated calibration and sensitivity analysis was performed for each model. This step started with selection of the most sensitive parameters using measured daily discharge at the outlet of the Gavilanes river catchment. Next, unique parameters were selected using statistics of fit and signature metrics for five segments of the daily flow duration curve. This step concluded with a temporally distributed sensitivity analysis to identify the dominance of parameters controlling different hydrological processes. The models were later run with the previously identified sets of "optimal" parameters and evaluated for streamflow at four Hydrological Response Units (HRUs) corresponding to the four monitoring micro-catchments with contrasting dominant land use.

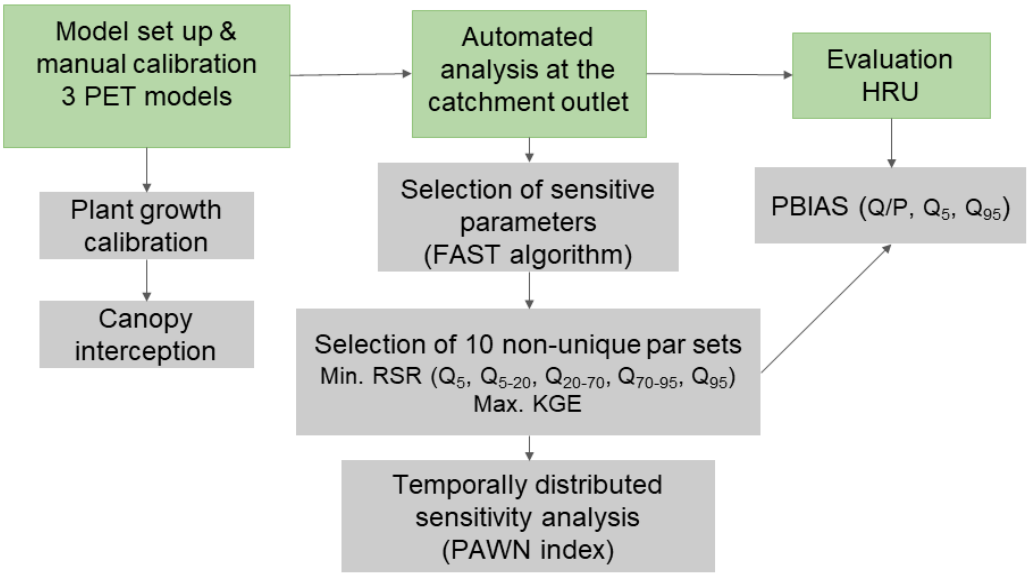

Figure 3-2: General modeling framework adopted in this study for the evaluation of SWAT-T.

3.3.4.1 Model set up and data preparation

The SWAT-T model was set up for land use conditions representing the year 2013 (Von Thaden et al., 2019). The land cover map contained seven classifications: pine, mature TMCF, intermediate age TMCF, crop, pasture, coffee, and human settlements. These land cover classes were input into the model setup using the categories from the SWAT database that are presented in Figure 3-1b: pine (PINE), forest-evergreen (FRSE), forest-evergreen (FRSE2), agricultural land-generic (AGRL), pasture (PAST), coffee (COFF), residential medium density (URMD). FRSE and FRSE2 have different LAI values corresponding to mature and intermediate TMCF, respectively. We assigned the characteristics of each category in the SWAT plant database (Neitsch et al., 2011). We used the soil classes from the INEGI database (INEGI, 2007) and field data to populate the soil database in SWAT-T (see Table 3-2 for more details).

The model was set up to capture the elevation, slope, land use, and soil class corresponding to the predominant conditions in the Gavilanes catchment and in the four monitored micro-catchments (Table 3-1). ArcSWAT version 2012 (Winchell et al., 2013) was used to set up the SWAT-T model. A digital elevation model (DEM) with a 15-m resolution (INEGI, 2012) was used to delineate the catchments. The study area was divided into 17 sub-catchments. Two slope classes were defined, with slope ranges of 0 - 35% and >35%, respectively. The sub-catchments were further subdivided into hydrological response units (HRUs). Small HRUs were removed from the model setup; specifically, HRUs with shares of total area below thresholds of 5, 20, and 20% for land use, soils, and slope were eliminated from the setup and their areas were apportioned to the remaining HRUs. These thresholds were selected for retaining the dominant land

covers, maintaining individual HRUs for the four monitored micro-catchments, and keeping the computational costs manageable. In total, the model setup resulted in 140 HRUs.

The list of hydroclimatological and spatial data used to set up the SWAT model is presented in Table 3-2. Maximum and minimum daily temperature and daily precipitation data were compiled from ten weather stations: four corresponding to the Mexican National Weather Service (SMN, 2020), three from López-Ramírez et. al. (2020), and three operated by the National Autonomous University of Mexico (UNAM). Monthly average relative humidity, solar radiation, and wind speed were available only for the UNAM and López-Ramírez (2020) stations, which were assigned to the rest of the weather stations, considering the similarity in terms of elevation and the shortest distance.

Table 3-2: Input data for the SWAT-T model setup, the data sources, and data processing steps.

Input dataset	**Source**	**Data preparation**
Topography	INEGI (2012)	Digital Elevation Model for Mexico in 15 m resolution.
Land use	Von Thaden et al., (2019)	Supervised classification of Landsat imagery from the dry season (> 500 ground-based land cover reference data)
Soil data	INEGI (2007), Daniel Geissert (unpublished data, 2010), and Nathaniel Looker (unpublished data, 2018)	Soil classes from (INEGI, 2007) and pooling soil data collected in more than 100 sites.
Climate	SMN, (2020), López-Ramírez et al., (2020), and UNAM	Daily min and max temperature and precipitation. Monthly average of solar radiation, wind speed and relative humidity. (Jan 2014- Dec 2017)
Discharge Gavilanes	Lyssette E. Muñoz-Villers (Unpublished data)	10 min discharge, resampled (mean) to daily (May 2015- Apr 2017)

Discharge micro catchments	López-Ramírez et al., (2020)	3 min discharge, resampled (mean) to daily (Jul 2016- Aug 2019)
Leaf area index	LAI ground measurements with LI-COR Biosciences (2019)	LAI measurements using LI-COR Canopy Analyzer.
	MODIS time series (Myneni et al., 2015)	MOD15A2 (500 m/8-day from Jun 2014 to Aug 2019)

3.3.4.2 Manual model calibration

In the study region, the TMCF consists of a mix of deciduous, semi-deciduous (e.g., leaf-exchanging) and evergreen species of tropical and temperate biogeographical origins (Williams-Linera,1999, Williams-Linera et al., 2013). Most of the semi-deciduous species are of temperate origin, which shed their leaves during the early and mid-dry season and leaf out during the mid to late dry season (Borchert et al., 2005). We manually defined the end of the dry season and the beginning of the rainy season (SOS1 = January, and SOS2 = February, respectively), where a new vegetation growth cycle takes place (Alemayehu et al., 2017). The SWAT-T parameters that control the shape, the magnitude and the temporal dynamics of LAI were manually adjusted to reproduce the values of the rescaled MODIS LAI for each land cover class (Table 3-3). This procedure was repeated for the parameterization of the maximum canopy storage capacity (CANMX). CANMX was determined for mature TMCF (3.3 mm), intermediate TMCF (1.8 mm), pine forest (1.2 mm), and shade coffee (1.6 mm). These values were obtained from measurements of throughfall and stemflow in these land covers at different elevations in the study catchments (González-Martínez and Holwerda, 2018, Holwerda et al., 2010, Holwerda et al., 2013, Muñoz-Villers et al., 2015).

Table 3-3: SWAT-T parameters used to manually calibrate LAI with their default and calibrated values, note: FRSE2 corresponds to Intermediate age forests and uses the same default parameters of FRSE.

Parameter	Parameter definition (unit)	Min	Max	Variable	Default (calibrated)				
					FRSE	FRSE2	PINE	PAST	COFF
BIO	Radiation-use efficiency ((kg/ha)/(MJ/m^2))	10	90	LAI	15(15)	15(15)	15(15)	34(10)	10(10)
BLAI	Maximum potential leaf area index (m^2 m^{-2})	0.5	10	LAI	5(6.43)	5(5.93)	5(5)	4(5)	1.35(3.9)
FRGRW1	Fraction of PHU corresponding to the first point on the optimal LAI curve	0	1	LAI	0.15(0.1)	0.15(0.1)	0.15(0.15)	0.05(0.15)	0.05(0.15)
FRGRW2	Fraction of PHU corresponding to the second point on the optimal LAI curve	0	1	LAI	0.25(0.25)	0.25(0.25)	0.25(0.5)	0.49(0.5)	0.4(0.5)
LAIMX1	Fraction of BLAI corresponding to the first point on the optimal LAI curve	0	1	LAI	0.7(0.75)	0.7(0.75)	0.7(0.7)	0.05(0.4)	0.05(0.7)
LAIMX2	Fraction of BLAI corresponding to the second point on the optimal LAI curve	0	1	LAI	0.99(0.98)	0.99(0.98)	0.99(0.98)	0.95(0.99)	0.95(0.99)
DLAI	Fraction of total PHU when leaf area begins to decline	0.15	1	LAI	0.99(0.15)	0.99(0.15)	0.99(0.15)	0.99(0.8)	0.99(0.3)
T_BASE	Minimum temperature for plant growth (◦C)	0	18	LAI	0(8)	0(8)	0(5)	12(5)	10(10)
ALAI_MIN	Minimum leaf area index for plant during dormant period (m^2 m^{-2})	0	0.99	LAI	0.75(3.5)	0.75(3.5)	0.75(3.5)	0(0.1)	0.75(2.5)
PHU	Total number of heat units needed to bring plant to maturity	0	6000	LAI	5708(5500)	5708(5500)	1800(4000)	1481(3000)	1800(4500)

3.3.4.3 Automated calibration and evaluation

Parameter selection

In a parameter screening, we ran a global sensitivity analysis (GSA) to the simulation of discharge at the Gavilanes catchment outlet for the SWAT-T models using each PET method to identify the most influential parameters. We explored 23 model parameters that are frequently calibrated in SWAT to simulate discharge (see Arnold et al., 2012, Mehdi et al., 2018, Schürz et al., 2019, Meins, 2013, for a description of the relevant model parameters controlling the water balance). The ranges and types of parameter changes represent typical procedures often found in the SWAT literature. An overview of the model parameters that were identified as influential and that were further used in the model is provided in Table 3-4. We employed the *Fourier Amplitude Sensitivity Test* (FAST) algorithm (Cukier et al., 1973) included in the R *fast* package (Reusser, 2015) and integrated as part of the *SWATplusR* workflow (Schürz, 2019) to screen and rank the model parameters. A parameter was selected as important if it was within the most sensitive parameters, employing the Kling–Gupta Efficiency criterion (KGE) for daily streamflow, including its three components (Gupta et al., 2009). The GSA performed for the model parameters of the three PET models yielded similar results for the first 14 parameters. However, LAT_TTIME is a function of two parameters (SLSOIL and SOL_K) (Neitsch et al., 2011), thus we decided to adjust the two independent parameters. Therefore, we employed 13 parameters during the calibration for the three models (Table 3-4).

Table 3-4: SWAT-T model parameters used during the sensitivity analysis and automated calibration for the three PET models of the Gavilanes catchment.

Parameter	Description	Alteration	min	max	Used for calibration
SOL_AWC	Available water capacity in the soil [-]	Multiply	-0.35	0.35	X
SOL_K	Saturated hydraulic conductivity of the soil [mm/hr]	Multiply	-0.8	0.8	X
SOL_Z	Depth of the soil layer [mm]	Multiply	-0.3	0.3	
ALPHA_BF	Base flow alpha factor (day^{-1})	Replace	0	0.3	X
GW_DELAY	Ground water delay [days]	Replace	0	500	X
GW_REVAP	Ground water revap coefficient [-]	Replace	0.02	0.2	
GWQMN	Threshold depth of water in the shallow aquifer required for return flow to occur [mm]	Replace	0	2000	
RCHRG_DP	Deep aquifer percolation fraction [fraction]	Replace	0	1	
REVAPMN	Threshold depth of water in the shallow aquifer for revap to occur [mm]	Replace	0	500	

Parameter	Description	Alteration	min	max	Used for calibration
GW_SPYLD	Specific yield of the shallow aquifer (m^3/m^3)	Replace	0	0.4	
CH_K2	Hydraulic conductivity of the channel [mm/hr]	Replace	5	130	X
CH_N2	Manning's coefficient of the channel [-]	Replace	0	0.3	X
ALPHA_BNK	Baseflow alpha factor for bank storage (day^{-1})	Replace	0	1	X
CANMX	Maximum canopy storage [mm]	Multiply	-0.3	0.3	
EPCO	Plant uptake compensation factor [-]	Replace	0	1	X
ESCO	Soil evaporation compensation factor [-]	Replace	0	1	X
HRU_SLP	Average slope steepness [m/m]	Multiply	-0.2	0.2	X
SLSUBBSN	Average slope length [m]	Multiply	-0.3	0.3	
LAT_TTIME	Lateral flow travel time	Replace	0	180	
SLSOIL	Slope length for lateral subsurface flow	Replace	0	150	X
DEP_IMP	Depth to impervious layer for modeling perched water tables	Replace	0	6000	X
CN2	Curve Number [-]	Add	-15	15	X
SURLAG	Surface runoff lag coefficient [-]	Replace	0	10	

Identification of non-unique parameter sets

To facilitate the analysis of the SWAT-T model performance and separate the effects of particular PET methods on model output, we selected a series of simulations with non-unique parameter sets (Schürz et al., 2019). We simulated daily discharge for each model, using the Latin Hypercube Sampling method, with the R package *lhs* (Carnell 2019), to select 3000 random samples for the parameter combinations of the 13 most influential parameters that we previously identified. We evaluated simulations using signature metrics and a statistical performance metric (KGE). The ratio of the root mean square error to the standard deviation (RSR, Moriasi et al., 2007) was calculated for five segments of the flow duration curve (FDC): very high (0-5% days of exceedance), high (5-20%), medium (20-70%), low (70-95%), and very low flows (95-100%), as suggested by Pfannerstill et al. (2014). RSR varies from an optimal value of 0, which indicates a perfect model simulation, to a large positive value. This evaluation method has been shown to lead to an improved selection of good calibration runs since it captures different parts of the hydrograph (Pfannerstill et al., 2014). We simultaneously identified the best 1500 runs out of 3000 for the five-signature metrics (Minimize RSR), followed by the selection and comparison of the best ten simulations with maximum KGE for each PET method.

Evaluation of streamflow in four micro-catchments with different land covers

All identified non-unique parameter sets were subsequently applied individually to the SWAT-T model (Mehdi et al., 2018), and the model simulations were evaluated in the four HRUs with contrasting dominant land covers (Table 3-1). These HRUs largely resemble the soil, slope, vegetation, and elevation conditions observed in the four monitored micro-catchments. First, we visually compared the simulated and observed FDCs. Second, we estimated the percentage bias (PBIAS) criteria for the annual ratio between average daily runoff and average daily rainfall (Q/P), for the mean annual daily high flow(Q_5), and for the mean annual daily low flow (Q_{95}).

Evaluation of Evapotranspiration (ET)

We compared the actual evapotranspiration (ET) predicted by SWAT-T with ET estimated from local meteorological data on the ET/ ET_0 ratios for different vegetation covers. First, we calculated the reference evapotranspiration (ET_0) following FAO guidelines (Allen et al., 1998) and using the available meteorological data for the study period at four sites with contrasting vegetation covers (Table 3-8). Next, ET was obtained by multiplying ET_0 by the ratio of ET to ET_0 reported for FRSE, FRSE2, and PINE by Muñoz-Villers et al. (2015) and for COFF by Holwerda et al. (2013). These ET values were directly compared with ET predicted in the corresponding HRUs by a calibrated SWAT-T model, applying the best set of previously identified parameters for each PET method.

Temporally distributed parameter sensitivity analysis

The temporally distributed parameter sensitivity analysis (TDSA) is used to identify deficiencies in the model structure as a function of time of year (Pfannerstill et al., 2015, Haas et al., 2015, Guse et al., 2014, Guse et al., 2016, Guse et al., 2019). A TDSA was applied to the three SWAT-T models to obtain daily temporal parameter sensitivities, which were later summarized at monthly intervals (Guse et al., 2016) to derive information about the dominant hydrological processes during the wet and dry seasons.

We simulated daily discharge for each model in the Gavilanes catchment, again using the Latin Hypercube Sampling to select 1500 random samples for the combinations of eight parameters (Table 3-5). To study the temporal dynamics of the parameterization on the simulation of daily discharge for the three PET methods we employed the R package *temPAWN* (Schürz, 2020), which calculates the daily PAWN (derived from the authors names) sensitivity index according to Pianosi and Wagener (2018) for each time step of a simulation. PAWN is moment-independent and is a suitable method for asymmetrically distributed outputs of models (Zadeh et al., 2017). PAWN (Pianosi and Wagener, 2015) has shown to be effective for parameter ranking, including various applications with the SWAT model (Zadeh et al., 2017, Pianosi and Wagener, 2018, Schürz et al., 2019). Table 3-5 lists the model parameters selected to assess parameter sensitivity for each hydrologic process: surface runoff, lateral flow, groundwater flow, evaporation, interception, and

soil water storage. The parameters that control surface runoff, soil water storage, lateral flow and rainfall interception were modified spatially, while the parameters controlling groundwater were altered globally.

Table 3-5: Selection of parameters and their ranges for the temporal sensitivity analysis. Parameters are paired with the hydrological process they control.

Parameter name	Abbreviation	Process	Alteration	min	max
Curve Number [-]	CN2	Surface runoff	Add	-0.15	0.15
Available water capacity in the soil [-]	SOL_AWC	Soil water storage	Multiply	-0.4	0.4
Hydraulic conductivity of the soil [mm/hr]	SOL_K	Lateral flow	Multiply	-0.8	0.8
Slope length for lateral subsurface flow	SLSOIL	Lateral flow	Replace	0	150
Groundwater delay [days]	GW_DELAY	Groundwater	Replace	0	500
Base flow factor [-]	ALPHA_BF	Groundwater	Replace	0	0.3
Maximum canopy storage [mm]	CANMX	Interception	Add	0	4
Soil evaporation compensation factor [-]	ESCO	Evapotranspiration	Replace	0	1

3.4 Results

3.4.1 LAI simulation

We evaluated the degree of agreement between daily MODIS LAI with the calibrated SWAT-T simulated LAI using visual comparisons and statistical measures. From the qualitative inspection (see Figure 3-3), it is apparent that the annual growth cycle of each land cover class from the calibrated SWAT-T model corresponds well with the MODIS LAI model rescaled with field data. In quantitative terms, the calibrated models exhibited generally strong correlations — 0.67 (FRSE), 0.89 (FRSE2), 0.92 (PAST), 0.47 (PINE), and 0.64 (COFF) — during the calibration period. The greatest mismatch in LAI was found for PINE, most likely because only one site was used to measure LAI for this land use.

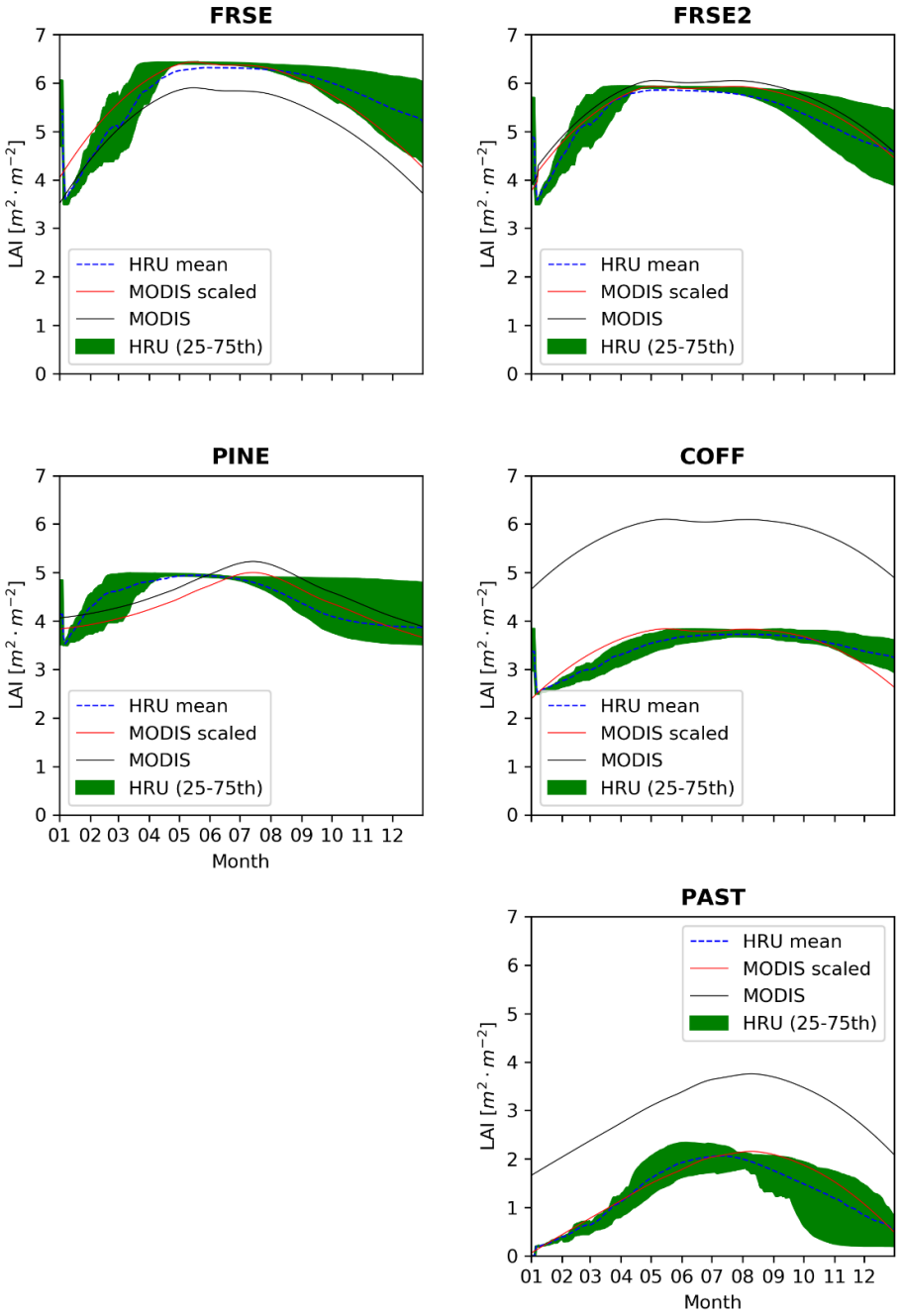

Figure 3-3: Annual LAI as simulated by SWAT-T plant growth using calibrated SWAT-T parameters and the rescaled MODIS annual growth model (red line). The black line represents the original smoothed MODIS annual growth model. The green band denotes the area between the 25 and 75th quantile of the corresponding HRUs. (See explanations in the text.)

3.4.2 Streamflow simulations at the Gavilanes catchment

Visual comparisons of daily simulated streamflow hydrographs with observed streamflow over the calibration period for the three PET methods suggest fairly good concordance (Figure 3-4a). However, the quantitative results presented in Table 3-6 show that the HA method exhibited a higher KGE and NSE while producing the lowest PBIAS. The PM method on the other hand showed the poorest ability of calibrated models to reproduce observed streamflow (lower NSE and KGE, and larger PBIAS). These statistical results were consistent with the results from the signature metric analysis, where HA consistently exhibited the lowest RSR for the five parts of the FDC, and, once again PM exhibited the larger RSR for all the segments of the FDC. These results are more evident in Figure 3-4b, where we can observe narrower uncertainty bands for HA. At very low flows, however, the three PET methods produced similar results, exhibiting high RSR values, due to the likely high uncertainty in the simulated and measured very low flows.

Table 3-6: Final selection of best model calibration runs after applying 5 FDC performance metric-based selection. The mean value for all indices of fit is presented for each PET method for comparison of performance.

Sim	PET	Calibration run	KGE	NSE	PBIAS	R^2	RSR				
							Q_5	$Q_{5\text{-}20}$	$Q_{20\text{-}70}$	$Q_{70\text{-}95}$	Q_{95}
1	PM	831	0.51	0.07	22.70	0.61	5.36	3.39	1.03	0.88	3.29
2	PM	2293	0.48	0.13	19.60	0.67	5.67	3.87	0.85	0.53	2.75
3	PM	1146	0.42	-0.08	27.10	0.64	5.97	4.26	1.22	0.57	2.24
4	PM	525	0.49	0.06	31.00	0.70	6.27	3.78	1.31	1.91	2.96
5	PM	1480	0.44	0.06	21.00	0.67	6.44	4.70	0.61	0.92	3.33
6	PM	875	0.38	-0.05	28.30	0.71	7.13	4.93	1.06	1.08	2.74
7	PM	2216	0.41	0.03	21.90	0.69	7.17	4.26	0.85	0.78	3.10
8	PM	2871	0.44	0.00	28.70	0.68	7.31	3.57	1.26	1.48	1.93
9	PM	2822	0.42	0.12	15.60	0.69	8.31	3.35	0.53	0.66	2.86
10	PM	515	0.45	-0.07	28.50	0.63	8.52	2.86	1.11	1.86	3.27
	Mean		0.44	0.03	24.44	0.67	6.81	3.90	0.98	1.07	2.85
1	PT	2953	0.63	0.20	12.20	0.48	1.24	2.14	0.72	0.64	2.87
2	PT	2311	0.58	0.34	18.70	0.71	3.51	3.80	0.79	0.62	2.52
3	PT	2873	0.59	0.21	27.20	0.66	3.52	3.50	1.12	2.07	3.02
4	PT	764	0.64	0.47	15.50	0.75	3.96	3.00	0.56	0.76	2.86
5	PT	1813	0.71	0.48	-16.20	0.70	4.23	0.99	1.15	1.44	0.90
6	PT	1938	0.68	0.45	9.80	0.66	4.36	1.59	0.40	0.78	3.33
7	PT	716	0.63	0.47	11.90	0.73	5.34	2.38	0.40	0.83	3.30
8	PT	456	0.58	0.23	23.20	0.66	5.74	2.63	0.94	1.77	3.33
9	PT	1544	0.66	0.42	10.40	0.67	6.60	1.30	0.30	0.97	3.32
10	PT	600	0.59	0.36	9.90	0.68	6.86	1.77	0.37	0.60	2.73
	Mean		0.63	0.36	12.26	0.67	4.54	2.31	0.67	1.05	2.82
1	HA	2059	0.74	0.47	14.90	0.62	1.36	1.42	0.62	1.69	2.55

Sim	PET	Calibration run	KGE	NSE	PBIAS	R^2	RSR				
							Q_5	Q_{5-20}	Q_{20-70}	Q_{70-95}	Q_{95}
2	HA	2312	0.80	0.61	8.20	0.70	1.51	1.31	0.31	1.02	2.57
3	HA	1880	0.83	0.65	-1.10	0.71	2.57	0.50	0.49	0.69	3.28
4	HA	770	0.71	0.51	8.10	0.69	2.79	2.05	0.44	0.42	2.52
5	HA	1513	0.84	0.69	3.80	0.74	2.84	0.58	0.22	0.88	3.33
6	HA	2787	0.72	0.44	6.00	0.61	2.91	1.44	0.40	0.73	3.16
7	HA	546	0.71	0.47	1.30	0.64	3.79	1.00	0.47	0.44	2.11
8	HA	541	0.71	0.52	7.90	0.69	5.50	1.18	0.27	0.92	3.43
9	HA	2638	0.70	0.51	3.20	0.69	5.54	0.84	0.39	0.48	2.63
10	HA	686	0.72	0.51	-5.90	0.67	5.75	0.45	0.69	0.47	2.03
	Mean		0.75	0.54	4.64	0.67	3.46	1.08	0.43	0.77	2.76

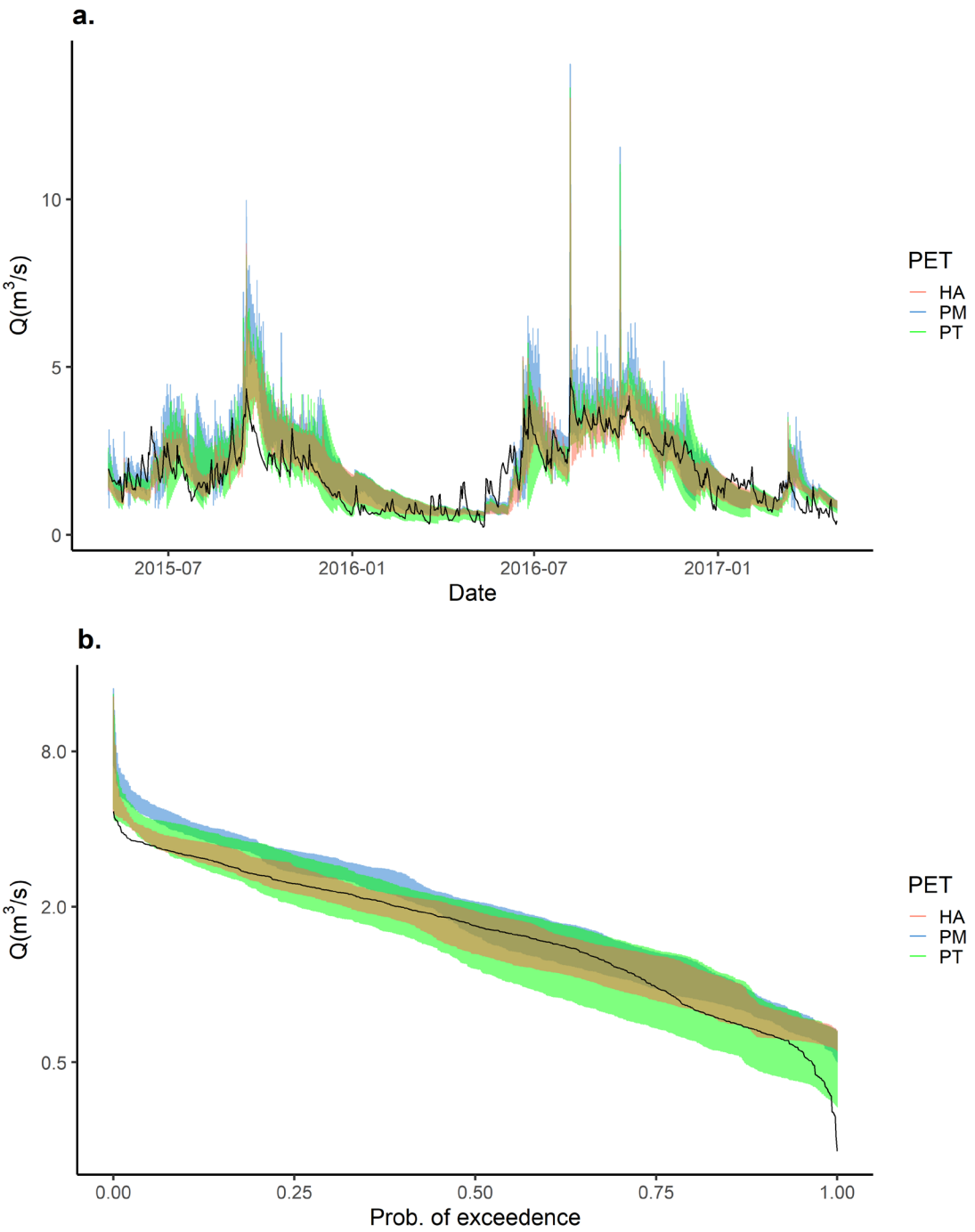

Figure 3-4: Calibrated simulations of discharge at the Gavilanes outlet using the best 10 sets of non-unique parameters for each PET method (a) and their corresponding flow duration curves (b), black line represents observed discharge. Figures include an alpha factor = 0.5, adding transparency to the color bands with darker tones indicating areas of overlap.

3.4.3 Model performance at the four micro-catchments

Qualitatively, the three PET methods showed good performance in simulating different phases of FDC for the MF and SC. Additionally, all PET methods accurately simulated the high, mid and low flows in the IF (Figure 3-5). However, SWAT-T clearly failed to capture the very low flows observed in IF. An unexpected result was that the model largely overestimated the low and very low flow dynamics in the IP, probably to due to the global calibration of groundwater parameters. The statistical results (Table 3-7) confirm these findings, where the three PET methods exhibited extremely high mean PBIAS (> 400) for mean annual low flow (Q_{95}) in the IP micro-catchment. Additionally, the three models underestimated Q_{95} in the MF and IF HRUs. For mean annual high flow (Q_5) the PM and PT methods exhibited slightly better performance than HA.

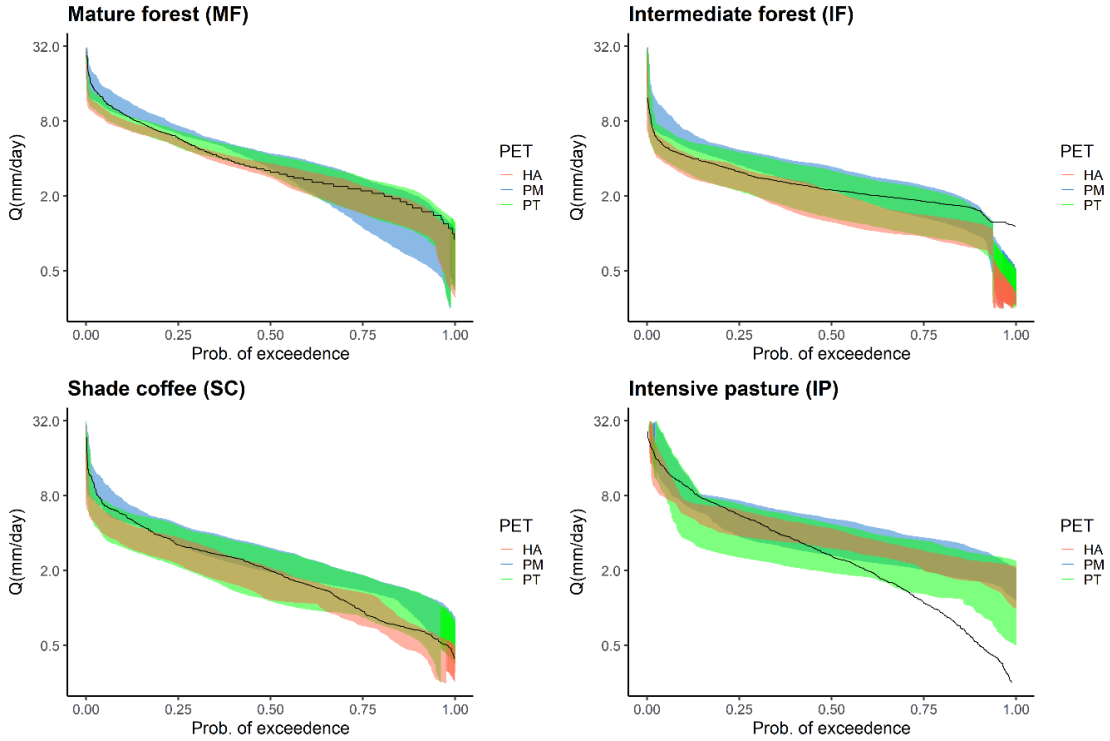

Figure 3-5: Streamflow simulations resulting from the identified sets of non-unique parameters evaluated at four micro-catchments with contrasting dominant land covers. Figure includes an alpha factor = 0.5, this adds transparency to the color bands and darker tones of the colors represent overlapping areas.

Table 3-7: PBIAS for different streamflow metrics in four monitored micro-catchments. Positive values indicate overestimation, values close to 0 are considered excellent and up to 25% are considered satisfactory (Moriasi et al., 2007).

	Metric	MF	IF	SC	IP
PM	PBIAS Q/P	4.30	5.19	24.08	2.83
	PBIAS Q_5	11.53	47.59	9.91	19.45
	PBIAS Q_{95}	-17.01	-55.12*	53.12	476.00*
PT	PBIAS Q/P	-7.82	-14.97	0.98	-9.62
	PBIAS Q_5	-6.08	19.18	-12.03	-2.88
	PBIAS Q_{95}	-11.42	-62.59*	24.54	420.80*
HA	PBIAS Q/P	-20.15	-39.12	-23.99	-18.64
	PBIAS Q_5	-16.35	-5.52	-26.90	-2.29
	PBIAS Q_{95}	-23.43	-72.17*	-20.66	410.20*

*Systematic errors

3.4.4 Evapotranspiration in contrasting land covers

Comparisons of ET as predicted by the best calibrated SWAT-T model using three PET methods with ET estimated based on local data from the ratio of the actual (ET) to potential (ET_0) evapotranspiration revealed that ET estimated using the HA method more closely matched ET based on local data (Table 3-8). However, our results also show that the HA method overestimates ET in COFF by 28% at lower elevations (1210 m a.s.l.), while underestimating ET in FRSE by 27% and by 8% in FRSE2 at 2170 (m a.s.l.). PM and PT methods present higher underestimation of ET for these same forest sites.

Table 3-8: Comparison of ET predicted by the best calibration run for each PET method in SWAT versus ET obtained using the FAO Penman-Monteith reference evapotranspiration method and local Kc values.

LC	Elevation (m a.s.l.)	Kc (ET/ET_0)	ET_0 (mm yr^{-1})	ET (mm yr^{-1})	ET SWAT (mm yr^{-1})		
					PM[c]	PT [d]	HA[e]
FRSE	2170	1.55[a]	919	1424	726	934	1044
FRSE2	2170	1.24[a]	919	1139	708	933	1044
PINE	2180-2480	0.58-1.00[a]	919	532-919	660	935	1044
COFF	1210	0.98[b]	1090	1069	845	1138	1366

[a] Muñoz-Villers et al. 2015
[b] Holwerda et al. 2013
[c] Calibration run 831, see Table 6 for details
[d] Calibration run 2953, see Table 6 for details
[e] Calibration run 2059, see Table 6 for details

3.4.5 Temporal sensitivity analysis

Monthly averages of sensitivity results for each model parameter were very similar for the three PET methods. A marked dominance of lateral flow was detected throughout the year, with an important contribution of groundwater. The highest significance of groundwater parameters occurred at the end of the wet season (October and November), during the transition between the wet and dry seasons (hydrograph recession). Low influence of surface runoff is observed, except in the middle of the rainy season (July-September) when this parameter plays a slightly more significant role. Evapotranspiration, interception, and soil water storage parameters did not influence streamflow (Figure 3-6); this may be due to the availability of water throughout the year, but it seems counterintuitive when contrasted against local data, as discussed in the following section.

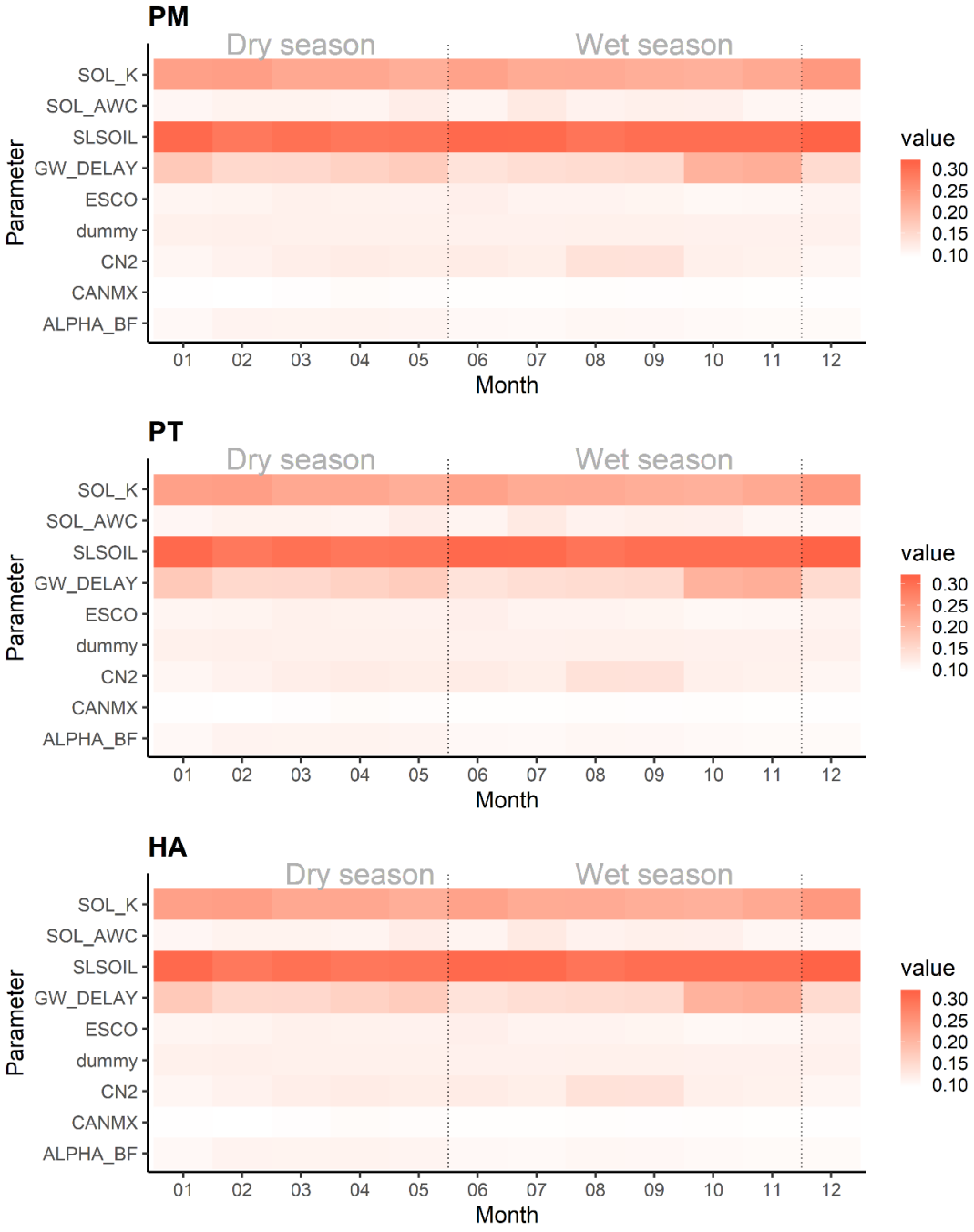

Figure 3-6: Mean monthly averaged parameter sensitivities for the three PET methods (PM, PT, and HA) evaluated at the Gavilanes catchment. Parameter sensitivity is presented relative to a dummy variable, parameters with a darker tone had a correspondingly more significant effect on streamflow. Dotted lines denote the beginning and the end of the wet and dry seasons. See the text for an explanation of each parameter.

3.5 Discussion

3.5.1 Suitability of the SWAT-T model to simulate discharge in a tropical montane catchment influenced by cloud forest

SWAT-T (Alemayehu et al., 2017) was capable of accurately simulating LAI in TMCF areas of central Veracruz, Mexico (Figure 3-3). Overall, the rescaled MODIS LAI model effectively represented the annual growth dynamics when compared with independent LAI observations. In mature TMCF, the average LAI measured for the dry and wet seasons was 4.1 and 5.9, respectively (González Martínez and Holwerda, 2018). The LAI model also provided good results when compared with shade coffee plantations where minimum LAI was 2.7 in December 2016 and maximum LAI was 3.9 in July 2017 (Holwerda and Meesters, 2019). Furthermore, the SWAT-T-simulated LAI corresponded well with the MODIS LAI annual growth model (an average R^2 of 0.71 for all land covers).

SWAT-T was capable of incorporating local data on the maximum canopy storage capacity for the land covers. However, the formulation of SWAT-T did not allow realistic simulation of the effect of rainfall interception in forested areas. In the study region, rainfall interception and canopy storage capacity have been reported in the literature using measurements of rainfall, throughfall, and stemflow combined with the Liu Model (Liu, 2001) in two mature TMFC sites (CANMX1 = 3.3 mm, I1 = 17% of P, CANMX2 = 1 mm, I2 = 15% of P) (Holwerda et al., 2010, González Martínez and Holwerda, 2018), a 19-year old TMCF site (CANMX1 = 1.5 mm, I = 8% of P) (Holwerda et al., 2010), and a shade coffee plantation (CANMX = 0.5 mm, I = 8% of P) (Holwerda et al., 2013). Results of rainfall interception were also reported for 10 yr-old and 30 yr-old pine (*Pinus patula*) plantations (I = 7% of P and 5% of P, respectively) (Muñoz-Villers et al., 2015). Furthermore, rainfall interception values reported for other montane cloud forests vary between 8 and 46% of P (Bruijnzeel et al., 2011). Thus far, all of the SWAT models underestimated rainfall interception (I <4 % of P, for all land covers).

These values strongly suggest that in these environments, interception is an important component of the water balance for mature TMCF. Thus, it follows that the conversion of mature TMCF to other land covers is associated with a decrease in rainfall interception from around 16% of P to 7% of P and that CANMX varies from 0 up to 4 mm. Nevertheless, the temporally distributed sensitivity analysis (Figure 3-6), tells a different story, where interception has a minimal effect on streamflow for all the SWAT models, even during the dry season. This result can be explained by the fact that SWAT limits daily evaporation from the canopy by daily PET (Figure 1 of Abiodun et al., 2018, Neitsch et al., 2011). This formulation underestimates the actual evaporation from the wet forest canopy, which is enhanced by the extraction of sensible heat from the atmosphere facilitated by the low aerodynamic resistance of forest (Stewart, 1977, Shuttleworth and Calder, 1979). This point requires further review, and we suggest that the SWAT model allow the canopy storage capacity to empty daily, as assumed by simpler, widely accepted interception models such as the Liu model (Liu, 2001).

The SWAT-T model was able to satisfactorily simulate streamflow during the calibration period as can be observed in Figure 3-4 and verified by acceptable goodness of fit indices (Table 3-6). The incorporation of a multi-metric framework that considers five segments of the FDC (Pfannerstill et al., 2014) improved the identification of the best parameter sets. However, calibrating the models was challenging for very high and low flow conditions. In our study, we were able to improve the model calibration by relaxing the conditions for the simultaneous selection of the best 50% quantile for the five segments of the FDC. While other researchers have used more restrictive conditions for selecting simulations, including the best 20% quantile by Pfannerstill et al. (2014), and the best 25% quantile used by Guse et al. (2020), we observed that our more relaxed approach was effective in enhancing overall model performance and parameter identification.

The temporally distributed sensitivity analysis suggested a low influence of surface runoff, an intermediate influence of groundwater, and the dominance of lateral flow in estimating streamflow response (Figure 3-6). Our results on surface runoff agree with a recent study in a neighboring catchment of similar size (60.6 km^2), where López-Hernández (2019) examined 159 storm events and found that only 3 to 7% of total streamflow occurred as quickflow. Moreover, Muñoz-Villers et al. (2016) reported long mean baseflow transit times (between 1.2 and 2.7 years) in Gavilanes catchment and 11 nested subcatchments (0.1 to 34 km^2), suggesting that deep subsurface flow paths, rather than shallow lateral flow, is the dominant flow path for runoff generation (Muñoz-Villers and McDonnell, 2012, 2013). These results agree with the high permeability observed at the soil–bedrock interface (5 to 30 mm h^{-1}).

A structural deficit in SWAT models can explain the contradiction in between the dominant flow path indicated by the SWAT model results and field observations. In SWAT, groundwater is divided into a shallow and a deep aquifer. The shallow aquifer represents an unconfined aquifer that may discharge into the channel. Alternatively, the deep aquifer is described as a confined aquifer that does not contribute to the streamflow (Neitsch et al., 2011). This suggests that the SWAT model's reliance on a single active groundwater storage compartment is insufficient for describing the fast recession phase together with the low flow with the same parameter set (Luo et al., 2012, Guse et al., 2014, Pfannerstill et al., 2014). In this regard, the parameter GWDELAY presents a tradeoff between both discharge phases. If GWDELAY represents a fast recession with a short number of days, the model produces a large amount of water available for contribution to streamflow. On the other end, a longer GWDELAY is required to represent the slow water release during the long low flow periods (Pfannerstill et al., 2014). Field results (streamflow) indicated a long recession phase, in turn the model responded with larger values of GWDELAY (around 400 days) during the calibration. In such a system, the shallow aquifer releases the water more slowly, and the system behaves more like a semipermeable layer, providing conditions that inaccurately imply the dominance of lateral flow (Hu and Li, 2018).

3.5.2 Relative performance of three PET methods

The finding of minimal influence of evapotranspiration (ET), interception (I), and soil water storage parameters was surprising (Figure 3-6), since ET accounts for 30-40% of the rainfall in the headwater catchments where most recharge occurs (Muñoz-Villers et al., 2012, Muñoz-Villers et al., 2015, Muñoz-Villers et al., 2016). Notwithstanding, these ET results agree with values of ET (19-50%) reported in other tropical montane mesoscale catchments (i.e., Crespo et al., 2012, Beck et al., 2013). Alemayehu et al. (2015) suggested that in terms of the ET simulation, more attention should be given to the appropriate selection of PET methods because the SWAT model parameters are sensitive to the choice of the PET estimation method, a result supported by our findings.

The Hargreaves (HA) method produced the best goodness of fit results, including an average KGE of 0.75, an NSE greater than 0.5, and the minimum average RSR for all segments of the FDC (Table 3-6). The Priestley-Taylor (PT) method yielded better results than the Penman Monteith (PM) method. This result was confirmed by a direct comparison between annual ET predicted by the calibrated SWAT-T models with annual ET estimated using locally derived data on the ratio of ET to ET_0 (Table 3-8). Overall, ET from the HA method more closely resembled ET values predicted based on local data. However, the HA method largely overestimated ET in shade coffee located in the lower elevations (elev. = 1210 m a.s.l.), while it underestimated ET in mature and intermediate age TMCF located in upper elevations of the TMCF belt (elev. of 2170 m a.s.l.).

TMCF environments exhibit reduced incoming solar radiation from clouds, high atmospheric humidity, and high presence of fog (Bruijnzeel et al., 2011; Fahey et al., 2015). In principle, the PT and PM methods explicitly account for the effect of lower radiation. Moreover, in our study areas suppression of transpiration by fog is minimal (Alvarado-Barrientos et al., 2014), especially in the lower areas where fog occurrence is practically absent (only 2% of the time, Holwerda, 2010). Nonetheless, fog is more frequent (around 32%, Alvarado-Barrientos et al., 2014) in the middle and upper sections of the cloud forest belt, and it is probable that a higher presence of fog is associated with higher epiphyte densities that may contribute to higher canopy storage capacities in these areas (González Martínez and Holwerda, 2018). These high interception capacities may in turn enhance wet canopy evaporation in forested areas driven by negative (downward) sensible heat flux rather than sustained by radiant energy alone (Holwerda et al., 2012, Mizutani et al., 1997). Under these environmental conditions, radiation-based methods such as PT and PM will significantly underestimate PET in the middle and upper parts of the cloud forest zone and consequently limit the models' capacity to accommodate evaporation from the forests. In principle, the aerodynamic term in the PM equation accounts for sensible heat advection. In SWAT the PM method will underestimate PET in forests, because it uses the surface resistance of alfalfa (100 s m^{-1}) (Neitsch et al., 2011) and the surface resistance is zero for a wet canopy. Moreover, this PET method calculates aerodynamic resistance considering a crop (height of 40 cm) (Neitsch et al., 2011), which is ~5 times larger than that of forest, contributing to the underestimation of PET. In the PT method, the aerodynamic term is represented by the PT coefficient (1.28,

Neitsch et al., 2011). However, Shuttleworth and Calder (1979) show that this is not sufficient to account for the high evaporation rates from wet forest canopies (i.e. energy input from sensible heat advection can be several times greater than that from radiation).

Temperature-based methods such as HA generally produce higher PET estimates (Table 3-8). Higher values of PET compensate for the low capacity of the model to accommodate the evaporation of intercepted rainfall in forests but also lead to overestimation of transpiration rates in other land covers. It is likely that the PT method also overestimates forest transpiration. Further, when we select the PT and HA models, SWAT does not explicitly model the effect of the LAI on transpiration for LAI > 3.0 (Neitsch et al., 2011), as observed by the very similar ET SWAT values obtained for FRSE, FRSE 2, and PINE when using the HA and PT methods (Table 3-8). This formulation reduces the effect of vegetation cover on hydrological flows when using these approaches. In conclusion, although the HA PET method performs better, it is not for the right reasons, and the use of this approach overestimates ET in areas with lower interception capacity such as shade coffee and pasture, especially in the lower parts of the catchment where the presence of fog is less important.

3.5.3 Assessment of the capacity of the SWAT model to simulate streamflow in four micro-catchments with contrasting land cover

Examining the performance of the SWAT model simulations of streamflow in micro-catchments with contrasting land cover is useful, since these results can help to better understand the strengths and limitations of the model to evaluate the potential effects of land use change on the streamflow dynamics. The three PET methods studied were capable of satisfactorily estimating annual runoff coefficients and mean annual high flows in all land covers, although the best results were obtained for MF and SC (Figure 3-5, Table 3-7). Major discrepancies were observed for the mean annual low flows, especially in the IF and IP micro-catchments (Table 3-7).

Previous studies in this region suggest that managed land covers such as pasture can increase the variability of the streamflow response, but that at the daily scale, indicators such as the mean annual runoff coefficient and the mean annual high flow tend to be largely determined by elevation and slope (López-Ramírez et al., 2020, Muñoz-Villers et al., 2013). This phenomenon was captured well by SWAT-T models, where higher runoff coefficients were observed at higher elevations, as expected (Ramírez et al., 2017; Sáenz et al., 2014). For slope, SWAT-T predicted higher peak flows in steeper slopes, which is consistent with the higher mean annual high flows observed in steeper slopes by López-Ramírez et al. (2020) and Muñoz-Villers et al. (2013). Steeper slopes have also been associated with higher quickflow, and lower time to peak responses (Mu et al., 2015; Nainar et al., 2018). Overall, the calibrated SWAT-T models produced acceptable Q/P and mean annual high flows (Q_5) predictions (PBIAS < 25) for most of the land covers. We attribute this result to the dense network of climate stations available (Figure 3-1) and the use of slope in the definition of HRUs.

In terms of dry-season baseflow, local studies indicate that both mature and intermediate TMCF forests exhibit higher mean annual low flows than pastureland and shade coffee (López-Ramírez et al., 2020, Muñoz-Villers et al., 2013), thus consistent with the ‘‘sponge-effect hypothesis’’ for forests (Bruijnzeel, 2004; Muñoz-Villers and McDonnell, 2013; Ogden et al., 2013, Muñoz-Villers et al., 2015). Our SWAT-T results, however, point in the opposite direction, with the model substantially overestimating mean annual low flow in the IP micro-catchment for all PET methods (PBIAS > 400, see Table 3-7), and underestimating mean annual low flow for all the PET methods in the mature and intermediate age TMCF micro-catchments (Table 3-7). This finding has serious implications when using hydrological models to analyze the effects of land use changes (e.g., deforestation, reforestation, and natural regeneration) on water budgets.

3.5.4 Potential limitations of this approach.

In our global sensitivity analysis, we did not consider the impact of model setup (number of subbasins and HRUs). However, our study addresses the uncertainty associated with model parameterizations, allowing the visualization of the effects of non-unique parameter sets. Many authors recognize that the impact of this factor is generally more significant than model setup by several orders of magnitude (Schürz et al., 2019, Jha et al., 2004). The selection of HRUs considers a land cover threshold of 5% given the significant computation time required to run this analysis. This threshold was used to reduce the computational costs without significantly compromising the simulation accuracy. However, we recognize that this practice reduces the effects of small land covers at the outlet (Schürz et al., 2019). Finally, we were not able to completely isolate the response of unique HRUs because the four studied micro-catchments were not entirely covered by a unique land use and slope class. These heterogeneities may have influenced our results.

3.6 Conclusions

SWAT-T was capable of accurately mimicking the annual vegetation growth in zones of TMCF in central Veracruz, Mexico. Moreover, SWAT-T was capable of accurately simulating streamflow at the main outlet and predicting a low influence of surface runoff. However, the model incorrectly predicted the dominance of lateral flow, instead of the deep groundwater flow observed by isotope-based studies. Our results thus support the hypothesis that the single active aquifer formulation of SWAT is unable to adequately reproduce the complex response in groundwater dominated catchments.

The HA method for PET produced the best goodness-of fit-results, followed by PT, and PM. The PT and PM PET methods underestimated forest evaporation in the wet conditions of the TMCF zone of central Veracruz. Temperature-based PET methods such as the HA method perform better in these areas, but not for the right reasons since the use of these approaches overestimates ET rates in areas with lower interception capacity (i.e.

non-forested). Incorporation of simpler and more widely accepted interception models such as Liu model (Liu, 2001) may improve results for the right reasons.

SWAT-T satisfactorily reproduced the Q/P and mean annual high flows in contrasting land covers (MF, IF, SC, IP). However, the model consistently overestimated the mean annual low flow in the IP micro-catchment and underestimated it in the MF and IF micro-catchments. This result suggests that the use of the SWAT-T models in TMCF areas with low influence of surface runoff is not recommended for conducting land-use change analysis, especially when interested in hydrological services such as baseflow sustenance. Overall, structural improvements informed by field data are required to better understand and model the effects of land-use change on hydrology in SWAT-T. Special attention should be given to the use of more reliable groundwater data during the development and calibration of hydrology models.

3.7 References

Abiodun, O.O., Guan, H., Post, V.E. A., Batelaan, O., 2018. Comparison of MODIS and SWAT evapotranspiration over a complex terrain at different spatial scales. Hydrology Earth System Sciences, 22, 2775–2794, https://doi.org/10.5194/hess-22-2775-2018.

Alemayehu, T., Griensven, A.V., Bauwens, W., 2015. Evaluating CFSR and WATCH Data as Input to SWAT for the Estimation of the Potential Evapotranspiration in a Data-Scarce Eastern-African Catchment. Journal of Hydrologic Engineering 21 (3): 05015028. https://doi.org/10.1061/(ASCE)HE.1943-5584.0001305

Alemayehu, T., Griensven, A., Woldegiorgis, B.T., Bauwens, W., 2017. An improved SWAT vegetation growth module and its evaluation for four tropical ecosystems. Hydrology and Earth System Science, 21, 4449–4467. https://doi.org/10.5194/hess-21-4449-2017

Allen, R.G., Pereira, L.S., Raes, D., Smith, M., 1998. Crop evapotranspiration guidelines for computing crop water requirements. FAO Irrigation and drainage paper 56. Last consulted on November 4, 2020 at: http://www.fao.org/docrep/X0490E/X0490E00.htm

Alvarado-Barrientos, M.S., Holwerda, F., Asbjornsen, H., Dawson, T.E., Bruijnzeel, L.A., 2014. Suppression of transpiration due to cloud immersion in a seasonally dry Mexican weeping pine plantation. Agricultural and Forest Meteorology, 186, 12–25. https://doi.org/10.1016/j.agrformet.2013.11.002

Aouissi, J., Benabdallah, S., Chabaâne, Z.L., Cudennec C., 2016. Evaluation of potential evapotranspiration assessment methods for hydrological modelling with SWAT—Application in data-scarce rural Tunisia. Agricultural Water Management 174, 39–51. http://dx.doi.org/10.1016/j.agwat.2016.03.004

Archibald, J. A., Walter, M. T., 2013. Do Energy-Based PET Models Require More Input Data than Temperature-Based Models? -An Evaluation at Four Humid FluxNet Sites. Journal of the American Water Resources Association 50, issue 2, 497-508. https://doi.org/10.1111/jawr.12137

Arnold, J.G., Moriasi, D.N., Gassman, P.W., Abbaspour, K.C., White, M.J., Srinivasan, R., Santhi, C., Harmel, R. D., Griensven, A.V., Van Liew, M.W., Kannan, N., Jha, M.K., 2012. Swat: Model Use, Calibration, and Validation. Transaction of ASABE 55, 1491–1508.

Arnold, J.G., Youssef, M.A., Yen, H., White, M.J., Sheshukov, A.Y., Sadeghi, A.M., Moriasi, D. N., Steiner, J.L., Amatya, D.M., Skaggs, R.W., Haney, E.B., Jeong, J., Arabi, M., Gowda, P.H., 2015. Hydrological processes and model representation: impact of soft data on calibration. American Society of Agricultural and Biological Engineers 58 (6), 1637-1660. DOI 10.13031/trans.58.10726.

Arnold, J.G., Srinivasan, R., Muttiah, R.S., Williams, J.R., 1998. Large area hydrologic modelling and assessment part I: model development. Journal of the American Water Resources association. 34, 73–89. https://doi.org/10.1111/j.1752-1688.1998.tb05961.x

Beck, H.E., Bruijnzeel, L.A., van Dijk, A.I.J.M., McVicar, T.R., Scatena, F.N., Schellekens, J., 2013. The impact of forest regeneration on streamflow in 12 mesoscale humid tropical catchments. Hydrology and Earth System Sciences. 17, 2613-2635. doi:10.5194/hess-17-2613-2013

Borchert, R., Robertson, K., Schwartz, M.D., Williams-Linera, G., 2005. Phenology of temperate trees in tropical climates. International Journal of Biometeorology 50: 57–65. DOI 10.1007/s00484-005-0261-7

Bremer, L.L., Hamel, P., Ponette González, A.G., Pompeu, P.V., Saad, S.I., Brauman, K.A., 2020. Who are we measuring and modeling for? Supporting multilevel decision-making in watershed management. Water Resources Research, 56, e2019WR026011. https://doi.org/10.1029/2019WR026011

Bruijnzeel, L.A., 2004. Hydrological functions of tropical forests: Not seeing the soil for the trees?. Agriculture, Ecosystems and Environment, 104, 185–228. https://doi.org/10.1016/j.agee.2004.01.015

Bruijnzeel, L.A., Mulligan, M., Scatena, F.S., 2011. Hydrometeorology of tropical montane cloud forests: Emerging patterns. Hydrological Processes, 25(3), 465–498. https://doi.org/10.1002/hyp.7974

Campos, C.A., 2010. Response of soil inorganic nitrogen to land use and topographic position in the Cofre de Perote Volcano (Mexico). Environmental Management 46: 213. https://doi.org/10.1007/s00267-010-9517-z

Carnell, R., 2019. Lhs: Latin hypercube samples. [online] Available from: https://CRAN.R-project.org/package=lhs.

Crespo, P., Bücker, A., Feyen, J., Vaché, K.B., Frede, H., Breuer, L., 2012. Preliminary evaluation of the runoff processes in a remote montane cloud forest basin using Mixing Model Analysis and Mean Transit Time. Hydrological Processes. 26, 3896–3910. DOI: 10.1002/hyp.8382

Cukier, R.I., Fortuin, C.M., Shuler K. E., 1973. Study of the sensitivity of coupled reaction systems to uncertainties in rate coefficients. I Theory. The Journal of Chemical Physics 59, 3873. https://doi.org/10.1063/1.1680571

Fahey, T.J., Sherman, R.E., Tanner, E.V.J., 2015. Tropical montane cloud forest: Environmental drivers of vegetation structure and ecosystem function. Journal of Tropical Ecology, 32, 355–367. https://doi.org/10.1017/S0266467415000176

Francesconi, W., Srinivasan, R., Pérez-Miñana, E., Willcock, S.P., Quintero, M., 2016. Using the Soil and Water Assessment Tool (SWAT) to model ecosystem services: A systematic review. Journal of Hydrology 535, 625–636. http://dx.doi.org/10.1016/j.jhydrol.2016.01.034

García, C.I., Martínez, A.A., Ramírez, A., Cruz, A.N., Rivas A.J., Domínguez, L., 2004. La relación agua-bosque: delimitación de zonas prioritarias para pago de servicios ambientales hidrológicos en la cuenca del río Gavilanes, Coatepec, Veracruz. Last consulted on November 4, 2020 at: http://www2.inecc.gob.mx/publicaciones2/libros/528/relacion.pdf

Garcia, E., 2004. Modificaciones al sistema de clasificación climática de Köppen (5th ed., p. 90). Mexico D. F.: Instituto de Geografía UNAM. http://www.igeograf.unam.mx/sigg/utilidades/docs/pdfs/publicaciones/geo_siglo21/serie_lib/modific_al_sis.pdf

González-Martínez, T.M., Holwerda, F., 2018. Rainfall and fog interception at the lower and upper altitudinal limits of cloud forest in Veracruz, Mexico. Hydrological processes 32, Issue 25, Pages 3717-3728. https://doi.org/10.1002/hyp.13299

Gupta, H.V., Kling, H., Yilmaz, K.K., Martinez, G.F., 2009. Decomposition of the mean squared error and NSE performance criteria: Implications for improving hydrological modelling, Journal of Hydrology 377, 80–91. https://doi.org/10.1016/j.jhydrol.2009.08.003

Guse, B., Reusser, D. E., Fohrer, N., 2014. How to improve the representation of hydrological processes in SWAT for a lowland catchment – Temporal analysis of parameter sensitivity and model performance, Hydrological Processes 28, 2651–2670, doi:10.1002/hyp.9777

Guse, B., Pfannerstill, M., Strauch, M., Reusser, D.E., Volk, M., Gupta, H.V., Fohrer, N., 2016. On characterizing the temporal dominance patterns of model parameters and processes. Hydrological Processes 30, 2255–2270. https://doi.org/10.1002/hyp.10764

Guse, B., Pfannerstill, M., Kiesel, J., Strauch, M., Volk, M., Fohrer, N., 2019. Analysing spatio-temporal process and parameter dynamics in models to characterise contrasting catchments. Journal of Hydrology 579, 863-874. https://doi.org/10.1016/j.jhydrol.2018.12.050

Guse, B., Kiesel, J., Pfannerstill, M., Fohrer, N., 2020. Assessing parameter identifiability for multiple performance criteria to constrain model parameters. Hydrological Sciences Journal, 65:7, 1158-1172, https://doi.org/10.1080/02626667.2020.1734204

Guswa, A.J., Brauman, K.A., Brown, C., Hamel, P., Keeler, B. L., Sayre, S.S., 2014. Ecosystem services: Challenges and opportunities for hydrologic modeling to support decision making. Water Resources Research, 50, 4535–4544, doi:10.1002/2014WR015497

Haas, M.B., Guse, B., Pfannerstill, M., Fohrer, N., 2015. Detection of dominant nitrate processes in ecohydrological modeling with temporal parameter sensitivity analysis. Ecological Modelling 314, 62–72. http://dx.doi.org/10.1016/j.ecolmodel.2015.07.009

Hamel, P., Riveros-Iregui, D., Ballari, D., Browning, T., Célleri, R., Chandler, D., Chun, K., Destouni, G., Jacobs S., Jasechko, S., Johnson, M., Krishnaswamy, J., Poca, M., Vieira P. P., Rocha, H., 2017. Watershed services in the humid tropics: Opportunities from recent advances in ecohydrology. Ecohydrology, 11(3), e1921. https://doi.org/10.1002/eco.1921

Hargreaves, G.H., Samani, Z.A., 1985. Reference crop evapotranspiration from temperature. Applied Engineering in Agriculture 1(2), 96-99. (doi: 10.13031/2013.26773) @1985 https://elibrary.asabe.org/abstract.asp?aid=26773

Heidari, A., Mayer, A., Watkins, D., 2019. Hydrologic impacts and trade-offs associated with forest-based bioenergy development practices in a snow-dominated watershed, Wisconsin, USA. Journal of Hydrology 574, 421-429. doi: https://doi.org/10.1016/j.jhydrol.2019.04.067

Holwerda, F., Bruijnzeel, L.A., Muñoz-Villers, L.E., Equihua, M., Asbjornsen, H., 2010. Rainfall and cloud water interception in mature and secondary lower montane cloud forests of Central Veracruz, Mexico. Journal of Hydrology, 384, 84–96. https://doi.org/10.1016/j.jhydrol.2010.01.012

Holwerda F., Bruijnzeel L.A., Scatena F.N., Vugts H.F., Meesters A.G.C.A., 2012. Wet canopy evaporation from a Puerto Rican lower montane rain forest: The importance of realistically estimated aerodynamic conductance. Journal of Hydrology 414–415, 1–15. doi:10.1016/j.jhydrol.2011.07.033

Holwerda, F., Bruijnzeel, L.A., Barradas, V.L., Cervantes, J., 2013. The water and energy exchange of a shaded coffee plantation in the lower montane cloud forest zone of central Veracruz, Mexico. Agricultural and Forest Meteorology 173,1– 13. http://dx.doi.org/10.1016/j.agrformet.2012.12.015

Holwerda, F., Meesters, A.G.C.A., 2019. Soil evaporation in a shaded coffee plantation derived from eddy covariance measurements. Journal of Geophysical Research: Biogeosciences 124. https://doi.org/10.1029/2018JG004911

Hrachowitz, M., Fovet, O., Ruiz, L., Euser, T., Gharari, S., Nijzink, R., Freer, J., Savenije, H. H., Gascuel-Odoux, C., 2014. Process consistency in models: The importance of system signatures, expert knowledge, and process complexity. Water Resources Research 50, 7445–7469. https://doi.org/10.1002/2014WR015484

Hu, G.R., Li, X.Y., 2018. Subsurface Flow. In: Li X., Vereecken H. (eds) Observation and Measurement. Ecohydrology. Springer, Berlin, Heidelberg. https://doi.org/10.1007/978-3-662-47871-4_9-1

Jha, M., Gassman, P.W., Secchi, S., Gu, R., Arnold, J., 2004. Effect of Watershed Subdivision on SWAT Flow, Sediment, and Nutrient Predictions. Journal of the American Water Resources Association 40, 811–825. https://doi.org/10.1111/j.1752-1688.2004.tb04460.x

Karlsen, R., 2010. Stormflow processes in a mature tropical montane cloud forest catchment, Coatepec, Veracruz, Mexico. MSc. thesis, VU Univ., Amsterdam, Netherlands, 110 pp.

LI-COR., 2019. LAI-2200C Plant Canopy Analyzer Instruction Manual. Copyright©2013–2019, LI-COR, Inc., Publication Number: 984–14112. Last consulted on November 4, 2020 at: https://licor.app.boxenterprise.net/s/fqjn5mlu8c1a7zir5qel

Liu, S.G., 2001. Evaluation of the Liu model for predicting rainfall interception in forests world-wide. Hydrological Processes 15 (12), 2341–2360. https://doi.org/10.1002/hyp.264

López-Hernández, J., 2019. Comportamiento hidrológico a varias escalas temporales de una cuenca periurbana, centro de Veracruz, México (BSc. Thesis). Universidad Nacional Autónoma de México, México City, México, p. 45.

López-Ramírez, S.M., Sáenz L., Mayer, A., Muñoz-Villers, L.E., Asbjornsen H., Berry, Z.C., Looker, N., Manson, R., Gómez-Aguilar, L.R., 2020. Land use change effects on catchment streamflow response in a humid tropical montane cloud forest region, central Veracruz, Mexico. Hydrological Processes 1–16. DOI: 10.1002/hyp.13800

Lu, J., Ge, S., Steven, M., Devendra, M. A., 2005. A Comparison of Six Potential Evapotranspiration Methods for Regional Use in the Southeastern United States. Journal

of the American Water Resources Association 41(3): 621-633. DOI: 10.1111/j.1752-1688.2005.tb03759.x

Luo, Y., Arnold, J., Allen, P., Chen, X., 2012. Baseflow simulation using SWAT model in an inland river basin in Tianshan Mountains, Northwest China. Hydrology and Earth System Science 16, 1259–1267, https://doi.org/10.5194/hess-16-1259-2012

Marín-Castro, B.E., Geissert, D., Negrete-Yankelevich, S., Gómez-Tagle, C.A., 2016. Spatial distribution of hydraulic conductivity in soils of secondary tropical montane cloud forests and shade coffee agroecosystems. Elsevier Geoderma 283, 57–67. http://dx.doi.org/10.1016/j.geoderma.2016.08.002

Mehdi, B., Schulz, K., Ludwig, R., 2018. Evaluating the Importance of Non-Unique Behavioural Parameter Sets on Surface Water Quality Variables under Climate Change Conditions in a Mesoscale Agricultural Watershed. Water Resources Management 32, 619–639. https://doi.org/10.1007/s11269-017-1830-3

Meins, F.M., 2013. Evaluation of spatial scale alternatives for hydrological modelling of the Lake Naivasha basin, Kenya, Master thesis, University of Twente. Last consulted on November 5, 2020 at: https://www.utwente.nl/en/et/wem/education/msc-thesis/2013/meins.pdf

Mizutani, K., Yamanoi, K., Ikeda, T., Watanabe, T., 1997. Applicability of the eddy correlation method to measure sensible heat transfer to forest under rainfall conditions. Agricultural and Forest Meteorology 86, 193-203. PIZ SO168-1923(97)00012-9.

Monteith, J.L., 1965. Evaporation and Environment.19th Symposia of the Society for Experimental Biology, 19. University Press, Cambridge, pp. 205–234. Last consulted on November 5, 2020 at: https://repository.rothamsted.ac.uk/item/8v5v7/evaporation-and-environment

Moore, D., 2005. Slug injection using salt in solution. Streamline watershed Management Bulletin Vol. 8, No. 2, printed in Canada, ISSN 1705-5989.

Moriasi, D., Arnold, J., Van Liew, M., Binger, R., Harmel, R., Veith, T., 2007. Model evaluation guidelines for systematic quantification of accuracy in watershed simulations. Transactions of the American Society of Agricultural and Biological Engineers 50, 885–900. https://doi.org/10.13031/2013.23153

Mu, W., Yu, F., Li, C., Xie, Y., Tian, J., Liu, J., Zhao, N., 2015. Effects of rainfall intensity and slope gradient on runoff and soil moisture content on different growing stages of spring maize. Water 7, 2990–3008. https://doi.org/10.3390/w7062990

Muñoz-Villers, L.E., McDonnell, J. J., 2012. Runoff generation in a steep, tropical montane cloud forest catchment on permeable volcanic substrate. Water Resources Research 48, W09528. doi:10.1029/2011WR011316

Muñoz-Villers, L.E., McDonnell, J. J., 2013. Land use change effects on runoff generation in a humid tropical montane cloud forest region. Hydrology and Earth System Sciences 17, 3543–3560. https://doi.org/10.5194/hess-17-3543-2013

Muñoz-Villers, L.E., Holwerda, F., Alvarado-Barrientos, M.S., Geissert, D., Marín-Castro, B., Gómez-Tagle, A., McDonnell, J., Asbjornsen H., Dawson, T., Bruijnzeel, L. A., 2015. Hydrological effects of cloud forest conversion in central Veracruz, Mexico. Bosque, 36(3), 395–407. https://doi.org/10.4067/S0717-92002015000300007

Muñoz-Villers, L.E., Geissert, D.R., Holwerda, F., McDonnell, J.J., 2016. Factors influencing stream baseflow transit times in tropical montane watersheds. Hydrology and Earth System Sciences 20, 1621-1635. doi:10.5194/hess-20-1621-2016

Myneni, R., Knyazikhin, Y., Park, T., 2015. MCD15A2H MODIS/Terra+Aqua Leaf Area Index/FPAR 8-day L4 Global 500m SIN Grid V006. NASA EOSDIS Land Processes DAAC. doi: 10.5067/MODIS/MCD15A2H.006. Accessed July 30, 2019.

Naeem, S., Ingram, J.C., Varga, A., Agardy, T., Barten, P., Bennett, G., Bloomgarden E., Bremer, L.L., Burkill, P., Cattau, M., Ching, C., Colby, M., Cook, D.C., Costanza, R., DeClerck, F., Freund, C., Gartner, T., Goldman-Benner, R., Gunderson, J., Jarrett, D., Kinzig, A. P., Kiss, A., Koontz, A., Kumar, P., Lasky, J. R., Masozera, M., Meyers, D., Milano, F., Naughton-Treves, L., Nichols, E., Olander, L., Olmsted, P., Perge, E., Perrings, C., Polasky, S., Potent, J., Prager, C., Quétier, F., Redford, K., Saterson, K., Thoumi, G., Vargas, M.T., Vickerman, S., Weisser, W., Wilkie, D., Wunder S. 2015. Get the science right when paying for nature's services. Science 347 (6227), 1206-1207. DOI: 10.1126/science.aaa1403

Nainar, A., Tanaka, N., Bidin, K., Annammala, K.V., Ewers, R.M., Reynolds, G., Walsh, R.P.D., 2018. Hydrological dynamics of tropical streams on a gradient of land-use disturbance and recovery: A multi-catchment experiment. Journal of Hydrology 566, 581–594. https://doi.org/10.1016/j.jhydrol.2018.09.022

National Institute of Statistics, Geography and Informatics (INEGI, by its name in Spanish). 2007. Conjunto de datos vectoriales edafológicos. Escala 1:250 000 Serie II. Last consulted on November 3, 2020 at: https://www.inegi.org.mx/temas/edafologia/

National Institute of Statistics, Geography and Informatics (INEGI, by its name in Spanish). 2012. Continuo de Elevaciones Mexicano 3.0, 15m resolution. Last consulted on November 1, 2020 at: https://www.inegi.org.mx/app/geo2/elevacionesmex/

National Weather Service (SMN, by its name in Spanish). 2020. Información estadística climatológica. Last consulted on November 2, 2020 at: https://smn.conagua.gob.mx/es/climatologia/informacion-climatologica/informacion-estadistica-climatologica

Neitsch, S.L., Arnold, J.G., Kiniry, J.R., Williams, J.R., 2011. Soil and water assessment tool theoretical documentation version 2009, Texas Water Resources Institute. Last consulted on November 3, 2020 at: https://swat.tamu.edu/media/99192/swat2009-theory.pdf

Ogden, F.L., Crouch, T.D., Stallard, R.F., Hall, J.S., 2013. Effect of land cover and use on dry season river runoff, runoff efficiency, and peak storm runoff in the seasonal tropics of Central Panama. Water Resources Research 49, 8443–8462. https://doi.org/10.1002/2013WR013956

Paré, L., Gerez, P., 2012. Al filo del agua: Cogestión de la subcuenca del río Pixquiac, Veracruz (1st ed.). Delegación Tlalpan, México, D.F., INE-Semarnat, ISBN 978-607-7908-89-0.

Pfannerstill, M., Guse, B., Fohrer, N., 2014. Smart low flow signature metrics for an improved overall performance evaluation of hydrological models. Journal of Hydrology, 510, 447–458. http://dx.doi.org/10.1016/j.jhydrol.2013.12.044

Pfannerstill, M., Guse, B., Reusser, D., Fohrer, N., 2015. Process verification of a hydrological model using a temporal parameter sensitivity analysis. Hydrology and Earth System Science 19, 4365–4376. https://doi.org/10.5194/hess-19-4365-2015

Pianosi, F., Wagener, T., 2015. A simple and efficient method for global sensitivity analysis based on cumulative distribution functions. Environmental Modelling & Software 67, 1–11. http://dx.doi.org/10.1016/j.envsoft.2015.01.004

Pianosi, F., Wagener, T., 2018. Distribution-based sensitivity analysis from a generic input-output sample. Environmental Modelling and Software 108, 197-207. https://doi.org/10.1016/j.envsoft.2018.07.019

Plesca, I., Timbe, E., Exbrayat, J.F., Windhorst, D., Kraft, P., Crespo, P., Vaché, K., Frede, H.G., Breuer, L., 2012. Model intercomparison to explore catchment functioning: results from a remote montane tropical rainforest. Ecological Modelling 239, 3–13. doi:10.1016/j.ecolmodel.2011.05.005

Priestley, C.H.B., Taylor, R.J., 1972. On the assessment of surface heat flux and evaporation using large-scale parameters. Monthly Weather Review 100, 81–92. https://doi.org/10.1175/1520-0493(1972)100<0081:OTAOSH>2.3.CO;2

Qiu, L., Zhen, F., Yin, R., 2012. SWAT-based runoff and sediment simulation in a small watershed, the loessial hilly-gullied region of China: capabilities and challenges. International Journal of Sediment Research 27, Issue 2, 226-234. https://doi.org/10.1016/S1001-6279(12)60030-4

Quintero, M., Wunder, S., Estrada, R.D., 2009. For services rendered? Modeling hydrology and livelihoods in Andean payments for environmental services schemes. Forest Ecology and Management 258, 1871–1880. doi:10.1016/j.foreco.2009.04.032

R Core Team (2019). R: A language and environment for statistical computing. R Foundation for Statistical Computing, Vienna, Austria. Available from: https://www.R-project.org/.

Ramírez, B.H., Teuling, A.J., Ganzeveld, L., Hegger, Z., Leemans, R., 2017. Tropical montane cloud forests: Hydrometeorological variability in three neighboring catchments with different forest cover. Journal of Hydrology 552, 151–167. https://doi.org/10.1016/j.jhydrol.2017.06.023

Reusser, D., 2015. Fast: Implementation of the fourier amplitude sensitivity test (fast). Available from: https://CRAN.R-project.org/package=fast.

Ripley B. D., 1998. Based on the cloess package of Cleveland, Grosse and Shyu. Available from: https://stat.ethz.ch/R-manual/R-devel/library/stats/html/loess.html

Sáenz, L., Mulligan, M., Arjona, F., Gutierrez, T., 2014. The role of cloud forest restoration on energy security. Ecosystem Services 9, 180–190. https://doi.org/10.1016/j.ecoser.2014.06.012

Salas-Martínez, R., Ibáñez-Castillo, L.A., Arteaga-Ramírez, R., Martínez-Menes, M.R., Fernández-Reynoso, D.S., 2014. Hydrological modelling of mixteco river watershed in the state of Oaxaca, México. Agrociencia 48, 1-15.http://www.colpos.mx/agrocien/Bimestral/2014/ene-feb/art-1.pdf

Samadi, Z.S., 2017. Assessing the sensitivity of SWAT physical parameters to potential evapotranspiration estimation methods over a coastal plain watershed in the southeastern United States. Hydrology research 48.2, 395-415. https://doi.org/10.2166/nh.2016.034

Sánchez-Galindo, M., Fernández-Reynoso, D.S., Martínez-Menes, M., Rubio-Granados, E., Ríos-Berber, J. D., 2017. Hydrological model of the Sordo River watershed, Oaxaca, México, using SWAT. Water Technology and Sciences (in Spanish) 8(5), 141-156. DOI: 10.24850/j-tyca-2017-05-10

Schürz, C., Hollosi, B., Matulla, C., Pressl, A., Ertl, T., Schulz, K., Mehdi, B., 2019. A comprehensive sensitivity and uncertainty analysis for discharge and nitrate-nitrogen loads involving multiple discrete model inputs under future changing conditions. Hydrology and Earth Systems Sciences 23, 1211–1244, https://doi.org/10.5194/hess-23-1211-2019

Schürz C., 2019. SWATplusR: Running SWAT2012 and SWAT+ Projects in R. doi: 10.5281/zenodo.3373859, R package version 0.2.7. Available from: https://github.com/chrisschuerz/SWATplusR.

Schürz C., 2020. temPAWN: Analyze SWATplusR simulations with temporal PAWN sensitivity analysis, doi: 10.5281/zenodo.4103887, R package version 0.1.0,). Available from: https://github.com/chrisschuerz/temPAWN

Shrestha, S., Shrestha, M., Shrestha, P.K., 2018. Evaluation of the SWAT model performance for simulating river discharge in the Himalayan and tropical basins of Asia. Hydrology Research 49 (3), 846–860. doi: https://doi.org/10.2166/nh.2017.189

Shuttleworth, W.J., Calder, I.R., 1979. Has the Priestley-Taylor equation any relevance to forest evaporation?. Journal of Applied Meteorology 18, 639-646. https://doi.org/10.1175/1520-0450(1979)018%3C0639:HTPTEA%3E2.0.CO;2

Soil Conservation Service. 1972. Section 4: Hydrology in National Engineering Handbook. SCS.

Stewart, J.B. (1977). Evaporation from the wet canopy of a pine forest. Water Resources Research 13(6), 915-921. https://doi.org/10.1029/WR013i006p00915

Strauch, M., Volk, M., 2013. SWAT plant growth modification for improved modeling of perennial vegetation in the tropics. Ecological Modelling, 269, 98–112. http://dx.doi.org/10.1016/j.ecolmodel.2013.08.013

Tuppad, P., Kannan, N., Srinivasan, R., Rossi, C.G., Arnold, J.G., 2010. Simulation of agricultural management alternatives for watershed protection. Water Resources Management 24 (12), 3115–3144. DOI 10.1007/s11269-010-9598-8

Van Liew, M.W., Veith, T.L., Bosch, D.D., Arnold J.G., 2007. Suitability of SWAT for the Conservation Effects Assessment Project: Comparison on USDA Agricultural Research Service Watersheds. Journal of Hydrologic Engineering 12, issue 2. https://doi.org/10.1061/(ASCE)1084-0699(2007)12:2(173)

Vigerstol, K.L., Aukema, J.E., 2011. A comparison of tools for modeling freshwater ecosystem services. Journal of Environmental Management 92, issue 10, 2403-2409. https://doi.org/10.1016/j.jenvman.2011.06.040

Vizcaíno-Bravo, Q., Williams-Linera, G., Asbjornsen, H., 2020. Biodiversity and carbon storage are correlated along a land use intensity gradient in a tropical montane forest watershed, Mexico. Basic and Applied Ecology 44, 24-34. https://doi.org/10.1016/j.baae.2019.12.004

Von Thaden, J., Manson, R.H., Congalton, R.G., López-Barrera, F., Salcone, J., 2019. A regional evaluation of the effectiveness of Mexico's payments for hydrological services. Regional Environmental Change 19(6), 1751-1764. https://doi.org/10.1007/s10113-019-01518-3

Williams-Linera, G., 1999. Leaf Dynamics in a Tropical Cloud Forest: Phenology, Herbivory, and Life Span. Selbyana, 20 (1), 98-105. Retrieved from https://journals.flvc.org/selbyana/article/view/120452

Williams-Linera, G., Toledo-Garibaldi, M., Gallardo-Hernández, C., 2013. How heterogeneous are the cloud forest communities in the mountains of central Veracruz, Mexico?. Plant Ecology 213, 685-701. https://doi.org/10.1007/s11258-013-0199-5

Winchell, M., Srinivasan, R., Di Luzio, M., Arnold, J., 2013. ArcSWAT interface for SWAT2012: user's guide. Blackland Research and Extension Center, Texas Agrilife Research. Grassland, Soil and Water Research Laboratory, USDA Agricultural Research Service, Texas, USA. Available from: http://swat.tamu.edu/software/arcswat/

Wright, C., Kagawa-Viviani, A., Gerlein-Safdi, C., Mosquera, G.M., Poca, M., Tseng, H., Chun, K.P., 2018. Advancing ecohydrology in the changing tropics: Perspectives from early career scientists. Ecohydrology 11(3). https://doi.org/10.1002/eco.1918

Zadeh, F.K., Nossent, J., Sarrazin, F., Pianosi, F., Griensven, A., Wagener, T., Bauwens, W., 2017. Comparison of variance-based and moment-independent global sensitivity analysis approaches by application to the SWAT model. Environmental Modelling and Software 91, 210-222. http://dx.doi.org/10.1016/j.envsoft.2017.02.001

4 Using the InVEST-SWY model to evaluate the potential hydrologic impacts of land conversion in two tropical montane cloud forest watersheds

4.1 Abstract

Hydrological services modeling is becoming increasingly popular to guide conservation policy. Moreover, deforestation rates are higher in the tropics, while most modeling tools were developed in temperate zones under site-specific assumptions. Work testing the performance of hydrological models used worldwide is key to increase model credibility and improve the model accuracy. Using streamflow data from two catchments influenced by tropical montane cloud forest in central Veracruz, Mexico, this work assesses the strengths and weaknesses of the Seasonal Water Yield model as part of the Integrated Valuation of Ecosystem Services and Tradeoffs framework (InVEST-SWY) to represent the water budget at annual and monthly scale. The sensitivity of simulated streamflow to changes in the routing parameters, and land use was evaluated. Rainfall interception was incorporated in forests at two altitudinal elevation bands using locally calibrated interception models and daily rainfall. It was found that the model is useful for quick assessments of catchment water budgets at annual scale. However, the interannual baseflow dynamics were not accurately represented; baseflow was underestimated during the dry season. Moreover, the model predicted a significant increase of baseflow as a result of land use intensification. This finding contradicted results from local monitoring studies that reported a decrease in the dry season baseflow in managed land covers. Future directions to improve the applicability of this model are suggested.

4.2 Introduction

Forests provide valuable contributions to people but continue to be threatened by land use change. However, the evaluation of the cobenefits in conservation is still a nascent practice (Börner et al., 2020). Payments for watershed services or payments for hydrological services (PHS) programs (Bösch et al., 2018) typically target upstream forest conservation as a proxy to the downstream provision of hydrological services (HS) such as water quantity (dry-season flows, aquifer recharge, flood protection) (Brouwer et al., 2011). However, inadequate targeting of areas with higher priority and the lack of hydrological modeling and monitoring of the effects of PHS on the hydrology (conditionality) constitute two key obstacles that may considerably hamper watershed management programs success (Wunder et al., 2020, Mokondoko et al., 2018). Moreover, local monitoring efforts are often disconnected from modeling, and modeling efforts are commonly guided by oversimplified assumptions which affects its credibility and impact (Bremer et al., 2020)

The central Veracruz area is one of the pioneers adopting PHS programs. This program started in 2003 as part of the National PHS program adopted by Mexico. Several studies

have shed light regarding the hydrologic functioning of contrasting land covers in these areas: including measurements of rainfall interception (i.e., Holwerda et al., 2010, Holwerda et al., 2013, González Martínez and Holwerda, 2018), monitoring of headwater catchments (Muñoz Villers et al., 2013, López Ramírez(a) et al., 2020), etc. However, most local hydrological modeling efforts have relied on secondary datasets (i.e., Mokondo et al., 2018). Further, most studies evaluating the targeting and economic efficiency of PHS programs in these areas have linked changes in forest cover to field-calibrated measures of water regulation (i.e., Mayer et al., 2020, Jones et al., 2020, Berry et al., 2020), overlooking the interactions with position related factors such as elevation and rainfall distribution. It is an unresolved issue if the location of areas with maximum hydrologic services is determined by the topographic, edaphic, climatic, and geologic characteristics that promote recharge, rather than influenced by functions associated with the protection of forests (Asbjornsen et al., 2017).

Targeting areas of greater risk of deforestation is often used as a surrogate for opportunity cost, this criterion aims to increase program additionality (Alix-Garcia et al., 2014). However, the benefits of paying for outcomes in terms of ES provision (i.e., additional cubic meters of dry season baseflow) rather than proxies of ES provision (i.e., forest cover maintained) are higher (Börner et al., 2017). Moreover, paying for outcomes may also decrease the risk of moral hazard (non-compliance among program participants). In most existing PHS programs, compliance is based on land-use proxies, because measuring ES provision and monitoring may be more costly than measuring actions (e.g., measuring forest conservation). In this regard, the use of hydrological models represents a more efficient way to manage and assess PHS schemes (Quintero et al., 2009, Bremer et al., 2020). A range of GIS-based tools have been used to map HS and facilitate the analysis of their magnitude (Mokondo et al., 2018). The Seasonal Water Yield model as part of the Integrated Valuation of Ecosystem Services and Tradeoffs (InVEST-SWY) framework has been increasingly used and enhanced to allow simulations of how land use/land cover (LULC) might contribute to HS provisioning (i.e., Sahle et al., 2019, Hamel et al., 2020). However, its application has been focused on the use of coarse datasets and few studies have validated the InVEST-SWY model with ground data. More research is needed to better understand the model's capacity to capture the dominant hydrological processes in tropical montane areas influenced by TMCF.

Studies of additionality of PHS programs have typically been limited to historical conversions and, thus, do not account for future changes in drivers of land-use conversion (Börner et al., 2017). Policy design scenarios provide a platform to explore the potential of improving ecosystem services outcomes by introducing and refining conservation programs (e.g., Tabor et al., 2018; Hewson et al., 2019). More research comparing targeting PHS to areas with maximum hydrological services versus targeting for proxies such as risk of deforestation is needed.

The goal of this paper is to model future ecosystem services outcomes in PHS programs in watersheds in Veracruz, Mexico. The primary advance of this work is the evaluation of targeting strategies by combining (a) a calibrated InVEST-SWY model (integrating

results from local monitoring across different scales in forested and managed land covers) with (b) a land change model (LCM) that simulates future land cover patterns in response to PHS program coverage and targeting strategies. To the best of our knowledge this is the first study to model rainfall interception in SWY using locally derived parameters for two elevation bands of TMCF forests. Moreover, this study reviews the InVEST-SWY strengths and weaknesses to represent monthly baseflow dynamics.

The specific research questions addressed are:

> What are the strengths and weaknesses of the InVEST-SWY model to simulate the effects of land-use changes in TMCF environments?
>
> How effective is the current PHS targeting areas of higher baseflow contribution?
>
> What are the effects of future land use and PHS targeting scenarios on baseflow and quick flow?

4.3 Methods

4.3.1 Study site

The Gavilanes catchment (Figure 4-1) (area = 4,132 ha) is the main source of water for the city of Coatepec, Veracruz, Mexico (García et al., 2004). Elevations in the catchment range from 1,180 to 2,960 m above sea level (m a.s.l.). The Pixquiac catchment (Figure 4-1) (area = 10,613 ha) provides 38% of the water supply for the Veracruz state capital of Xalapa (Paré and Gerez, 2012). Elevations range from 1,040 to 3,740 m a.s.l. in the Pixquiac catchment. The two catchments comprise part of the Antigua River basin (area = 1,565 km^2). The general climate is temperate humid (García, 1988) with about 80% of the annual rainfall occurring during the wet season (May - October), followed by a prolonged dry season (November - April). Maximum groundwater recharge and runoff also occurs during the wet season (Muñoz-Villers and McDonnell, 2013). Mean annual rainfall ranges from 1,120 mm to 3,185 mm. Mean daily temperatures ranges from 19° to 5°C (Holwerda et al., 2013; Muñoz-Villers et al., 2012).

The Payments for Hydrological Services program, managed by the National Forest Commission (CONAFOR), began operating in the catchments in 2003 and today covers 27% of the area of the studied catchments. Most parcels receiving payments in the watersheds are now operated by nongovernmental organizations in concert with the two cities of Coatepec and Xalapa (Nava-López et al., 2018; Von Thaden et al., 2019).

The soils in these areas are mainly classified as Umbric Andosols derived from volcanic ash, with clay and silty clay as dominant textures (Campos, 2010; Paré and Gerez, 2012). Soil profiles are generally deep (A + B horizons > 1 m and C + Cr horizons > 10 m on ridges and backslopes) and moderately well developed (Karlsen, 2010), favoring good

water storage. The soils in the region have high permeabilities ranging from 0.05 to 0.08 mm hr^{-1} (Karlsen, 2010; Muñoz-Villers and McDonnell, 2012).

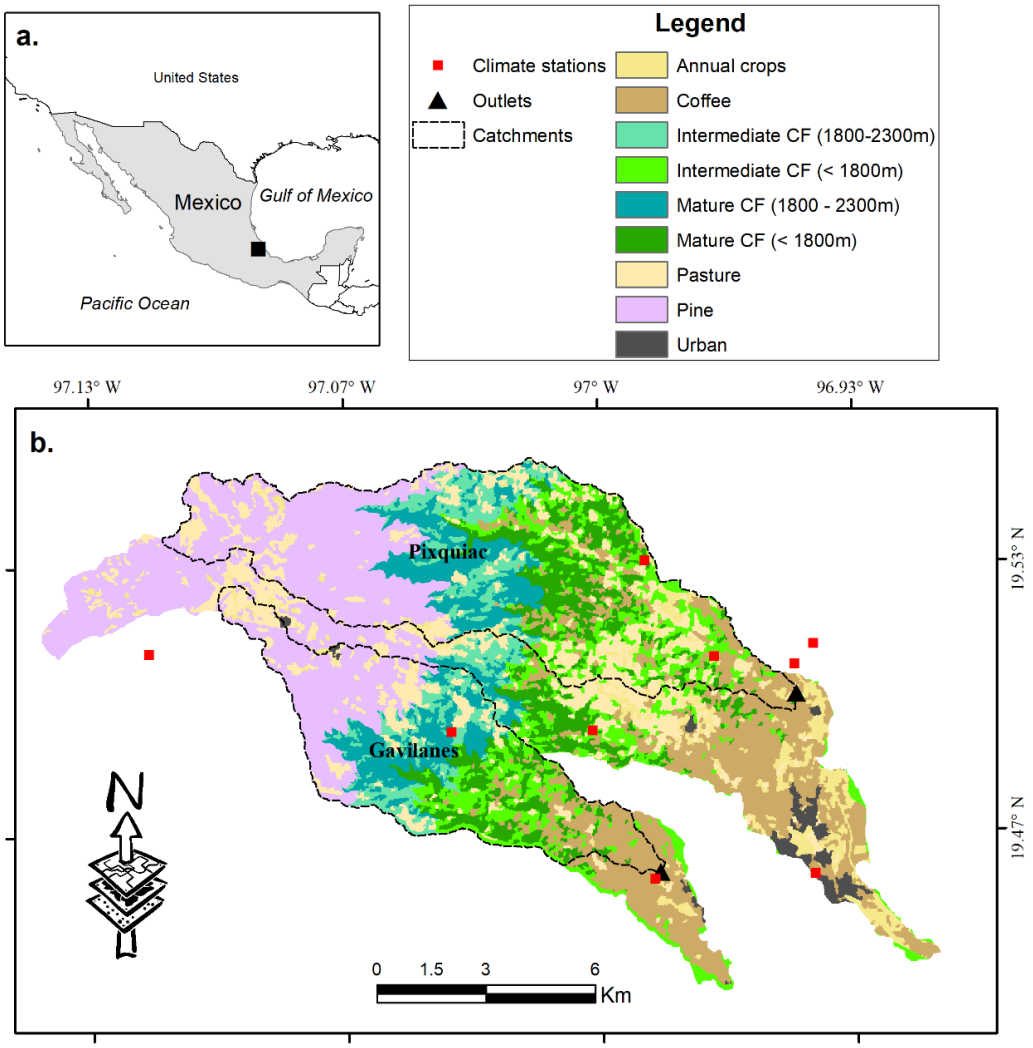

Figure 4-1: General location (a), the study area, including the Gavilanes and Pixquiac catchments (b). Figure distinguishes two cloud forest (CF) elevation bands and two ages of forest.

4.3.2 The InVEST-SWY model

The InVEST-SWY model provides a spatial estimation of baseflow production in a catchment. The model also provides monthly estimates of surface runoff. This model offers sensitivity to land use and explicit representation of routing. The model relies on basic principles of water partitioning (precipitation, runoff and evapotranspiration) and routing (upgradient water becoming available to downgradient parcels). A full model description can be found in the user's guide (Sharp et al., 2020). Four main computational

steps can be identified. First, the model calculates the monthly quickflow (QF) on each pixel based on a modification of the NRCS curve number approach based on monthly precipitation and the number of rainfall events per month (Guswa et al., 2018). Next, the model partitions the monthly available water between local recharge and evapotranspiration. On a given pixel, partitioning is governed by upgradient recharge, and three parameters, α, β, and γ, which control the availability of subsurface water for evapotranspiration (Hamel et al., 2020).

Monthly evapotranspiration is computed as follows being either limited by the demand (potential evapotranspiration - PET) or by the available water.

$$AET_{i,m} = min(PET_{i,m}; P_{i,m} - QF_{i,m} + \alpha_m \beta_i Lsum.avail_{,i}) \ldots\ldots\ldots\ldots [1]$$

Where $PET_{i,m}$ is the monthly potential evapotranspiration and is computed using a monthly crop factor for the pixel's LULC ($Kc_{,i,m}$) and the monthly reference evapotranspiration ($ET0_{,i,m}$). $Lsum.avail_{,i}$ is the sum of upgradient subsurface water that is potentially available at pixel i, α and β represent the fraction of annual recharge from upslope pixels that is available to a downslope pixel for evapotranspiration in a given month. α is a function of precipitation seasonality: recharge from a given month can be used by downslope areas during later months, depending on the subsurface travel times. In the default parameterization, α is set to 1/12.

β reduces the available water based on local topography, geology and position *(0-1),* (i.e., the recharge from the pixel just above the pixel of interest is less likely to be lost than the pixels much further away). γ is the fraction of pixel recharge that is available to downslope pixels (default is 1).

Thirdly, the model computes local recharge (L, equation 2), which represents the potential contribution to baseflow.

$$L_i = P_i - QF_i - AET_i \ldots\ldots\ldots\ldots\ldots\ldots [2]$$

where P_i is annual precipitation, QF_i is the annual quickflow, and AET_i is the annual actual evapotranspiration.

Finally, the model estimates the baseflow index (B) which represents the actual contribution of a pixel to baseflow (i.e. water that reaches the stream). If the local recharge is negative, then the pixel did not contribute to baseflow so *B* is set to zero. If the pixel contributed to groundwater recharge, then *B* is a function of the amount of flow leaving the pixel and of the relative contribution to recharge of this pixel.

4.3.3 Data for the InVEST-SWY model evaluation

We used a two-year streamflow series from the Gavilanes catchment streamflow gauge (5/2/2015 - 4/30/2017) and from Pixquiac catchment (9/17/2015 - 10/31/2017), see

Figure 4-1. Water levels were measured every 10 min using water level sensors paired with barometric pressure recorders. Recorded levels were converted to streamflow (L s^{-1}) using experimental stage-discharge relationships based on rating curves derived from salt dilution measurements of discharge (Moore, 2005). The streamflow data were resampled (mean) to monthly timesteps (Figure 4-7).

4.3.4 Model set up and data preparation

The list of hydroclimatological and spatial data used to set up the InVEST-SWY model is presented in Table 4-1. Maximum and minimum monthly temperature and daily precipitation data were compiled from ten weather stations: four corresponding to the Mexican National Weather Service (SMN, 2020), three from López-Ramírez et. al. (2020), and three operated by the National Autonomous University of Mexico (UNAM). Monthly average relative humidity, solar radiation, and wind speed were available only for the UNAM and López-Ramírez (2020) stations, which were assigned to the rest of the weather stations, considering the similarity in terms of elevation and the shortest distance. We calculated the reference evapotranspiration (ET_0) following FAO guidelines (Allen et al., 1998) and using the available meteorological data (Table 4-1).

Table 4-1: Input data for the InVEST-SWY model setup, the data sources, and data processing steps.

Input dataset	**Source**	**Data preparation**
Topography	INEGI (2012)	Digital Elevation Model for Mexico in 15 m resolution.
Land use	Von Thaden et al. (2019)	Supervised classification of Landsat imagery from the dry season (> 500 ground-based land cover reference data)
Soil data	López-Ramirez (b) et al. (2020)	Soil groups developed from (INEGI, 2007) and pooling soil hydraulic conductivity data collected in more than 100 sites.
Climate	SMN, (2020), López-Ramírez (a) et.al., (2020), and UNAM	Monthly min and max temperature and precipitation, average of solar radiation, wind speed, and relative humidity.
Discharge main outlets	Lyssette E. Muñoz-Villers (Unpublished data)(05/2015- 10/ 2017)	10 min discharge, resampled (mean) to daily.

Input dataset	Source	Data preparation
Crop coefficients, Kc	Transpiration + Rainfall Interception	Transpiration values from Muñoz-villers et al., 2015. Rainfall interception from the Liu Model (Liu, 2001), parameters reported in the literature (Holwerda et al., 2010, Holwerda et al., 2013, González Martínez and Holwerda, 2018)

Rainfall interception in forested land covers

Variation among rainfall interception among different types of TMCF usually reveal large differences (González-Martínez and Holwerda, 2018). In the study area, researchers have consistently studied rainfall interception by comparing rainfall with net rainfall, the latter being the sum of throughfall and stemflow, and measuring meteorological variables to optimizing the parameters for the widely accepted interception model (Liu, 2001). We used the reported optimal interception parameters in combination with observed daily rainfall, under the assumption that the canopy dries every day, to estimate monthly values of interception for forested land covers (equation 3).

$$I = C_m \left[1 - exp\left(-\frac{k}{C_m}P\right)\right]\left[1 - \frac{\underline{E}}{k\underline{R}}\right] + \frac{\underline{E}}{\underline{R}}P \quad \text{.....[3]}$$

where I is the daily modelled interception loss (mm), C_m is the canopy storage capacity (mm), k is the canopy cover fraction (adimensional), $\underline{E}$ is the mean evaporation from the wet canopy (mm hr^{-1}), and $\underline{R}$ is the mean rainfall intensity (mm hr^{-1}). We used the annual parameters reported in the literature (Holwerda et al., 2010, Holwerda et al., 2013, González Martínez and Holwerda, 2018). Results from the model are reported in Figure 4-2.

To incorporate the effects of land cover on the model we added the monthly transpiration (E_t) plus the interception loss (I) for forests. For each month we used the annual values reported of the ratio of transpiration (E_t) by the reference evapotranspiration (ET_0) (E_t/ET_0) of 0.92 for mature and intermediate forests (Muñoz-Villers et al., 2015). Then we added the estimated monthly I divided by the monthly ET_0 (Figure 4-3).

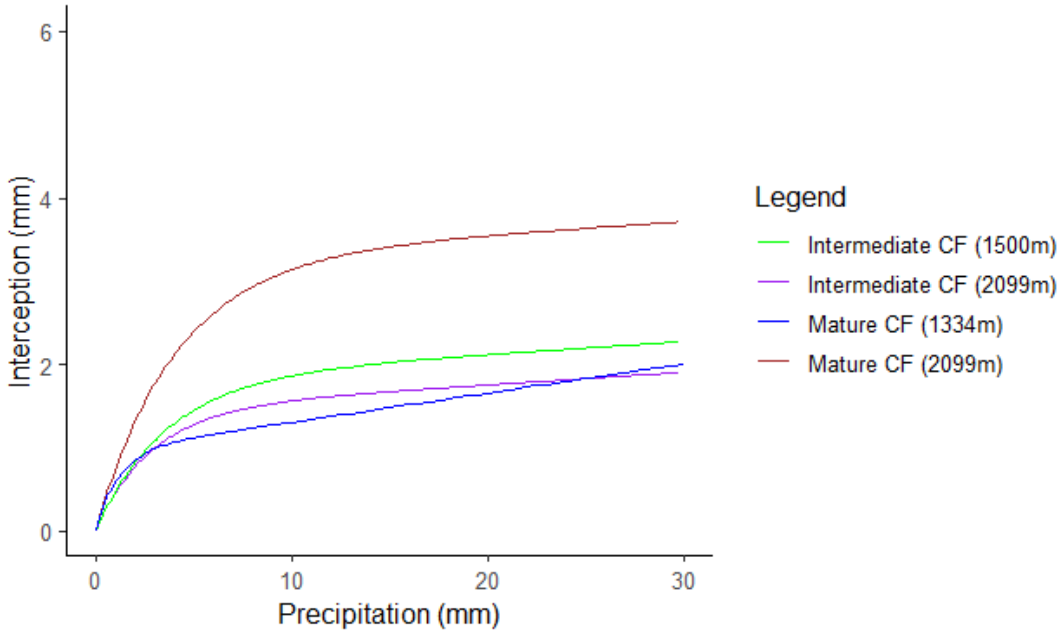

Figure 4-2: Fitted Liu rainfall interception model, relationship between incident rainfall and interception loss for all data including only events with P < 30 mm. See text for further explanation.

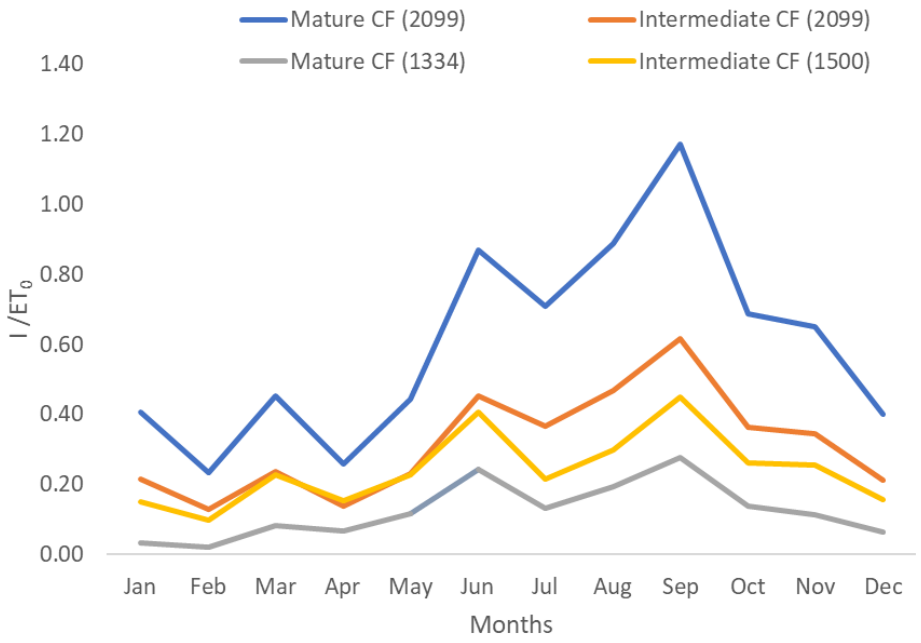

Figure 4-3: Monthly ratio of interception loss (I) and reference evapotranspiration (ET_0). Used to parameterize the InVEST-SWY model.

4.3.5 Monthly baseflow

The InVEST-SWY model was developed and validated against annual baseflow and does not produce monthly baseflow outputs, instead, it aggregates it annually (Sharp et al., 2020). We disaggregated the monthly baseflow from the annual one by running the model with all the monthly inputs set to a specific month and then dividing the produced baseflow by 12, this procedure was repeated for all months. This approach mimics the current annual aggregation method and produces the same results as if the model had the capacity to disaggregate monthly baseflow results (Personal communication with NatCap Software support team).

4.3.6 Sensitivity analyses and model calibration

To better understand the effect of the availability parameters (α and β), we conducted one-at-a-time sensitivity analysis. First, with the default value for α (1/12), we varied β from 0 to 1 by increments of 0.2. A value of 0 for β means that there is no upslope contribution, while a value of 1 means that the entire contribution from upslope pixels is available for evapo-transpiration downgradient (Hamel et al., 2020). To assess the effect of α, we repeated the above analysis for values of α equal to 0, 1/12, 2/12, 3/12, up to 6/12 (for all pixels). A value of $\alpha = 0$ means that local recharge from upgradient is not available for evapo-transpiration locally, representing the same case as $\beta = 0$. A value of 6/12 for α means that one half (0.5) of the annual recharge, i.e. the equivalent of six average months, is potentially available downstream on a given month. This might occur in a watershed with slow release of recharged water.

4.3.7 Effectiveness of PHS at targeting zones with higher baseflow contribution

To explore the spatial relationship between areas with higher baseflow contribution and PHS payments in our study areas, we used the annual baseflow map produced by the InVEST-SWY model. Levels of simulated baseflow were divided into five equally distributed categories (very low, low, medium, high, and very high) and were overlapped with areas in the Pixquiac and Gavilanes watersheds that are receiving PHS.

4.3.8 Scenarios

A business as usual (BAU) scenario, two pessimistic scenarios, and three alternative PHS targeting scenarios were previously developed (Mayer et al., 2020, in review). The BAU scenario projects land cover to 2027 based on historical land cover transitions and the current coverage (~30%) of PHS in the watersheds. The pessimistic scenarios include a no PHS scenario ("No PHS") and a doubling of deforestation rates ("Double Defor"). The "No PHS" scenario approximates what future land cover would look like if the conservation policy were to end. Land cover transitions on forests outside of PHS were used to approximate future changes with no conservation policy in areas receiving PHS.

The second pessimistic scenario illustrates outcomes under increasing pressures to forests outside of conservation protection (Figure 4-4).

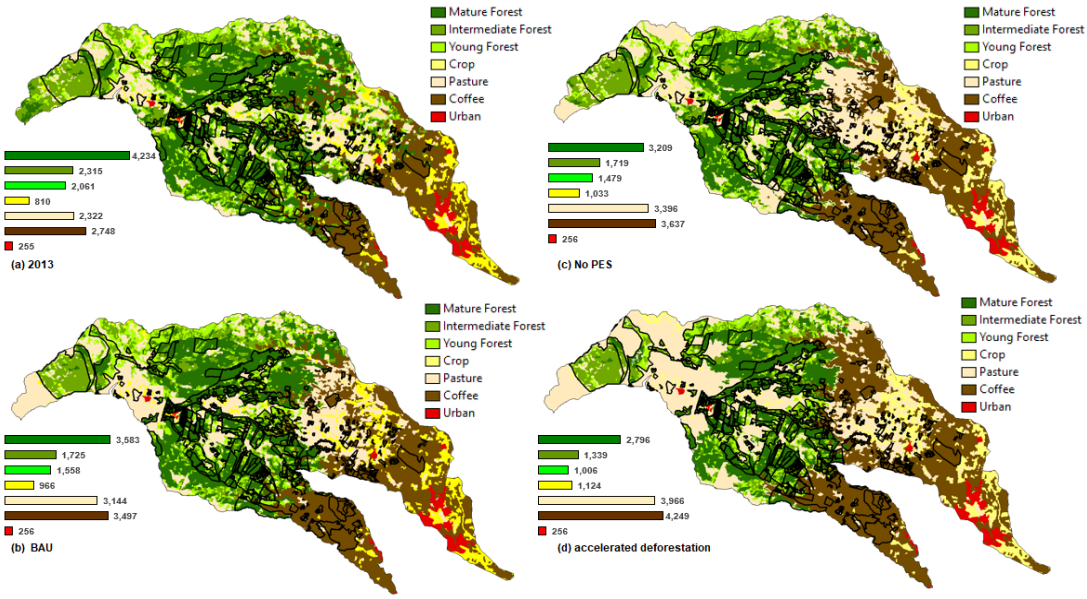

Figure 4-4: Land cover maps and PHS coverage (bold lines) for the study catchments for (a) 2013 base year, (b) 2027 business as usual (BAU) scenario prediction, (c) No PHS program scenario prediction, and (d) 2027 double deforestation risk. Bar charts indicate the area of land cover for the base year or future scenario (Mayer et al., 2020).

The three PHS design scenarios double the current land area under PHS by applying alternative targeting schemes. The first scenario increases the payment area by selecting land areas likely to participate based on the characteristics of the lands currently enrolled, "Current" targeting strategy (See Mayer et al., 2020, Jones et al., 2019, Jones et al., 2020). The second PHS scenario increases the conservation area by selecting new areas according to the highest deforestation rates ("Defor risk" targeting strategy). A deforestation risk map was generated based on deforestation trends for all forested classes combined in the study region from 1993 to 2013 (Von Thaden et al., 2019). The third future PHS scenario increases the conservation area by targeting new areas with the highest groundwater recharge rates ("Hydro" targeting strategy). A hydrologic model was developed with the SWAT software platform (Arnold et al., 2012) and calibrated using two stream gauges at the two watershed outlets (Shinbrot et al., 2020). Output from the SWAT model was used to map average annual groundwater recharge rates over the study area and subsequently select land parcels in order to maximize the overall groundwater recharge rate (Figure 4-5).

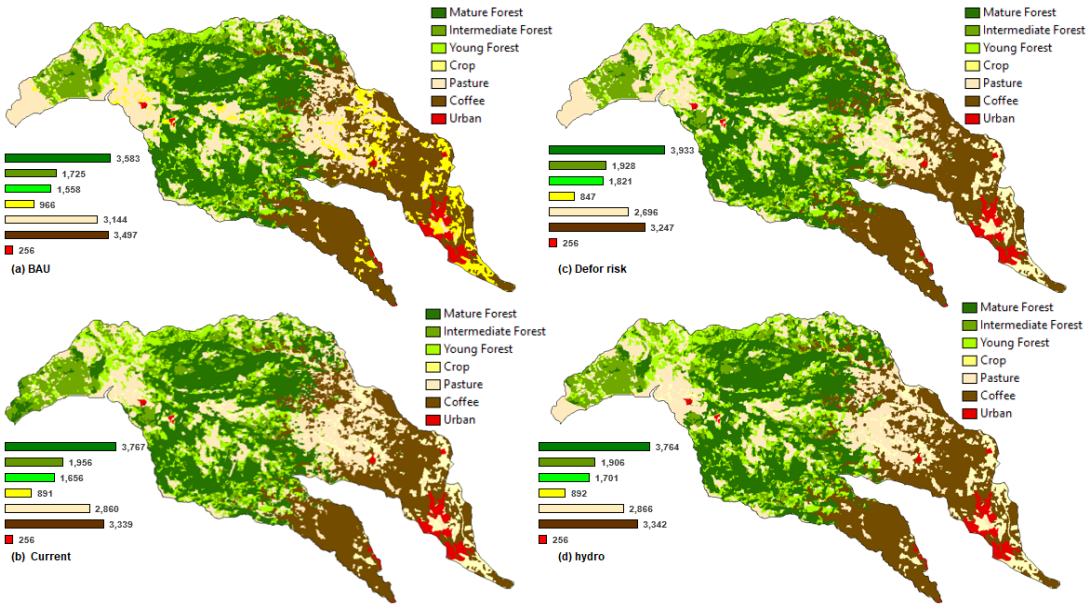

Figure 4-5: Land cover maps for the study watersheds for (a) 2027 Business as usual, (b) 2027 Current targeting, (c) 2027 Defor risk targeting, and (d) 2027 hydro targeting. Bar charts indicate the area of land cover for the future scenario (Mayer et al., 2020).

4.4 Results

4.4.1 Sensitivity analysis to routing parameters

The sensitivity analysis highlighted similar roles of the flow routing parameters α and β. In all cases, the values of α and β indicate a minimum potential for more recharge to be removed by evapotranspiration. Thus, there is a reduced chance to decrease baseflow. Both parameters showed that modeled values of baseflow were similarly sensitive to α and β, only a slight decrease from 1380 to 1320 mm was obtained when either of the parameters are modified to increase evapotranspiration.

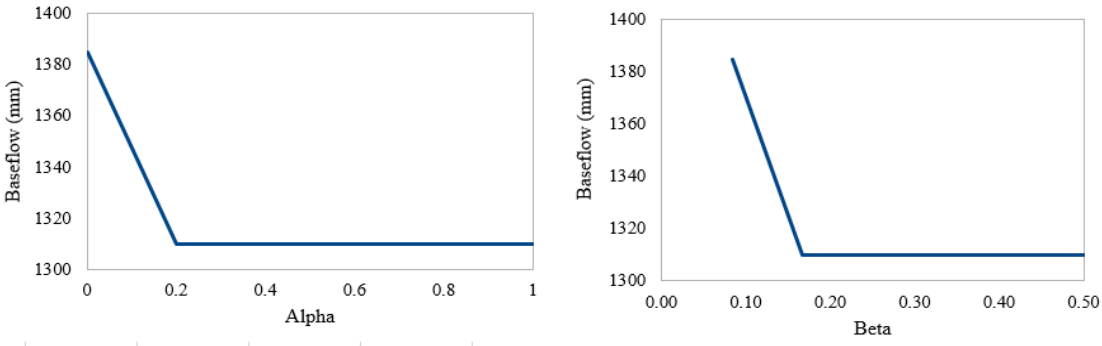

Figure 4-6: One-at-a-time sensitivity analysis of the InVEST-SWY model baseflow, B, to α (right) and β (left) parameters.

4.4.2 Comparison with observed data

The comparison with observed monthly streamflow data in the Gavilanes (Figure 4-7a, Table 4-2) and Pixquiac (Figure 4-7b, Table 4-2) showed consistent results. The observed annual runoff is 1356 mm/yr for Gavilanes, and 1283 mm/yr for Pixquiac (adding reported water extractions). InVEST-SWY predicted the average annual streamflow well. However, the model overestimated streamflow for Gavilanes and underestimated it for Pixquiac. The largest discrepancy was observed in the monthly values. In the two catchments the model overestimated streamflow in the wet season and largely underestimated it during the dry season. Partitioning between quickflow and baseflow showed that quickflow plays a less important role in these areas. This process is well represented by the InVEST-SWY model as explained in the discussion chapter.

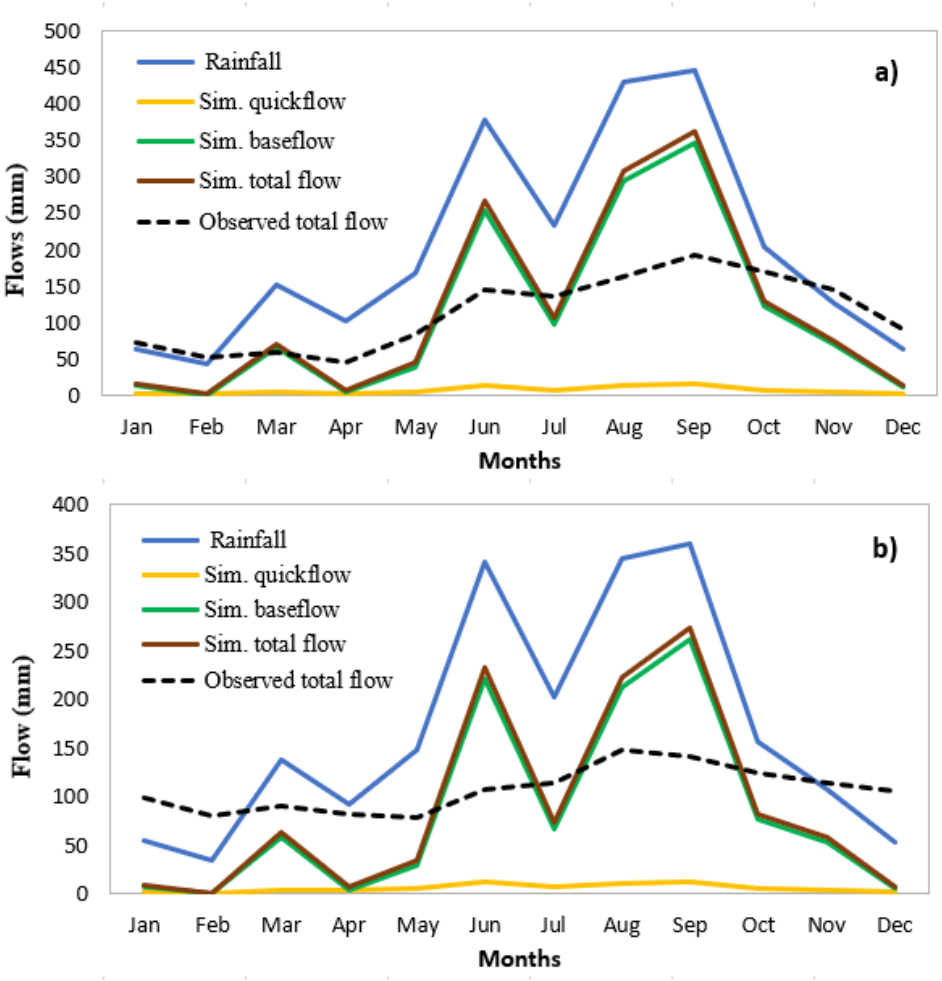

Figure 4-7: Comparison between InVEST-SWY model predictions and monthly observations at two stream gauges a) Gavilanes, b) Pixquiac. Hydrographs represent modeled quickflow and baseflow.

Table 4-2: Monthly observed and simulated discharge at the two streamflow gauges. All units in mm.

Catchment	Month	Rainfall	Sim. quickflow	Sim. baseflow	Sim. total flow	Observed total flow
Gavilanes	Jan	63.5	2.2	12.9	15.1	72.4
	Feb	43.6	1.6	0.0	1.6	53.1
	Mar	151.0	5.3	65.1	70.4	59.9
	Apr	101.8	3.6	4.4	7.9	45.5
	May	167.2	5.9	39.4	45.4	83.2
	Jun	379.3	13.3	253.7	267.0	144.4
	Jul	234.5	8.0	98.4	106.4	135.7
	Aug	429.9	15.0	293.8	308.8	162.3
	Sep	445.5	15.7	346.2	361.9	193.8
	Oct	204.8	7.3	122.9	130.1	169.5
	Nov	126.7	4.5	70.3	74.8	145.8
	Dec	63.9	2.2	12.0	14.2	90.8
	Annual	**2,411.8**	**84.6**	**1,319.1**	**1,403.7**	**1,356.4**
Pixquiac	Jan	54.0	1.8	7.4	9.1	98.9
	Feb	33.9	1.1	0.0	1.1	79.6
	Mar	138.0	4.7	57.8	62.5	90.6
	Apr	92.0	3.2	3.3	6.5	81.1
	May	148.7	5.0	29.6	34.7	78.6
	Jun	342.0	11.7	221.7	233.4	107.6
	Jul	201.7	6.5	66.4	72.9	114.1
	Aug	343.9	11.1	212.2	223.4	147.8
	Sep	360.1	11.9	262.2	274.1	141.0
	Oct	156.9	5.1	76.0	81.1	124.1
	Nov	107.6	3.6	53.8	57.4	114.2
	Dec	52.5	1.7	5.0	6.7	105.6
	Annual	**2,031.1**	**67.4**	**995.5**	**1,063.0**	**1,283.2**

4.4.3 Current PHS targeting efficiency

Areas of high to very high baseflow contribution generally occurred in the middle and upper zones of the Los Gavilanes and the south-west part of the Pixquiac catchment (Figure 4-8). In both catchments the PHS payments cover more areas of high and very high importance for baseflow (Figure 4-9). The proportion of PHS polygons receiving payments located in areas of high, and very high water recharge was greater in the Gavilanes (61%) versus Pixquiac catchment (50%).

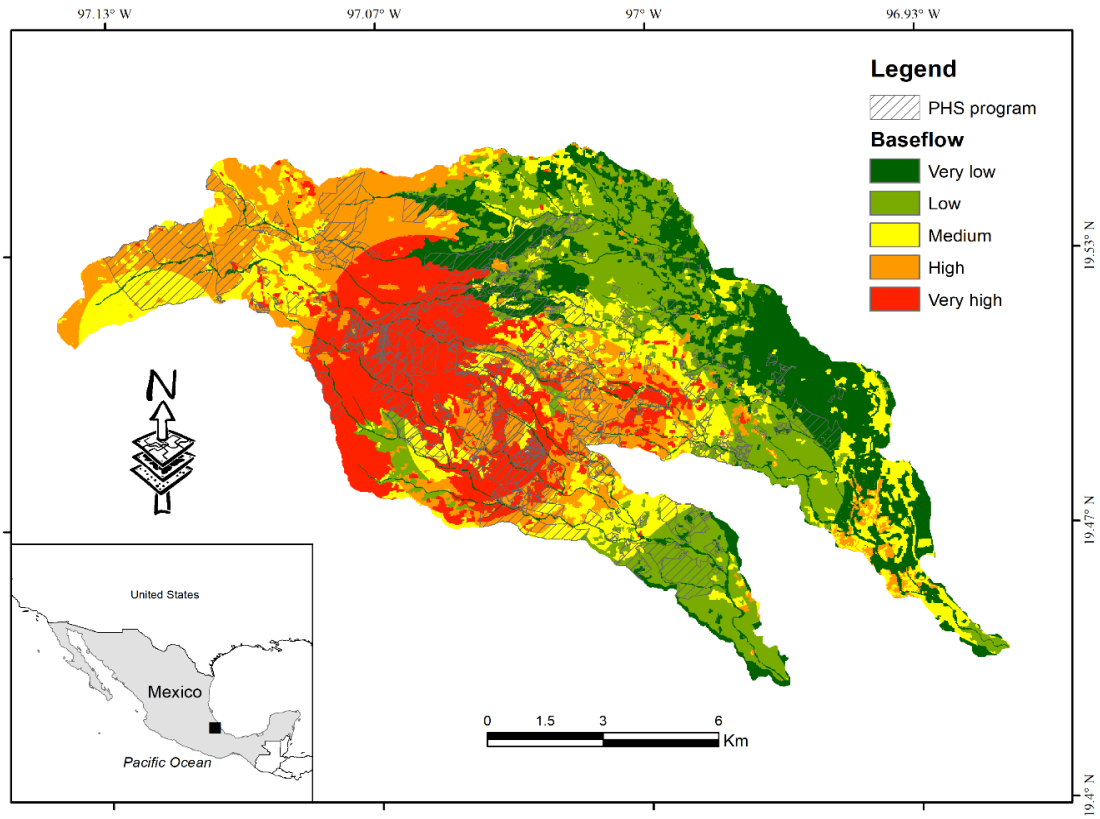

Figure 4-8: Map comparing areas of different levels of recharge with those receiving payments for hydrologic services (PHS) during the period 2003–2020 in the Pixquiac and Gavilanes watersheds.

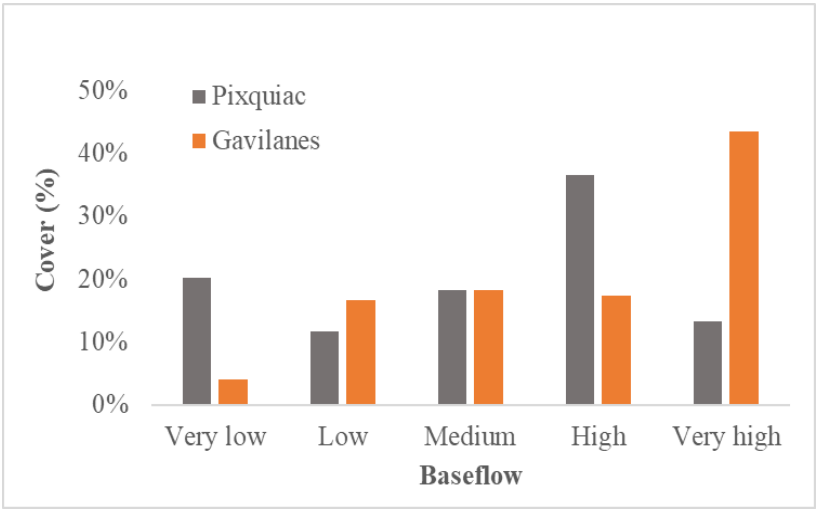

Figure 4-9: Comparison of the proportion of zones with different levels of recharge within the Gavilanes and Pixquiac catchments versus the coverage of land parcels receiving payments for hydrologic services (PHS) during the period 2003–2020.

4.4.4 Effect of scenarios in baseflow

Table 4-3 and Figure 4-10 show the effects of various scenarios on quickflow and baseflow contribution. In general, a moderate decrease in the total flow is expected as a result of the conservation of PHS. Although the annual changes are very mild for both catchments. This response is primarily controlled by baseflow (Table 4-2). In this regard, the pasture scenario; an extreme hypothetical case, where pasture would entirely cover the study area, offered the highest baseflow contribution. These results are not realistic in the light of the finding from the monitored micro-catchments discussed in chapter 2 and will be further analyzed in the discussion section.

Table 4-3: Effects of different land use scenarios on the quickflow and baseflow in the Gavilanes and Pixquiac watersheds.

Catchment	Description	Forest	Managed	Baseflow (mm)	Quickflow (mm)	Total flow (mm)
Gavilanes	2013	71.3%	29%	1,271.5	86.4	1,358.0
	BAU	59.0%	41%	1,276.7	86.6	1,363.4
	No PES	51.2%	49%	1,292.8	86.6	1,379.4
	Deforestation	40.8%	59%	1,294.4	86.8	1,381.2
	Current	59.4%	41%	1,279.0	86.5	1,365.5
	Def. risk	65.8%	34%	1,274.4	86.5	1,360.9
	Hydro targeting	60.7%	39%	1,274.6	86.5	1,361.2
	Holistic	67.1%	33%	1,263.3	86.1	1,349.4
	Pasture	0.0%	100	1,414.0	87.6	1,501.6
	Forest	100.0%	0	1,213.3	84.1	1,297.4
Pixquiac	2013	73%	26%	924.3	68.3	992.6
	BAU	63%	37%	938.1	68.4	1,006.5
	No PES	61%	39%	956.8	68.5	1,025.3
	Deforestation	52%	48%	946.1	68.7	1,014.7
	Current	68%	32%	937.0	68.4	1,005.3
	Def. risk	70%	30%	930.3	68.3	998.6
	Hydro targeting	68%	32%	936.1	68.4	1,004.5
	Holistic	76%	24%	922.8	68.3	991.1
	Pasture	0%	100%	1,041.9	69.1	1,111.0
	Forest	100%	0%	858.1	67.2	925.3

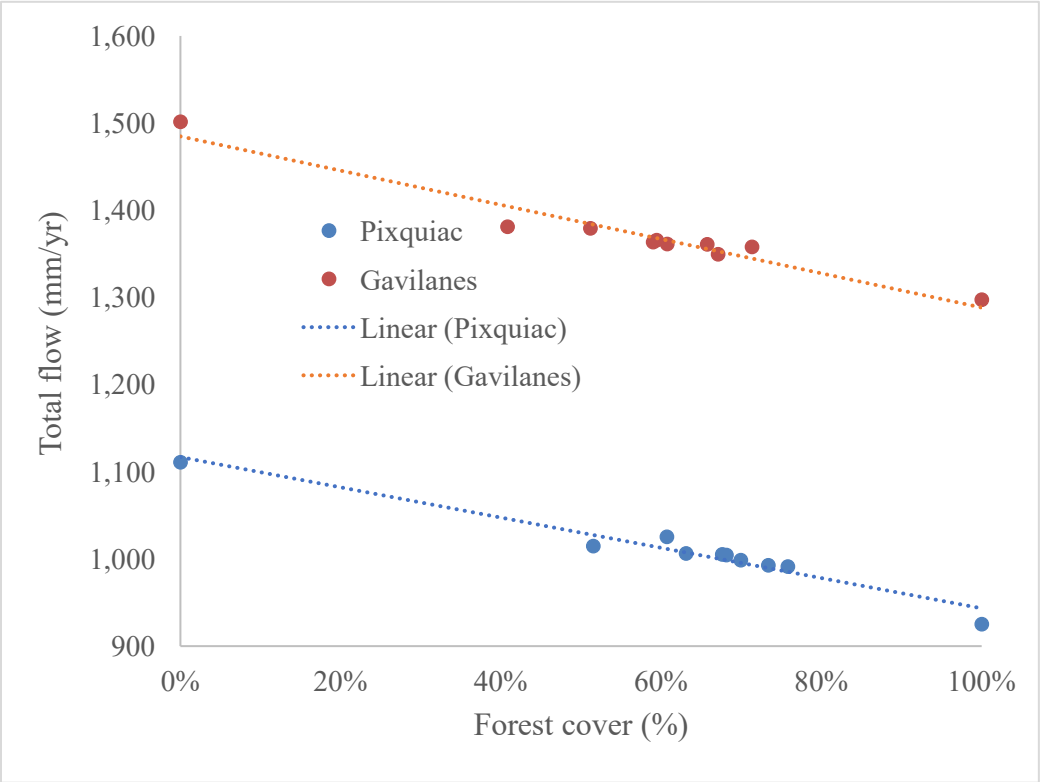

Figure 4-10: Comparison of the effects of changes of forest cover in total flow.

4.5 Discussion

What are the strengths and weaknesses of the InVEST-SWY model to simulate the effects of land-use changes in TMCF environments?

The model showed very low sensitivity to routing parameters (Figure 4-6). These results are expected as the uncertainty about flow routing will decrease in wetter regions, when water deficit for evapotranspiration is low (Hamel et al., 2020). Our results confirm this hypothesis. In this regard, careful attention should be given to the climate and vegetation parameter inputs (Wang et al., 2018).

The model accurately predicted low influence of quickflow (≈ 6% of total streamflow) for both catchments and the dominance of baseflow (≈ 94% of total streamflow) (Table 4-2). These results agree with a recent study in the Pixquiac Catchment, where López-Hernández (2019) examined 159 storm events and indicated that only 3 to 7% of total streamflow occurred as quickflow. The dominance of baseflow predicted by the model is also realistic, as reported by long mean baseflow transit times (between 1.2 and 2.7 years) estimated in Gavilanes catchment and 11 nested subcatchments (Muñoz-Villers et al.,

2016), suggesting that baseflow is the dominant flow path for runoff generation (Muñoz-Villers and McDonnell, 2012, 2013).

The model yields realistic annual estimates of baseflow and quickflow. However, it exhibited a poor interannual performance (monthly). Results from the one-at-a-time sensitivity analysis indicate that the current routing algorithm is incapable of accounting for the groundwater response in our study area, where deep and well-developed soils play a significant role to infiltrate and store water. Improvements regarding the routing algorithm are required to enhance the applicability of this model in ground water dominated regions and to increase the model interannual performance (Figure 4-7).

How effective is the current PHS targeting areas of higher baseflow contribution?

Our results agree with the findings reported by Asbjornsen et al. (2017), such that areas receiving PHS payments are located in zones with high and very high relevance for baseflow contribution (Figure 4-8 and Figure 4-9). Indicating that the current PHS targeting is very effective in these environments. Moreover, our results divided the cloud forest belt in two elevation bands to account for altitudinal gradients in rainfall interception reported by González-Martínez and Holwerda (2018). The incorporation of these findings indicated that the highest evapotranspiration rates associated with forests took place in the upper cloud forest zone, where the highest rainfall takes place. These results indicated that these cloud forests promote the catchments capacity to modulate extreme rainfall events.

What are the effects of future land use and PHS targeting scenarios on baseflow and quick flow?

Overall, conservation policy has a very low impact on water quantity. For both catchments the InVEST-SWY model predicted a slight decrease in total streamflow (Table 4-3, Figure 4-10). Further, the model was unable to mimic the effects of forest conservation on dry-season baseflow. InVEST-SWY exhibited a poor performance at interannual scale and needs improvements to incorporate the water storage capacity of the soils. This limitation constrains the model's capacity to assist the evaluation of land use scenarios. i.e., the hypothetical scenario, where pasture would entirely cover the catchments produced the highest baseflow contribution. While this trend is somewhat realistic due to the increase in transpiration and evaporation observed in forests (Muñoz-Villers et al., 2015), it does not represent the critical drought conditions in the study area. Results from monitoring presented in Chapter 2 indicated that pastures exhibited a significant reduction on the mean annual low flow conditions (Q_{95}), this result agrees with previous finding reported by Muñoz-Villers et al. (2013) in a pasture dominated micro-catchment located at a higher elevation. This result supports the hypothesis that the sustenance of dry season baseflow in extreme drought conditions is related with the interaction between recharge and slow movement across long and deep pathways as suggested by Muñoz-Villers et al. (2016). Thus, future efforts in the calibration and

development better routing algorithms in the InVEST-SWY model should consider reliable groundwater dataset under contrasting land covers.

4.6 Conclusions

InVEST-SWY model presents the advantage of being parsimonious. Moreover, this model is able to integrate local evapotranspiration knowledge, such as locally derived crop coefficients in forested areas. Our results indicate that the model structure is useful for quick assessments of catchment water budgets. However, the model exhibits limitations to assist the analysis of land-use change scenarios, specially to capture interannual baseflow dynamics and the baseflow response in micro-catchments with contrasting land covers. More research is needed to improve the model routing algorithm using detailed streamflow datasets from a small catchment with dominant land covers.

4.7 References

Allen, R.G., Pereira, L.S., Raes, D., Smith, M., 1998. Crop evapotranspiration guidelines for computing crop water requirements. FAO Irrigation and drainage paper 56. Last consulted on November 4, 2020 at: http://www.fao.org/docrep/X0490E/X0490E00.htm

Alix-Garcia, J., G. Aronson, V. Radeloff, C. Ramirez-Reyes, E. Shapiro, K. Sims, and P. Yañez-Pagans. 2014. Environmental and socioeconomic impacts of Mexico's Payments for Ecosystem Services Program. 3ie Grantee Final Report. International Initiative for Impact Evaluation, New Delhi, India.

Asbjornsen, H., Manson, R.H., Scullion, J.J., Holwerda, F., Muñoz-Villers, L.E., Alvarado-Barrientos, M.S., Geissert, D., Dawson, T.E., McDonnell, J.J., Bruijnzeel, L.A., 2017. Interactions between payments for hydrologic services, landowner decisions, and ecohydrological consequences: synergies and disconnection in the cloud forest zone of central Veracruz, Mexico. Ecology and Society 22(2): 25. https://doi.org/10.5751/ES-09144-220225

Berry, Z.C., Jones, K., Gomez Aguilar, L.R., Congalton, R., Holwerda, F., Kolka, R.,..., López Ramírez, S.M., 2020. Evaluating ecosystem service trade-offs along a land-use intensification gradient in central Veracruz, Mexico. Ecosystem Services. https://doi.org/10.1016/j.ecoser.2020.101181

Börner, J., Baylis, K., Corbera, E., Ezzine-De-Blas, D., Honey-Rosés, J., Persson, M., Wunder, S., 2018. The Effectiveness of Payments for Environmental Services. World Development 96, 359–374. http://dx.doi.org/10.1016/j.worlddev.2017.03.020

Börner, J., Schulz, D., Wunder, S., Pfaff, A., 2020. The Effectiveness of Forest Conservation Policies and Programs. The Annual Review of Resource Economics 12, 45-64. https://doi.org/10.1146/annurev-resource-110119-025703

Bösch, M., Elsasser, P., Wunder, S., 2019. Why do payments for watershed services emerge? A cross-country analysis of adoption context. World Development 119, 111–119. https://doi.org/10.1016/j.worlddev.2019.03.010

Bremer, L.L., Hamel, P., Ponette González, A.G., Pompeu, P.V., Saad, S.I., Brauman, K.A., 2020. Who are we measuring and modeling for? Supporting multilevel decision-making in watershed management. Water Resources Research, 56, e2019WR026011. https://doi.org/10.1029/2019WR026011

Brouwer, R., Tesfaye, A., Pauw, P. (2011). Meta-analysis of institutional-economic factors explaining the environmental performance of payments for watershed services. *Environmental Conservation, 38,* 380-392.

Campos, C.A., 2010. Response of soil inorganic nitrogen to land use and topographic position in the Cofre de Perote Volcano (Mexico). Environmental Management 46: 213. https://doi.org/10.1007/s00267-010-9517-z

González-Martínez, T.M., Holwerda, F., 2018. Rainfall and fog interception at the lower and upper altitudinal limits of cloud forest in Veracruz, Mexico. Hydrological processes 32, Issue 25, Pages 3717-3728. https://doi.org/10.1002/hyp.13299

Guswa, A.J., Hamel, P., Meyer, K., 2018. Curve number approach to estimate monthly and annual direct runoff. Journal of Hydrologic Engineering 23, https://ascelibrary.org/doi/10.1061/%28ASCE%29HE.1943-5584.0001606

Hamel, P., Valencia, J., Schmitt, R., Shrestha, M., Piman T., Sharp, R. P., Francesconi, W., Guswa A. J., 2020. Modeling seasonal water yield for landscape management: Applications in Peru and Myanmar. Journal of Environmental Management 270. https://doi.org/10.1016/j.jenvman.2020.110792

Holwerda, F., Bruijnzeel, L.A., Muñoz-Villers, L.E., Equihua, M., Asbjornsen, H., 2010. Rainfall and cloud water interception in mature and secondary lower montane cloud forests of Central Veracruz, Mexico. Journal of Hydrology, 384, 84–96. https://doi.org/10.1016/j.jhydrol.2010.01.012

Holwerda, F., Bruijnzeel, L.A., Barradas, V.L., Cervantes, J., 2013. The water and energy exchange of a shaded coffee plantation in the lower montane cloud forest zone of central Veracruz, Mexico. Agricultural and Forest Meteorology 173,1– 13. http://dx.doi.org/10.1016/j.agrformet.2012.12.015

Jones, K.W., Foucat, S. A., Pischke, E. C., Salcone, J., Torrez, D., Selfa, T., Halvorsen, K. E. (2019). Exploring the connections between participation in and benefits from payments for hydrological services programs in Veracruz State, Mexico. *Ecosystem services, 35*, 32-42.

Jones, K.W., Mayer, A., Von-Thaden, J., Berry, C., Lopez-Ramirez, S.., Salcone, J., Manson, R.H., Asbjornsen, H. (Accepted). Measuring the net benefits of payments for hydrological services programs in Mexico. *Ecological Economics.*

Karlsen, R., 2010. Stormflow processes in a mature tropical montane cloud forest catchment, Coatepec, Veracruz, Mexico. MSc. thesis, VU Univ., Amsterdam, Netherlands, 110 pp.

Liu, S. G. (2001). Evaluation of the Liu model for predicting rainfall interception in forests world-wide. Hydrological Processes, 15(12), 2341–2360. https://doi.org/10.1002/hyp.264

López-Ramírez, S.M.(a), Sáenz L., Mayer, A., Muñoz-Villers, L.E., Asbjornsen H., Berry, Z.C., Looker, N., Manson, R., Gómez-Aguilar, L.R., 2020. Land use change effects on catchment streamflow response in a humid tropical montane cloud forest region, central Veracruz, Mexico. Hydrological Processes 1–16. DOI: 10.1002/hyp.13800

López-Ramírez, S.M.(b), Mayer, A., Sáenz, L., Muñoz-Villers, L.E., Holwerda, F., Looker, N., Schürz, C., Berry, Z.C., Manson, R., Lezama, C., Asbjornsen, H., Kolka, R., 2020. Performance of the SWAT model in predicting streamflow responses of contrasting land covers in tropical montane areas of Central Veracruz, Mexico. Journal of hydrology, In review.

López-Hernández, J., 2019. Comportamiento hidrológico a varias escalas temporales de una cuenca periurbana, centro de Veracruz, México (BSc. Thesis). Universidad Nacional Autónoma de México, México City, México, p. 45.

Mayer, A., Jones, K., Asbjornsen, H., Hunt, D., Lopez Ramirez, S.M., Manson, R., Salcone, J., Wright, T.M., Ávila-Foucat, S., Ugalde, J.V.T., 2020. Assessing ecosystem service outcomes from future deforestation threats and payment for hydrological services program designs with integrated modeling, Nature Sustainability, In review.

Mokondoko, P., Manson, R.H., Ricketts, T.H., Geissert, D., 2018. Spatial analysis of ecosystem service relationships to improve targeting of payments for hydrological services. PLoS ONE 13 (2): e0192560. https://doi.org/10.1371/journal.pone.0192560

Moore, D., 2005. Slug injection using salt in solution. Streamline watershed Management Bulletin Vol. 8, No. 2, printed in Canada, ISSN 1705-5989.

Muñoz-Villers, L.E., McDonnell, J. J., 2012. Runoff generation in a steep, tropical montane cloud forest catchment on permeable volcanic substrate. Water Resources Research 48, W09528. doi:10.1029/2011WR011316

Muñoz-Villers, L.E., McDonnell, J. J., 2013. Land use change effects on runoff generation in a humid tropical montane cloud forest region. Hydrology and Earth System Sciences 17, 3543–3560. https://doi.org/10.5194/hess-17-3543-2013

Muñoz-Villers, L.E., Holwerda, F., Alvarado-Barrientos, M.S., Geissert, D., Marín-Castro, B., Gómez-Tagle, A., McDonnell, J., Asbjornsen H., Dawson, T., Bruijnzeel, L. A., 2015. Hydrological effects of cloud forest conversion in central Veracruz, Mexico. Bosque, 36(3), 395–407. https://doi.org/10.4067/S0717-92002015000300007

Muñoz-Villers, L.E., Geissert, D.R., Holwerda, F., McDonnell, J.J., 2016. Factors influencing stream baseflow transit times in tropical montane watersheds. Hydrology and Earth System Sciences 20, 1621-1635. doi:10.5194/hess-20-1621-2016

National Institute of Statistics, Geography and Informatics (INEGI, by its name in Spanish). 2007. Conjunto de datos vectoriales edafológicos. Escala 1:250 000 Serie II. Last consulted on November 3, 2020 at: https://www.inegi.org.mx/temas/edafologia/

National Institute of Statistics, Geography and Informatics (INEGI, by its name in Spanish). 2012. Continuo de Elevaciones Mexicano 3.0, 15m resolution. Last consulted on November 1, 2020 at: https://www.inegi.org.mx/app/geo2/elevacionesmex/

National Weather Service (SMN, by its name in Spanish). 2020. Información estadística climatológica. Last consulted on November 2, 2020 at: https://smn.conagua.gob.mx/es/climatologia/informacion-climatologica/informacion-estadistica-climatologica

Nava-López, M., Selfa, T.L., Cordoba, D., Pischke, E.C., Torrez, D., Ávila-Foucat, S., Halvorsen, K.E. and Maganda, C., 2018. Decentralizing payments for hydrological services programs in Veracruz, Mexico: Challenges and implications for long-term sustainability. Society & natural resources, 31(12), pp.1389-1399. https://doi.org/10.1080/08941920.2018.1463420

Paré, L., Gerez, P., 2012. Al filo del agua: Cogestión de la subcuenca del río Pixquiac, Veracruz (1st ed.). Delegación Tlalpan, México, D.F., INE-Semarnat, ISBN 978-607-7908-89-0.

Quintero, M., Wunder, S., Estrada, R.D., 2009. For services rendered? Modeling hydrology and livelihoods in Andean payments for environmental services schemes. Forest Ecology and Management 258, 1871–1880. doi:10.1016/j.foreco.2009.04.032

Sahle, M., Saito, O., Fürst, C., Yeshitela K., 2019. Quantifying and mapping of water-related ecosystem services for enhancing the security of the food-water-energy nexus in tropical data–sparse catchment. Science of the Total Environment 646, 573–586. https://doi.org/10.1016/j.scitotenv.2018.07.347

Sharp, R., Douglass, J., Wolny, S., Arkema, K., Bernhardt, J., Bierbower, W., Chaumont, N., Denu, D., Fisher, D., Glowinski, K., Griffin, R., Guannel, G., Guerry, A., Johnson, J., Hamel, P., Kennedy, C., Kim, C.K., Lacayo, M., Lonsdorf, E., Mandle, L., Rogers, L.,

Silver, J., Toft, J., Verutes, G., Vogl, A. L., Wood, S, and Wyatt, K. 2020. InVEST 3.8.9 User's Guide. Available online:https://storage.googleapis.com/releases.naturalcapitalproject.org/invest-userguide/latest/index.html (accessed on 30 Oct 2020).

Shinbrot, X., Muñoz-Villers, L., Mayer, A., Purata, M., Jones, K., López-Ramírez, S.M., Lezama-Alcocer, C., Ramos-Escobedo, M., Manson, R. 2020. Quiahua, the first citizen science rainfall monitoring program in Mexico: Filling critical gaps in rainfall data for evaluating a Payment for Hydrologic Services program. Citizen Science: Theory and Practice. http://doi.org/10.5334/cstp.316

Von Thaden, J., Manson, R.H., Congalton, R.G., Lopez-Barrera, F., Salcone, J., 2019. A regional evaluation of the effectiveness of Mexico's payments for hydrological services. Regional Environmental Change 19, 1751–1764. https://doi.org/10.1007/s10113-019-01518-3

Wang, Z., Lechner, A.M., Baumgartl, T., 2018. Ecosystem Services Mapping Uncertainty Assessment: A Case Study in the Fitzroy Basin Mining Region. Water 10, 88; doi:10.3390/w10010088

Wunder, S., Börner, J., Ezzine-de-Blas, D., Feder, S., Pagiola, S., 2020. Payments for Environmental Services: Past Performance and Pending Potentials. Annual review of resource economics 12, issue 1, 209-234. https://doi.org/10.1146/annurev-resource-100518-094206

5 Final conclusions and recommendations

The conversion of forest degrades the soil´s capacity to store and infiltrate rainfall. Our work showed that managed land covers such as pasture and shade coffee decreased the soil´s hydraulic conductivity and increased the soil's bulk density. On the other hand, it was shown that 20 years of forest regeneration largely restores these soil properties.

Monitoring of high temporal resolution of rainfall and runoff at micro-catchments (areas < 0.5 km2) with dominant land covers, made clear that the degradation of their soil properties, due to intensive management, reduced their hydrological services. For instance, the micro-catchment covered by intensive pasture exhibited a significant reduction in its capacity to modulate peak flows and sustain dry season baseflow.

Structural improvements informed by field data are required to better understand and model the effects of land-use change on hydrology in SWAT. Special attention should be given to improve rainfall interception modeling in forests. In some forests, such as the studied mature cloud forest, evaporation may exceed transpiration. Failure to capture this process forced the model to overestimate transpiration in areas with lower rainfall interception, providing the right answers for the wrong reasons. We suggest the incorporation of simpler and widely accepted interception models such as Liu model (Liu 2001) that may improve results for the right reasons.

The InVEST-SWY model had the advantage of being parsimonious and useful to integrate local knowledge in terms of the high evapotranspiration rates in forests. Further, this model proved useful to provide a quick assessment of the catchment water budget at annual scale. However, the model was unable to capture the interannual baseflow dynamics, especially during the dry season.

The complex model (SWAT) and the parsimonious model (InVEST-SWY) exhibited deficiencies in their baseflow routing algorithms and failed to capture the baseflow dynamics in small catchments with contrasting land covers. More research is needed to enhance our modeling capacity to conduct land use scenario analysis. Promising research directions in the modeling of land use change need model calibration and development using streamflow datasets from small catchments dominated with contrasting land covers. Moreover, the development of hydrological models in catchments with deep soils that have high infiltration and storage capacities needs to take advantage of novel experimental methods to better understand the flow pathways and the factors controlling the ground water response. The use of isotope-based studies and high temporal resolution monitoring of streamflow offers a promising avenue in this regard.

A Copyright documentation

Communication with Tess Harrison, Editorial Office and Doerthe Tetzlaff, Editor-in-Chief, *Hydrological Processes*, regarding permission to reprint a published paper as Chapter 2 of this document.

Email from: Sergio Miguel Lopez Ramirez
Sent: 26 November 2020 02:09
To: Dörthe Tetzlaff
Cc: Mayer, Alex
Subject: Inquiry: Permission to place my published paper in my Ph.D. dissertation
Dear Prof. Doerthe Tetzlaff,

I am a Ph.D. Candidate at Michigan Technological University and I am asking you to kindly grant me permission to reprint my paper in my Ph.D. dissertation. The Paper is titled " Land use change effects on catchment streamflow response in a humid tropical montane cloud forest region, central Veracruz, Mexico", Hydrological Processes. 2020; 34: 3555–3570. DOI: 10.1002/hyp.13800.

I thank you in advance for your help.

Best regards,
Sergio M. López Ramírez

From: Dörthe Tetzlaff
Sent: 26 November 2020 06:23
To: Sergio Miguel Lopez Ramirez; HYP Editorial Office; Harrison, Tess
Cc: Mayer, Alex
Subject: AW: Inquiry: Permission to place my published paper in my Ph.D. dissertation

Dear Tess,
please see below - can one of you look into this and get back to the authors please?

best wishes
Doerthe

From: Harrison, Tess
to: Dörthe Tetzlaff, Sergio Miguel Lopez Ramirez, HYP Editorial Office
cc: Mayer, Alex
date: Nov 26, 2020, 6:45 AM
subject: RE: Inquiry: Permission to place my published paper in my Ph.D. dissertation

Dear Doerthe

Thanks for copying me in – Sergio, it is no problem for you to use your published paper in your PHD dissertation. Best of luck.

Thanks
Tess